F 1503/2

BULETINUL INSTITUTULUI POLITEHNIC DIN IAŞI

Tomul XXXVII (XLI)

Fasc. 1–4

Secţia II

CHIMIE ŞI INGINERIE CHIMICĂ

1991

ORSZÁGOS MŰSZAKI KÖZPONT ÉS KÖNYVTÁR INFORMÁCIÓS 1883

BULETINUL INSTITUTULUI POLITEHNIC DIN IAŞI

Tomul XXXVII (XLI)

Fasc. 1–4

Secţia II

CHIMIE ŞI INGINERIE CHIMICĂ

1991

EDITORIAL STAFF

Prof. dr. ing. **VITALIE BELOUSOV** (President)

Prof. dr. doc. **D. I. MANGERON** (Honorary President)

Conf. dr. ing. **MIRCEA MANOLOVICI** (Secretary)

Conf. dr. ing. **MATEI MACOVEANU**

Prof. dr. doc. ing. **ALFRED BRAIER** (Editor)

Prof. dr. ing. **HUGO ROSMAN** (Editor)

Prof. dr. ing. **MIHAIL VOICU** (Head of the Exchange Service)

Prof. dr. **AUREL BEJANCU**

Prof. dr. ing. **VICTOR BULACOVSCHI**

Prof. dr. ing. **MIHAI LUCANU**

Prof. dr. ing. **SPIRIDON CREȚU**

Prof. dr. ing. **ADRIAN RADU**

Conf. dr. ing. **AURELIA GRIGORIU**

BULETINUL INSTITUTULUI POLITEHNIC DIN IAŞI
BULLETIN OF THE POLYTECHNIC INSTITUTE OF JASSY
ИЗВЕСТИЯ ЯССКОГО ПОЛИТЕХНИЧЕСКОГО ИНСТИТУТА
Tomul XXXVII (XLI), Fasc. 1—4 1991

Secţia II

CHIMIE ŞI INGINERIE CHIMICĂ

SUMAR

Pag.

D. I. MANGERON I

O. VICOL, N. FOCA, L. ALDINI şi AL. IORDAN, Compoziţia şi stabilitatea complecşilor din sistemul $K_2[PdCl_4]$ — cisteină (engl., rez. rom.) 1

I. ROŞCA, M. PALAMARU, D. SIBIESCU şi D. SUTIMAN, Stabilitatea compuşilor Cu_2S, ZnS şi CdS folosiţi în stratul subţire al convertoarelor solare şi condiţiile de obţinere şi utilizare a acestora (germ., rez. rom.) 5

N. AELENEI şi E. BUTUC, Unele aspecte termochimice ale reacţiei de obţinere a monomerului 4,4′-diclordifenilsulfoxid (engl., rez. rom.) 13

N. HURDUC şi N. HURDUC, Studiul cinetic al copolimerizării anionice a ε-caprolactamei cu izoprenul (germ., rez. rom.) 19

I. MAZILU, I. COCÎRLĂ, L. TĂTARU, M. VÂŢĂ, D. SCUTARU şi T. LIXANDRU, Contribuţii la sinteza şi polimerizarea unor fenilacetilene *p*-substituite (engl., rez. rom.) 23

I. SIMINICEANU şi C. PETRILĂ, Un nou model termodinamic pentru procesul de sinteză a ureei (rom., rez., engl.) 29

A L. SZÉP, GH. MIHĂILĂ, R. SMOCOT şi M. IVANICIUC, Studiul procesului de descompunere termică a magnezitei (engl., rez. rom.) 37

C. HAGIU, R. DIACONESCU şi A. MĂRGINEAN, Analiza instalaţiei Norsk-Hydro de obţinere a nitrofosfaţilor (I) (franc., rez. rom.) 41

GH. CRISTIAN, N. VOICULESCU, M. PINTEALĂ, R. OGHINĂ, D. CRISTIAN şi R. ARDELEANU, Modelarea reacţiei de obţinere a fenilclorsilanilor (engl., rez. rom.) 49

S. PETRESCU, Transferul de masă solid—lichid la dizolvare (engl., rez. rom.) 55

C. ŞOLDEA şi O. ONISCU, Hidrazide şi hidrazone provenite din acizii morfolinosulfonil-fenoxiacetici (engl., rez. rom.) 59

M. POPA, CL. VASILIU-OPREA şi E.G. IOANID, Evaluarea rezistenţei reale a polimerilor solicitaţi la tracţiune (engl., rez. rom.) 65

A. AZZOUZ (Algeria), E. DUMITRU şi V. HULEA, Aspecte termodinamice şi cinetice privitoare la disproporţionarea catalitică a toluenului (engl., rez. rom.) 69

S. IFRIM şi F. SCHIEBER, Încleierea hîrtiei cu ulei de tall (franc., rez. rom.) 75

RECENZII 81

BULETINUL INSTITUTULUI POLITEHNIC DIN IAŞI
BULLETIN OF THE POLYTECHNIC INSTITUTE OF JASSY
ИЗВЕСТИЯ ЯССКОГО ПОЛИТЕХНИЧЕСКОГО ИНСТИТУТА
Tome XXXVII (XLI), Fasc. 1—4 1991

Section II

CHEMISTRY AND CHEMICAL ENGINEERING

CONTENTS

	Pp.
D. I. MANGERON	I
O. VICOL, N. FOCA, L. ALDINI and AL. IORDAN, Composition and Stability of some Complexes in the System $K_2[PdCl_4]$ — Cisteine (English, Romanian summary)	1
I. ROŞCA, M. PALAMARU, D. SIBIESCU und D. SUTIMAN, Die Beständigkeit von Cu_2S, ZnS und CdS, während der Erzeugung und Verwendungsbedingungen der in Sonnen-Elektroenergie Dünnschicht Konversionsverrichtungen (German, Romanian summary)	5
N. AELENEI and E. BUTUC, Some Thermochemical Aspects concerning the 4,4′-dichlorodiphenylsulphoxide Synthesis (English, Romanian summary) . .	13
N. HURDUC und N. HURDUC, Kinetisches Studium der Anionen-Kopolymerisation des ε - Kaprolaktams mit Isopren (German, Romanian summary)	19
I. MAZILU, I. COCÎRLĂ, L. TĂTARU, M. VĂŢĂ, D. SCUTARU and T. LIXANDRU, Contributions to the Synthesis and Polymerization of some *p*-Substituted Phenylacetylenes (English, Romanian summary)	23
I. SIMINICEANU and C. PETRILĂ, New Termodynamic Model of the Urea Synthesis Process (English, Romanian summary)	29
AL. SZÉP, GH. MIHĂILĂ, R. SMOCOT and M. IVANICIUC, On Kinetics of the Magnesite Thermal Decomposition (English, Romanian summary) . . .	37
C. HAGIU, R. DIACONESCU et A. MĂRGINEAN, Analyse de l'installation Norsk-Hydro pour l'obtention des nitro-phosphates (I) (French, Romanian summary)	41
GH. CRISTIAN, N. VOICULESCU, M. PINTEALĂ, R. OGHINĂ, D. CRISTIAN and R. ARDELEANU, The Modelling of Phenylchlorosilane Synthesis (English, Romanian summary)	49
S. PETRESCU, Mass Transfer at Solid—Liquid Dissolution (English, Romanian summary)	55
C. ŞOLDEA and C. ONISCU, Hydrazides and Hydrazones of Morpholino-sulphonyl-phenoxyacetic Acide (English, Romanian summary)	59
M. POPA, CL. VASILIU-OPREA and E.-G. IOANID, The Evaluation of the Real Strength of the Tensile Stressed Polymers (English, Romanian summary)	65
A. AZZOUZ (Algier), E. DUMITRIU and V. HULEA, Thermodynamic and Kinetic Aspects of Catalytic Disproportionation of Toluene (English, Romanian summary)	69
S. IFRIM et F. SCHIEBER, L'encollage du papier avec du talloïl (French, Romanian summary)	75
BOOK REVIEWS	81

BULETINUL INSTITUTULUI POLITEHNIC IAŞI
Tomul XXXVII (XLI), Fasc. 1—4, 1991
Secţia II
CHIMIE ŞI INGINERIE CHIMICĂ

Acad. Prof. Dr. DIMITRIE I. MANGERON
(1906—1991)

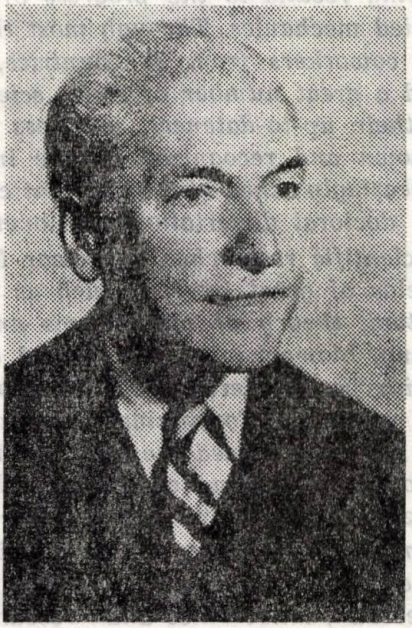

Professor Dr. Dimitrie I. Mangeron, member of the Romanian Academy, a leading figure of the romanian science and high technical teaching, was born in 15/28 November 1906, in Kishinev. After brilliant studies, he graduated in Jassy the Faculty of Sciences of the University „Al. I. Cuza". Then, after two years of more studies in Italy, he became doctor in mathematical sciences, with a remarkable work, devoted to some nonlinear differential equations with partial derivatives. These researches contain in germ what will be later called as „Mangeron equations".

Returned at home, between 1935—1941, he covers all the university ranks, until that of professor. Since 1940 and for all his life, professor Mangeron works with an outstanding passion at the Polytechnic Institute „Gh. Asachi" in Jassy, rapidly becoming a great scientist and a great teacher. He delivered courses on mathematics, but

especially he remains the fascinating professor in theoretical mechanics, for countless series of students, from all the faculties. He enchanted his audience through a wide intellectual opening, striking the listener imagination by a great capacity to penetrate with him in the heart of the more actual scientific problems. For a long time he worked hardly as head of the Departments of Theoretical Mechanics and Mathematics.

During more than sixty years, until the last moment, professor M a n g e r o n was an almost unique example of devotion in the service of teaching and science. With an contaminating enthusiasm and outstanding generosity, he created well-known schools of scientific researches. Open minded and exceptionally gifted, he contributed with remarkable and lasting results to the progress of mathematics and of theoretical and applied mechanics. Through most than 600 papers, written alone or with coworkers from 25 countries, professor Dimitrie M a n g e r o n solved a great number of sharp scientific problems, very impressive due to their up-to-dateness, widtness and variety. He became very soon known and recognized by the international scientific community, who inceasingly asked him to present conferences, to deliver courses or to guide doctoral dissertations, all over the world.

Through his scientific researches, professor M a n g e r o n put his mark on various fields of great interest, such as analytical mechanics, mechanics of vibration, theory of mechanisms and machines, optimal control in engineering, biomechanics, theory and applications of differential equations with partial derivatives, variational methods, history of mathematics and mechanics. Continuing his remarkable achievements, notorious specialists have introduced them in the international scientific circuit, as „Mangeron polyvibrating equations", „Mangeron operators", „Mangeron generalized equations in analytical mechanics", etc.

Scientist of enciclopedic style, profesor Dimitrie M a n g e r o n kept up a vast correspondence with an incredible number of scientists, editorial staffs of reviews, universities and research institutes from all the continents. Simultaneously, he spend incessantly much energy to spead over the world our scientific achievements and to keep up a lively exchange of scientific information. As nobody else, profesor M a n g e r o n contributed to make known the Polytechnic Institute „Gh. Asachi". He was elected member of numerous scientific societies, academies, editorial staffs of prestigious international journals from Europe, Nord and South America and Asia.

One great achievement of professor M a n g e r o n remains the foundation, in 1946, of the now well known „Bulletin of the Polytechnic Institute «Gh. Asachi», Jassy". He succeeded in securing it a high scientific level, who attracted very large contributions of numerous remarkable scientists from all geographical regions. Owing to professor M a n g e r o n, our „Bulletin" has acquired a high international prestige and

a strong capacity to penetrate in the international scientific media, on the basis of material exchange with a wide range of similar issues.

Professor Dimitrie I. Mangeron, member of the Romanian Academy, is definitively entered into the first ranks of our great scientists and teachers of this century. He remains alive in the memory of all who know him and cannot forget his largely open mind to universality, his inexhaustible desire to know and skill to spread knowledge, his unquestionable competence and profound humanism.

Editorial Staff of the
„Bulletin of the Polytechnic
Institute «Gh. Asachi», Jassy"

BULETINUL INSTITUTULUI POLITEHNIC DIN IAŞI
Tomul XXXVII (XLI), Fasc. 1—4, 1991
Secţia II
CHIMIE ŞI INGINERIE CHIMICĂ

D.C. 547.466.8 ; 661.298

COMPOSITION AND STABILITY OF SOME COMPLEXES IN THE SYSTEM $K_2[PdCl_4]$ — CISTEINE

BY

OLGA VICOL, N. FOCA, LIGIA ALDINI and ALEXANDRA IORDAN

1. Introduction

The simple or complex salts of Pd(II) such as $PdCl_2$ and respectively $H_2[PdCl_4]$ ($PdCl_2$ in acid medium and $K_2[PdCl_4]$ in neutral medium), react especially with aminoacids which contain in their molecuIs, besides amino and carboxyl groups, the group —SH. This results in complex combinations of a great variety and stability [1] ... [4].

This paper presents the results of the interaction Pd (II) — ligand (L), where :

$$L = \begin{array}{l} H_2C-SH \\ | \\ HC-NH_2 \\ | \\ COOH \end{array}$$

The reaction of $PdCl_2$ in acid medium with cisteine (weak alkaline solutions) is a fast process, starting at the moment of reactants mixing. Thus, according to the metal—ligand ratio, a large series of complex combination precipitate.

If we work with $K_2[PdCl_4]$ in DMF, the precipitation of complexes is a slow process, offering the possibility of a spectrophotometric study of the $K_2[PdCl_4]$ — cisteine reaction.

2. Experimental Part

The present study used $K_2[PdCl_4]$ solved in a mixture of DMF and H_2O, in a well-defined ratio (85% DMF — 15% H_2O). This is due to the fact that, although $K_2[PdCl_4]$ is water-soluble, it is unstable and suffers a decomposition process.

The ligand (L) — cisteine, can be used in aqueous weak alkaline solution or in a mixture of solvents DMF—H_2O. In this work we used the ligand both in aqueous solution and in a mixture of solvents DMF—H_2O.

The solution of $K_2[PdCl_4]$ in DMF – H_2O (1.10^{-3}/moll) is longterm stable, while the cisteine solution, after about 36 hours produces a white precipitate, due to an oxidation process:

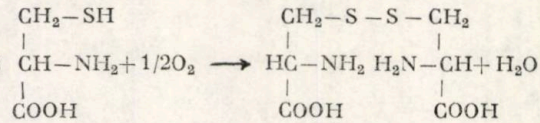

Cisteine *Cistine*

For this reason, the solution of cisteine were prepared at the moment of starting the determinations.

In the study of this system the DMF is recommended as a solvent since an increased concentration in water leads to a rapid precipitation of the complexes, which is observed as the coming out of some yellow-coloured precipitates [1], [2],

Using the DMF as a solvent results in no precipitation, as it was found experimentally, that all complexes separated in solid state and mosts of intermediate ones, resulted from their decomposition, are DMF-soluble.

3. Results and Discussions

In order to study the reaction of $K_2[PdCl_4]$ with cisteine, in solution, the electronic spectra of reactants and reaction products, were initially recorded. The cisteine – ligand in aqueous solution is colourless and presents absorbtion bands in UV range (Fig. 1).

The kalium tetrachlorpaladit in aqueous solution shows a well-defined absorbtion band in visible range, with $\lambda_{max} = 430$ nm (s. Fig. 2).

The electronic spectra of the $K_2[PdCl_4]$ – cisteine system (1 : 1 and 1 : 2) were recorded only in the visible range. That is because DMF is active in UV and no well-defined absorbtion bands can be obtained in this range.

The absorbtion spectra of the above mentioned systems are illustrated in Figs. 3 and 4. An analysis of the electronic spectra shows that in both cases the metal–ligand systems 1 : 1 and 1 : 2 have a time evolution (Figs. 3 and 4). This can be seen from modification of the absorbance value (A) ; after an hour it remains constant. A more rapid evolution is found in the study of $K_2[PdCl_4]$ – cisteine 1 : 1, showing that the system tends to molar ratio 1 : 2.

Comparing the values of the absorbance, A, read after one hour, both for the 1 M : 1 L and 1 M : 2 L systems, we found that they are approximately equal.

The analysed absorbtion bands in the visible range are in fact a prolongation of the better-defined UV-absorbtion bands. The analysis of these bands must be done in a relatively short time interval. The reading of the absorbances after a longer time interval is neither possible or a correct one, as with probes containing more water, the precipitation of the complexes starts and the solution becomes opalescent.

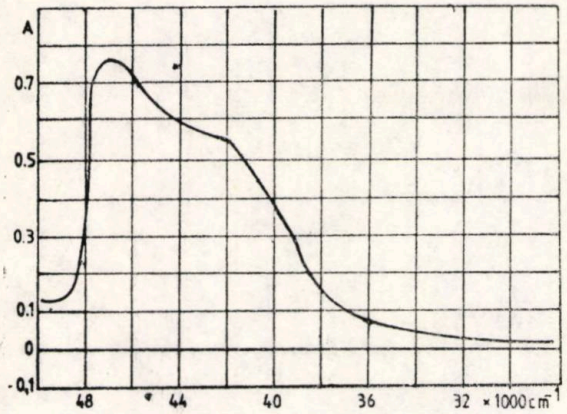

Fig. 1. — UV absorbtion spectrum of cisteine in aqueous solution; $C = 1 \times 10^{-3}$ mol.l^{-1}; sample volume = 1 cm.

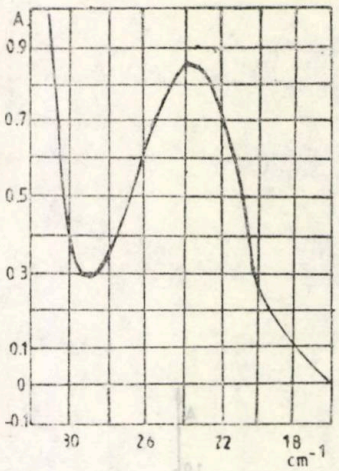

Fig. 2. — Electronic spectrum of $K_2[PdCl_4]$; $C = 1 \times 10^{-3}$ mol. l^{-1} sample volume = 1 cm.

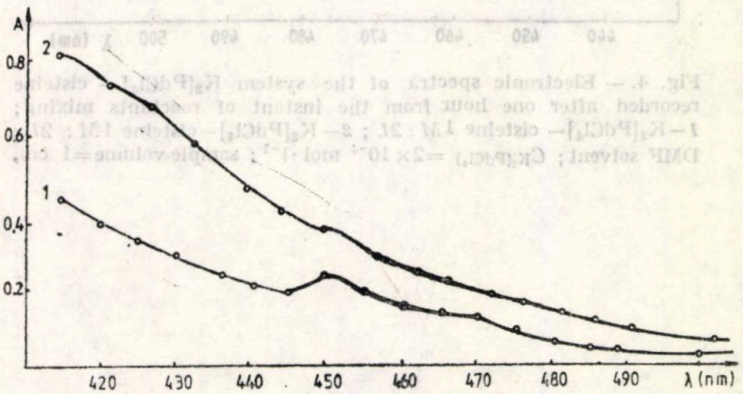

Fig. 3. — Electronic spectra of the system $K_2[PdCl_4]$ — cisteine at the instant of reactants mixing: *1* — $K_2[PdCl_4]$ — cisteine $1M : 1L$; *2* — — $K_2[PdCl_4]$ — cisteine $1M : 2L$; $C_{K_2[PdCl_4]} = 2 \times 10^{-4}$ mol $\cdot l^{-1}$; sample volume = 1 cm.

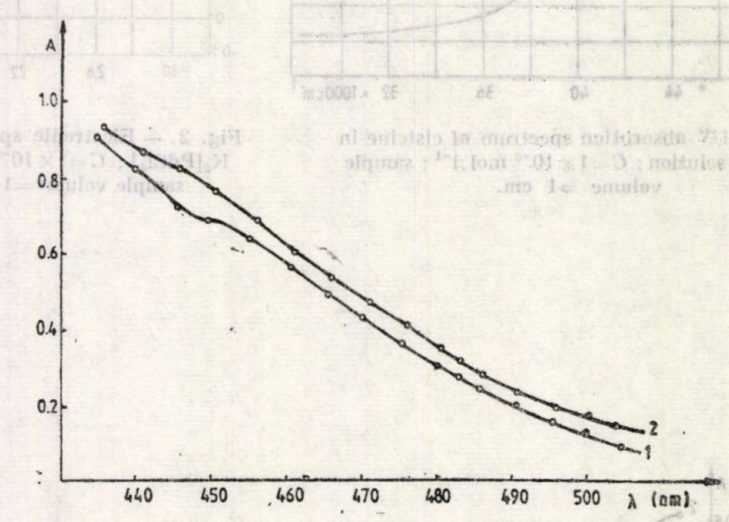

Fig. 4. — Electronic spectra of the system $K_2[PdCl_4]$ — cisteine recorded after one hour from the instant of reactants mixing; *1* — $K_2[PdCl_4]$ — cisteine $1M : 2L$; *2* — $K_2[PdCl_4]$ — cisteine $1M : 2L$; DMF solvent; $C_{K_2[PdCl_4]} = 2 \times 10^{-4}$ mol $\cdot l^{-1}$; sample volume = 1 cm.

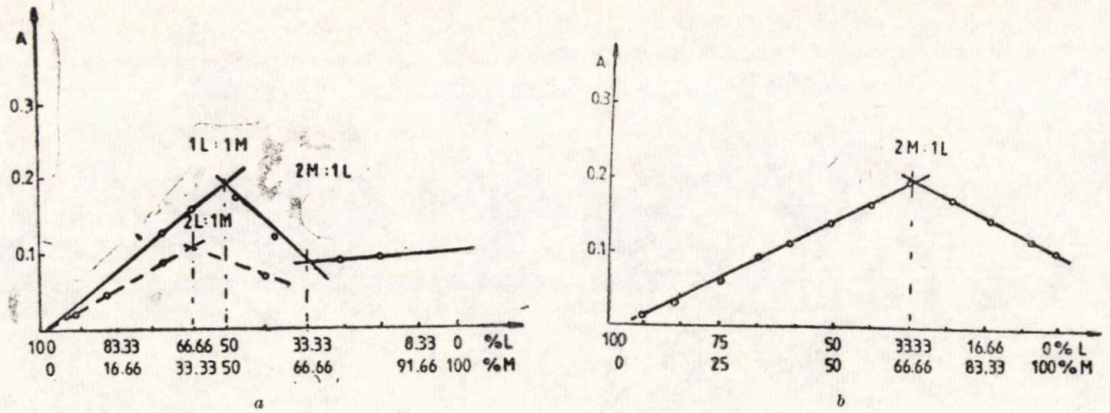

Fig. 6. — Data referring to the composition of the complexes in the system $K_2[PdCl_4]$ — cisteine using the J o b's method ; $C_M = 1.33 \times 10^{-4}$ mol.l^{-1} ; sample thickness = 1 cm.

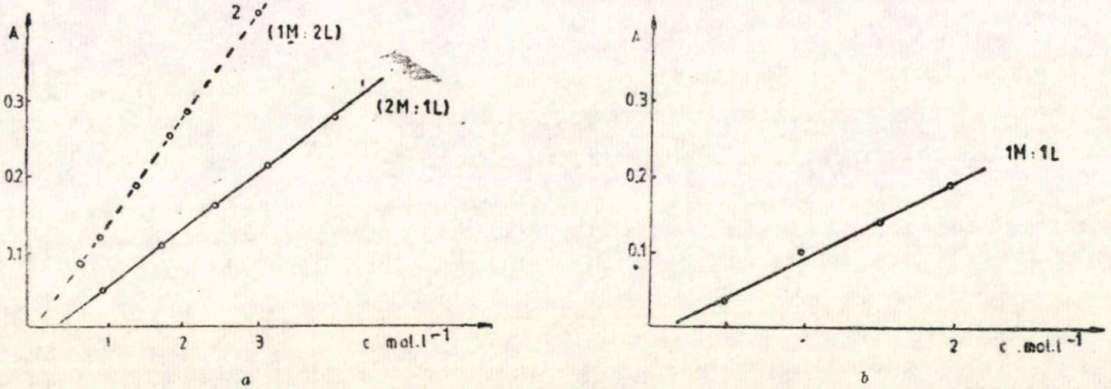

Fig. 7 — Checking the L a m b e r t-B e e r law for the complexes resulted from the reaction of $K_2[PdCl_4]$ with cisteine in a mixture of solvents DMF—H_2O.

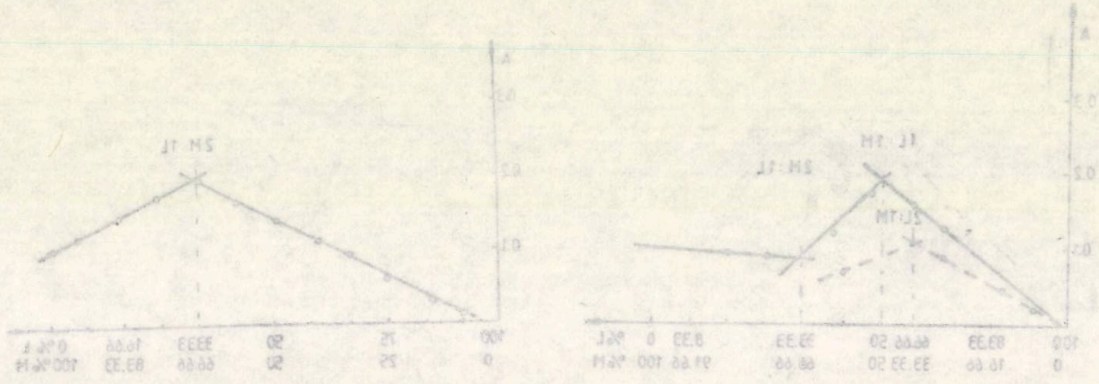

Fig. 6. — Data referring to the complexation of the complexes in the system $K_2[PdCl_4]$ — triethine using the Job's method; $C_M = 1.33 \times 10^{-4}$ mol.l^{-1}; sample thickness = 1 cm.

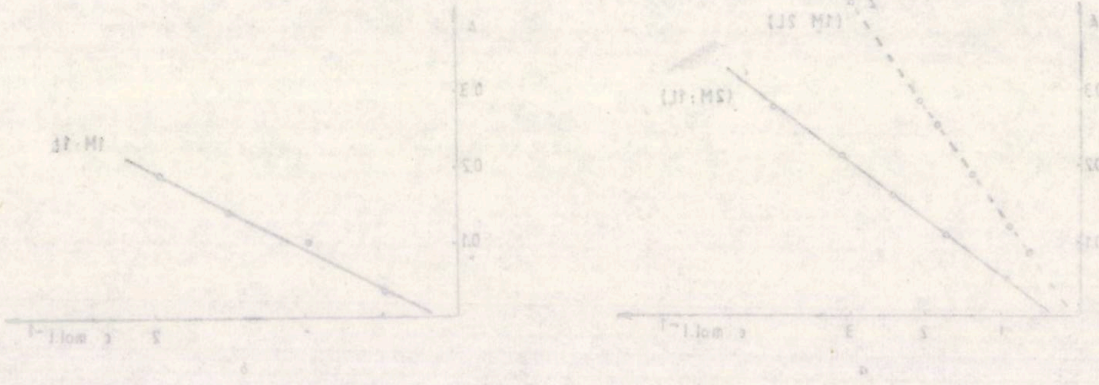

Fig. 7. — Checking the Lambert-Beer law for the complexes resulted from the reaction of $K_2[PdCl_4]$ with triethine in a mixture of solvents DMF–H_2O.

3.1. Determination of the Combination Ratio Pd(II) – Cisteine

The combination ratio $K_2[PdCl_4]$: cisteine was determined using the absorbtion spectra of the complex species in the visible range, applying a series of spectrophotometric methods, such as molar ratio method [5], continuous variation method [6] and the logarithmic method [7].

The determination of the combination ratio metal—ligand was effected in DMF—H_2O solution. The absorbance was read at 445 nm, using a Spekol apparatus ; in this range only the complex species absorbs.

3.2. Molar Ratio Method

The molar ratio method was applied first letting C_L=const. and then holding C_M=const. We obtained data confirming the formation of complexes which correspond to combination ratios of $1M:1L$ and $1M:2L$ (Fig. 5).

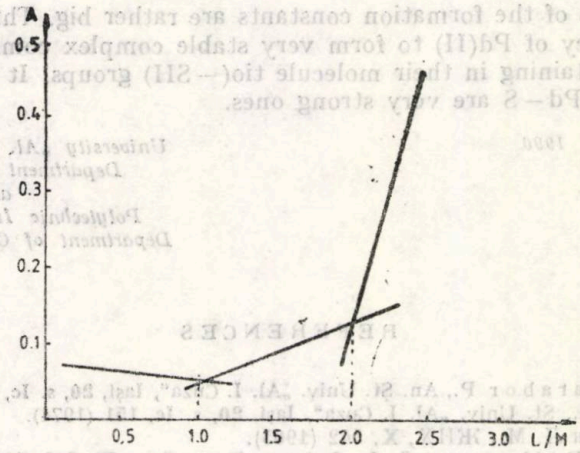

Fig. 5. — Data referring to the determination of the combination ratio $K_2[PdCl_4]$ — cisteine using the molar ratio method: C_M=const. ; C_L=variable ; V= 7.5 cm³ ; sample volume=1 cm.

By spectrophotometric analysis, using the continuous variation method, more complete data about the composition of the system $K_2[PdCl_4]$ — cisteine are obtained. They confirm the complex evolution of this system.

Thus, besides evidencing combination ratios of 1 M : 1 L and 1 M : 2 L, a complex characterized by $2M:1L$ (Figs. 6 *a* and *b*) is also evidenced.

3.3. Checking of Lambert-Beer's Law

The reaction of $K_2[PdCl_4]$ with cisteine, in the DMF—H_2O system, evidence a complex Pd(II) — L interaction. The applied spectrophotometric methods evidence the formation of three complex combination ratios of 1 M: 1 L, 1 M : 2 L and 2 M : 1 L. For this reason, the Lambert-Beer's law checked for the values of the combination ratios we obtained, that is 1 M :

1 L, 1 M : 2 L and 2 M : 1 L. The data are listed in Fig. 7 and they confirm the mentioned values of the combination ratios.

3.4. Stability of Complexes in the System $K_2[PdCl_4]$ – Cisteine

The formation constants were determined for combination ratios of 1 M : 1 L and 1 M : 2 L.

The determination of the formation constant of the 1 M : 1 L complex used the Turner–Anderson's method [9] while for the 1 M : 2 L complex, the Edmonds and Birnbaum's method [10] was used. The formation constants were also calculated using the Harvey-Manning's method [10].

The calculated values, using the above mentioned methods, are close to each other, their average being :

$$K_1(1\,M:1\,L) = 4.36\times10^{13}\ \text{l. moles}^{-1};\quad K_2(1\,M{:}2\,L)=5.62\times10^{15}\ \text{l}^2\text{. moles}^{-2}.$$

The values of the formation constants are rather big. This reflects very well the tendency of Pd(II) to form very stable complex combinations with aminoacids, containing in their molecule tio(–SH) groups. It is to mention that the bonds Pd–S are very strong ones.

Received, April 10, 1990

University „Al. I. Cuza", Jassy,
Department of Chemistry
and
Polytechnic Institute, Jassy,
Department of Organic Chemistry

REFERENCES

1. Vicol O., Harabor P., An. Şt. Univ. „Al. I. Cuza", Iaşi, **20**, s. Ic, 117 (1974).
2. Vicol O., An., Şt. Univ. „Al. I. Cuza", Iaşi, **20**, s. Ic, 151 (1974).
3. Волштейн Л. М., ЖНХ, **X**, 542 (1965).
4. Gray H. B., Balhausen C. J., J. Amer. Chem. Soc., **85**, 260 (1963).
5. Foca N., Vicol O., Hurduc N., Bul. Inst. polit., Iaşi, **XXX (XXXIV)**, *1–4*, s. II, 13–18 (1984).
6. Vicol O., Hurduc N., Schneider I.A., J. Inorg. Nucl. Chem., **41**, 309–315 (1979).
7. Joe, Jones A., Ind. Eng, Chem. Anal., **16**, 111 (1944).
8. Job A., Ann. Chem., **113** (1928).
9. Turner S.E., Anderson R.J., J. Amer. Chem. Soc. **71**, 912 (1949).
10. Edmonds S., Eirnbaum, J. Amer. Chem. Soc., **63**, 1 471 (1941).
11. Harvey A.E., Manning D.L., J. Amer. Chem. Soc., **72**, 4 488 (1950).

COMPOZIŢIA ŞI STABILITATEA COMPLECŞILOR DIN SISTEMUL $K_2[PdCl_4]$ – cisteină

(Rezumat)

Se prezintă rezultatele studiului compoziţiei şi stabilităţii combinaţiilor complexe în sistemul Pd(II) – cisteină. Au fost stabilite raportul de combinare $M : L$ şi au fost calculate constantele de stabilitate ale complecşilor.

BULETINUL INSTITUTULUI POLITEHNIC DIN IAŞI
Tomul XXXVII (XLI), Fasc. 1—4, 1991
Secţia II
CHIMIE ŞI INGINERIE CHIMICĂ

D.K. „74" ; 546.561.221 ; 661.847.2 ; 621. 383.2

DIE BESTÄNDIGKEIT VON Cu_2S, ZnS und CdS, WÄHREND DER ERZEUGUNG UND VERWENDUNGSBEDINGUNGEN DER IN SONNEN-ELEKTROENERGIE DÜNNSCHICHT KONVERSIONS VERRICHTUNGEN

VON

I. ROŞCA und DANIEL SUTIMAN

1. Allgemeine Schätzungen

Unter der vielfaltigen chemischen Komponenten die in den Sonnen-Elektroenergie, Direktkonversionsvorrichtungen angewandt werden, sind Cu_2S, CdS und ZnS, die zur Erzeugung der Sonnenzellen mit einer Dünnschicht Heterojunktur verwendet werden [1] ,..., [8].

Wie bekannt, sind die elektrophysischen Eigenschaften, wie auch die Sonnenzellenleistungen dieser Typen wesentlich vom Aufrechthalten der Güte der Zusammensetzungs-Konstante und von der Sulfidschichten-Struktur über Zeit abhängig. Aus den von einigen Verfasser durchgeführten Forschungen [9], [10] wurde festgestellt, daß man für die Sonnenzellen die Cu_xS als orthorombisches Cu_2S (Kalkocit) oder kupferreiche Phasen, zum Beispiel $Cu_{1,96}S$ (Djurleit) enthalten, maximale Wirkungsgrade erzielen kann.

Demzufolge ist es erforderlich daß durch die angewendte Verfahrenstechnik der Junkturbildung ein Cu_xS mit einem kupferreichem Inhalt (Kalkocit oder Djurleit mit $x=2$ bzw. 1,967) erzeugt werden soll, und diese Strukturen abbaufrei zu behalten.

Die Sonnenzellen des Typus Cu_2S-CdS mit hohen Leistungen werden normaler Weise nach dem Clevite-Verfahren hergestellt [11], wo die Cu_2S-Schicht durch „dipping" erzeugt wird. Es erfolgt durch das Eintauchen der mit CdS beschichtete Unterlage in einer (70° ... 90°C), warmen CuCl-Lösung mit eine teilweise Ersetzung der Cd^{2+} mit Cu^{+}-Ionen und am Ende eine 1 000 ... 2 000 Å dicke Cu_2S-Schichtbildung.

Die Bildung dieser Cu_2S-Schicht in den obenangegebenen oder anderen Bedingungen wurde theoretisch ermittelt [12] und experimentell festgestellt [11],..., [13].

Durch die über die CdS-Schicht, bildende Cu_2S-Schicht, verformt sich das hexagonal. CdS-Netz, leidet eine Umstaltung und geht zu einem orthorombischen Cu_2S-Netz über (Kalkocit).

Zwecks Erzielung hoherer Leistungen wurde die CdS-Schicht mit einer $Zn_xCd_{1-x}S$ schicht ersetzt, wo $x<0,25$ [8].

Da die Funktionen und Leistungen dieser Sonnenzellen von der Beständigkeit des dünnschichtigen Cu_2S, CdS und ZnS abhängig sind, ist es sinnvoll zu wissen ob diese Zusammensetzungen während der Herstellung und Verwendung als Dünnschichten in den Sonnen in Elektroenergie direkten Conversionsverrichtungen sich nicht in Zeit abbauen.

2. Abbau des Cu_2S, CdS und ZnS in Herstellungs- und Verwendungsbedingungen der Dünnschichten in den Sonnen-Elektroenergie Konversionsvorrichtungen

2.1. Die Thermodynamik des Abbauprozesses für CdS, Cu_2S und ZnS

Da die Komponente der atmosphärischen Umwelt auf Dünnschichtigen CuS, CdS und ZnS wirken, wie Temperatur, Sonnenstrallungen, ist es notwendig den Beständigkeitsberreich dieser Sulfide, die in den Sonnenernegie Konversionsvorrichtungen verwendet werden können, theoretisch und experimentell zu ermitteln. Zur Mechanismusbestimmung des Abbauprozeßes für Cu_2S, CdS und ZnS, in Dünnschicht des Abbauherstellungs- und Sonnenstrahlaustellungsbedingungen, ist es erforderlich die wichtigsten Reaktionen die zur chemischen Umwandlung der Sulfide führen, festzulegen. Unter Berücksichtigung daß die Atmosphäre aus H_2, O_2, geringe H_2O, C_2O und Edelgase-Mengen Zusammengesetzt ist, ergibt zich daß der Sauerstoff der als einzige Komponente ein hohen Oxidationscharakter hat, mit allen Sulfide eine temperaturabhängige Wechselwirkung verursachen kann, da S^{2-} reduktive Eigenschaften besitzt. Im Falle Cu_2S, weisen die Cu^+-Ionen ihren reduktiven sowie oxidativen Charakter bedingungsabhängig auf, und gehen in Cu^{2+} b. z. w. Cu über.

Es ist bekannt daß die aus der Dissoziation verschiedener Zusammensetzungen in wasserigen Lösungen stammenden Cu^+-Ionen, leicht übergangsfähig sind, und folgendes Gleichgewicht aufweisen:

$$2Cu^+ \rightleftarrows Cu^{2+} + Cu, \qquad K = 10^6.$$

Einige Verfasser, wie N a k a y a m a [9], sind der Meinung daß in dieser Weise sich längst der interkristallinen Grenzen, der in CdS befindlichen Defekte, Cu-Knoten bilden die, die Heterojunktur kurzschließen.

Bekannt ist auch, daß jedwelche chemische Reaktion in der Richtung der die Summe der freien Enthalpien der Reaktionprodukte kleiner als die Summe der freien Enthalpien der Reaktanten ist, spontan ablauft [9]. Der Prozeß hört auf sobald sich ein Gleichgewicht durch Nullwerden dieser freien Enthalpiedifferenzen einstellt.

Das thermodynamische Algorithmus beruht auf folgender Gleichung:

$$\Delta_R G_T^0 = \Delta_R H_T - T\Delta_R S_T^0,$$

wo: $\Delta_R G_T^0$ — freie Reaktionsenthalpie in Standardbedingungen bei Temperatur T; $\Delta_R H_T^0$ — Reaktionsenthalpie in Standardbedingungen bei Temperatur T; $\Delta_R S_T^0$ — Reaktionsentropie in Standardbedingungen bei Temperatur T;

$$\Delta_R H_T^0 = \Delta_R H_{298}^0 + \int_{298}^{T} \sum \nu_i C_{pi} \mathrm{d}T, \quad C_p = f(T); \quad \Delta_R H_{298}^0 = \sum \nu_i \Delta H_{fi},$$

mit: C_{pi} — spezifische Wärme der Komponente i; ν_i — stöekiometrischer Koeffizient für der Komponente i; H_{fi} — Bildungsenthalpie der Komponente i;

$$\Delta_R S_T^0 = \Delta_R S_{298}^0 + \int_{298}^{T} \frac{\sum \nu_i C_{pi}}{T} dT, \quad \Delta_R S_{298}^0 = \sum \nu_i S_{mi}^0,$$

wo S_{mi}^0 — molare Standardentropie der Komponente i.

Die möglich stattfindenden Reaktionen sind in Tabelle 1 dargestellt, wo die $\Delta_R G_T^0$ - Werte entsprechend für jeden Prozeß im Temperaturbereich 298°...473°K, unter Verwendung der Fachliteratur-Daten erfaßt sind [4].

Tabelle 1

Werte die $\Delta_R G_T^0$ entsprechend für jeden Prozess im Temperaturebereich 298°...473°K

No.		$\Delta_R G_T^0$, [KJ/mol]		
		298°K	373°K	473°K
1	$Cu_2S + \frac{3}{2} O_2 = Cu_2O + SO_2$	— 385,5	— 352,3	— 318,1
2	$Cu_2S + 2Cu_2O = 6Cu + SO_2$	86,6	76,4	63,4
3	$Cu_2S + O_2 = 2Cu + SO_2$	— 210,6	— 209,4	— 208,3
4	$Cu_2S + 2O_2 = 2CuO + SO_2$	— 307,5	— 289,5	— 265,5
5	$Cu_2S + 6CuO = 4Cu_2O + SO_2$	11,0	2,6	— 22,3
6	$Cu_2S + 2CuO = 4Cu + SO_2$	63,9	51,8	34,3
7	$Cu_2S + \frac{5}{2} O_2 = CuSO_4 + CuO$	— 744,6	— 674,6	— 627,0
8	$3Cu_2S + 5O_2 = 2CuSO_4 + 4Cu + SO_2$	—1 355	—1 310	—1 232
9	$ZnS + 2O_2 = ZnSO_4$	— 677	— 649	— 615
10	$ZnS + \frac{3}{2} O_2 = ZnO + SO_2$	— 422,5	— 417	— 410,5
11	$CdS + 2O_2 = CdSO_4$	— 674,6	— 654	— 619
12	$CdS + \frac{3}{2} O_2 = CdO + SO_2$	— 386	— 380,8	— 373,3

Laut Tabelle 1 ist die Reaktion 3 eine Summe der Reaktionen 1 unde 2 oder 4 und 6, und Reaktion 1 kann als eine aus Reaktionen 4 und 5 stammend beachtet werden.

Desgleichen kann Reaktion 3 als eine aus Summe der Reaktionen 6 und 7 stammend betrachtet werden.

In Betrachtnahme daß in normalen Betriebsbedingungen der Sonnenzellen die Temperatur nicht 100°C überschreitet bedeutet das, daß bis zu dieser Temperatur laut der thermodynamischen Festlegungen alle Sulfide aus welchen die Dünnschichten hergestellt sind, in Gegenwart des athmosphärischen Sauerstoffes sich oberflächig abbauen (der Abbau erfolgt intensiver bei Temperaturen über 100°C).

Im Falle daß die in Tabelle 1 angeführten Reaktionen sich in Wirklichkeit entwickeln, ergibt sich daß in Stelle Cu_2S, CdS und ZnS sich folgende feste Stoffe ergeben könnten : $CuSO_4$, CuO, Cu_2O, Cu, $CdSO_4$, CdO, $ZnSO_4$

und ZnO die nicht mehr als Dünnschichten in den Sonnen—Elektroenergie Direktconversionsvorrichtungen verwendet werden können.

Aus den thermodynamischen Festlegungen ergibt sich die Geschwindigkeit dieser Reaktionen, bzw. die Zeit in welcher sich die Cu_2S, CdS und ZnS Dünnschichten Abbauen (Tabelle 1).

2.2. Experimentelle Begründungen über den Abbau des dünnschichigen Cu_2S, CdS und ZnS

Obwohl die Treibkraft jedwelcher Umwandlungen chemischer Kombinationen, bei einem Phasen- oder Strukturnetzübergang die freie Enthalpiedifferenz zwischen den Anfangs- und Endbefindniß, oder die Differenz zwischen den freien Enthalpien der Reaktionsprodukte und der Ausgangsstoffe darstellt, hat diese Differenz nicht immer in Wirklichkeit als Folge die Bewirkung und Abwiklung des betreffenden Prozeß da dieser verhindert werden kann.

In den physikalisch-chemischen Umwandlungen treten oft solche Hinderniß ein, die das Einstellen aus thermodynamischen Standpunkt, den stabilen Gleichgewichtzunstand hemmen. Diese Hindernisse sind Sperren die das Anfangsbefindniß vom Endbefindniß trennen.

Im Falle der chemischen Reaktionen erklären sich diese Sperren, durch die Tatsache daß die Verbindungen der Ausgangsprodukte geschwächt werden müßen, um verschiedener schwächerer Teile der Moleküle die Möglichkeit zu bieten sich neu einordnen zu können, zwecks neuer Struktur Erhaltung.

Diese Verbindungschwächung erfolgt mittels einem Energieverbrauch. Der Energiezahlwert zur Überwindung dieset Sperre, gemessen auf der Ebene des Ausgangsystems, nennt sich Beschleunigungsenergie des Umwandlungsprozeßes und ist eine der wichtigsten Eigenschaften des Prozeßes.

Die Umwandlungsgeschwindigkeit ist durch die Größe der Beschleunigungsenergie, Thermoenergie des Ausgangssystems vom welchen die Größe der Partikelbruchteile a5hängig ist, Moleküle oder andere Strukturnetze die über genügend Energie zur Überwindung der betreffende Sperre verfügen bestimmt.

Falls die Beschleunigungsenergie die die zwei Zustände trennt, groß und die Thermoenergie klein ist (die Temperatur ist verhältnismäßig klein) findet der Prozeß nicht bei bemerkbarer Geschwindigkeit mit gewöhnlichen Mitteln statt.

Aus diesem Standpunkt, von großer Bedeutung ist das Studium des Cu_2S, CdS und ZnS Verhalten, allein unter Wärmewirkung, und gleichzeitig mit den chemischen Wirkstoffe der Umwelt, da allein die Wärme ein Zersetzungserreger ist, aber öfters in der Praxis beschleunigt diese die Wirkung der Abbauwirkstoffe wie: Sauerstoff, Feuchtigkeit verschiedene Unreinigungen, Katalisator u.s.w.

Es wurde festgestellt daß der dünnschichten Abbau der Sonnenzellen, vom angewandtem Herstellungsverfahren dieser, abhängig ist.

Zum Beispiel die Cu_2S-Schicht hat eine höhere Beständigkeit, wenn diese durch „trockene" Methoden (thermisches Verdampfen in Vakuum), gegenüber zu der, die durch Eintauchen einer Unterlage in einer heissen CuCl Suspension, auf der sich CdS absetzt, hergestellt wird.

Das erklärt sich durch die Übergangsfähigkeit in wässrigen Lösungen der Cu^+- und Cu-Ionen :

$$2Cu^+ = Cu^{2+} + Cu.$$

Falls die Cu_2S-Scicht im direkten Kontakt mit der umgebenden Atmosphäre kommt, wird ein Abbau in Zeit dieser Sulfide, die sich in unwirksame Komponente für die Sonnenzellen umwandeln festgestellt. Das ist möglich und mittels thermodynamischer Festlegungen begründet worden, durch die Sauerstoff-Teilnahme an der Reaktion (Tab. 1), und in der Tat, daß das auf der Sonnenzellenschicht Oberfläche als Mikrofilm bildende Wasserkondensat die Cu^+-Ionendissoziation, begunstigt.

Folge dieser Umwandlungen, geht Cu_2S in Cu_xS ärmere Phasen über, wie $Cu_{1,96}S$; $Cu_{1,8}S$ und sogar CuS.

Es wurde festgestellt daß der Kurzschluß-Stromwert der Sonnenzellen nach einer geradliniegen Funktion mit der Cupfermenge Abnahme des Cu_2S absinkt. Dies wurde auch von D i m a und Mitarbeiter bestätigt [2], [3].

Aus der in relative Einheiten ausgedrückte Spektralcharakteristik-Kurve der Offenkreiss-Spannung V_{CD} (Abb 1, Kurve *1*) unmittelbar nach der Sonnenzellenbildung, graphisch umgesetzt (Cu_2S-CdS), sind dei charakteristische Maximalwerte ersichtlich, und zwar ; Calcocit für $x=1{,}995$ und $\lambda = 0{,}98\ \mu m$; Djurlit mit $x=1{,}96$ und $\lambda = 0{,}74\ \mu m$ und CdS für $\lambda=0{,}52\ \mu m$ (Abb. 1, Kurve *2*) entsprechend des Djurlit.

Dar Maximalwert von 0,52 μm der, der Übergänge Band — Band in CdS entspricht, bleibt praktisch unverändert.

Diese Änderungen in der spektralen Charakteristik beruhen auf thermodynamisch festgelegten chemischer Umwandlungen des CuS (Tab. 1) und sind in Übereinstimmung mit der in 5-geschildertem Kurzschluß-Stromverringung. In Abb. 1 ist die Spannungsvariation im Offenkreis (in relative Einheiten ausgedruckt) der Zelle mit Cu_2S-CdS, von der Wellenlänge abhängig represäntiert, worin: *1* — unmittelbar nach der Sonnenzellen Bildung ; *2* — nach Aussetzen in der Luft der Sonnenzelle für eine Zeitspanne von 1 Jahr.

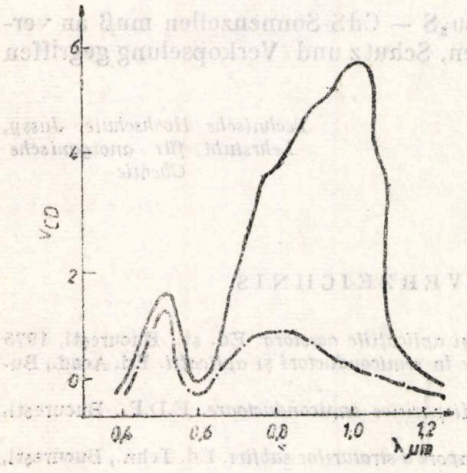

Abb. 1

Auf Grund der chemischen Analyse und aus dem IR-Absorbtionsspektrums der in gewöhnlicher Atmosphäre für 6 Monate, Zeitspanne ausgesetzten Cu_2S-CdS Schichten, wird, wie auch in [12], [13], die Anwesenheit einer $CuSO_4$ - Spuren, die eine Schutzschicht für Cu_2S gegen der Umweltwirkstoffe bilden, festgestellt.

Der Cu_2S Abbau hängt von der Herstellungsmethode, stärke Dichte, Porosität der Schicht, wie von der Temperatur und chemischen Zusammen-

setzung der Atmosphäre mit welcher die Sonnenzellenschicht im Kontakt kommt, ab.

Demzufolge sind die experimentelle Ergebniße, falls nicht alle Bedingungen konstant gehalten werden, sehr unterschiedlich.

In Arbeit [2] wird ein Studium hinsichtlich der Thermostabilität einiger Metallsulfide vorgelegt, unter welchem auch Cu_2S, CdS und ZnS, wo folgende Endreaktionsprodukte ersichtlich sind, wie : CuO, $CuSO_4$, CdO, $CdSO_4$, ZnO, $ZnSO_4$, SO_2. Als Zwischenproducte bilden sich Oxisälze der Typus $xMO.yMSO_4$. Die Reaktionsprodukte-Bildung hängt hauptsächlich von der Sauerstoff-Diffusion durch die feste Schicht und Temperatur ab, und sind mit den in dieser Arbeit geschilderten thermodynamischen Festlegungen und experimentellen Daten übereinstimmend.

3. Schlussfolgerungen

1. Aus den thermodynamischen Berechnungen und den experimentellen Daten geht hervor daß die Cu_2S, CdS und ZnS Dünnschichten sich im Kontakt mit der Athmosphäre und abhängig der umgebenden Temperatur zersetzen und demzufolge eine Leistungsverringerung der aus diesen Schichten hergestellten Sonnenzellen verursachen.

2. Der Abbau dieser Dünnschichten ist abhängig von der Herstellungsmethode, Stärke, Dichte und Porosität der Schicht, von der Athmosphärezusammensetzung, Haftung, Dichte der neuen Reaktionsprodukte, die echte Schutzschichten mit Störung der Sauerstoffdifusion werden können.

3. Es wurde festgestellt daß die Feuchtigkeitswirkung im Sonnenstrahl-Austellungsbedingungen der Zelle kräftiger wird.

4. Bei gewöhnlicher Temperatur wird nur Cu_2S praktisch merkbar abgebaut.

5. Zwecks Abbauverhütung der Cu_2S — CdS Sonnenzellen muß an verbesserte Dünnschichtherstellungsverfahren, Schutz und Verkopselung gegriffen werden.

Eingegangen am 6. Juni 1991

Technische Hochschule, Jassy, Lehrstuhl für anorganische Chemie

LITERATURVERZEICHNIS

1. Spînulescu I., *Fizica straturilor subţiri şi aplicaţiile acestora.* Ed. şt., Bucureşti, 1975
2. Dima I., Licea I., *Fenomene fotoelectrice în semiconductori şi aplicaţii.* Ed. Acad., Bucureşti, 1980.
3. Dima I., Munteanu I., *Materiale şi dispozitive semiconductoare.* E.D.P., Bucureşti, 1980.
4. Moroşanu E. C., *Depunerea chimică din vapori a straturilor subţiri.* Ed. Tehn., Bucureşti, 1981.
5. Spînulescu I., *Celule solare.* Ed. şt. şi encicl., Bucureşti, 1983.
6. Mimila A., Rev. Phys. Appl., **12**, 423 (1977).
7. Barnett M. A., Rothworth A., IEEE Trans., Electron Dev., **E-27**, 615 (1980).
8. Bath K. P., Solar Energy Materials, **1**, 215 (1979).
9. Nakayama N., Jap. J. Appl. Phys., **10**, 1 415 (1971).

10. Robertson J. M., Woods J., Proc. 2nd E. C. Photovoltaic Solar Energy Conference Berlin, April, 1979.
11. Shirland A. F., Advanced Energy Conversion, **6**, 201 (1966).
12. Roşca I., Nation. Symp. „Vorteil der Sonnen-Electroenergie, Jassy, Oct. 1982.
13. * * *, Patent USA *7 500 376* (1975).

STABILITATEA COMPUŞILOR Cu_2S, ZnS şi CdS FOLOSIŢI ÎN STRATUL SUBŢIRE AL CONVERTOARELOR SOLARE ŞI CONDIŢIILE DE OBŢINERE ŞI UTILIZARE A ACESTORA

(Rezumat)

Se prezintă rezultatele studiilor privind stabilitatea Cu_2S, ZnS, CdS, în condiţiile realizării şi utilizării straturilor subţiri în dispozitivele de conversie directă a energiei solare în energie electrică.

Din calculele termodinamice şi din datele experimentale rezultă că straturile subţiri formate din sulfurile respective se degradează în contact cu atmosfera în funcţie de temperatura la care sînt supuse determinînd scăderea randamentului celulelor fotovoltaice. Degradarea acestor straturi subţiri depinde de metoda de obţinere, grosimea, compactitatea şi porozitatea stratului, de aderenţa stratului pe suport, de peliculele de acoperire protectoare, de componentele atmosferei etc.

La temperatură obişnuită practic numai Cu_2S este sensibil degradat.

O mare importanţă au datele experimentale privind variaţia tensiunii în circuit deschis a celulei formate din Cu_2S—CdS în funcţie de lungimea de undă în variantele : imediat după formarea celulei şi după expunerea timp de un an.

BULETINUL INSTITUTULUI POLITEHNIC DIN IAŞI
Tomul XXXVII (XLI), Fasc. 1—4, 1991
Secţia II
CHIMIE ŞI INGINERIE CHIMICĂ

D.C. 541. 113547 279. 323

SOME THERMOCHEMICAL ASPECTS CONCERNING THE 4,4′-DICHLORODIPHENYLSULPHOXIDE SYNTHESIS

BY

N. AELENEI and ELENA BUTUC

1. Introduction

In the last years a large scale utilization of the aromatic polysulphones in the electronic, electrotechnic and medical technique industries is observed. These polysulphones are thermoplastic polymers having excellent electrical and mechanical properties, as well as a very good chemical and thermal stability [1], [2]. Among these polymers that obtained by the condensation of 4,4′-dichlorodiphenylsulphoxide with the sodium salt of 4,4′-dihydroxydiphenylpropan (biphenol *A*) is one of the most used polymers.

The synthesis of 4,4′-dichlorodiphenylsulphoxide monomer can be achieved by various methods, but the synthesis based on the reaction of monochlorobenzene with thionyl chloride in the presence of the anhydrous aluminium chloride is frequently used. This method is analogous with the synthesis of corresponding sulphone [3] ... [5], and the reaction mechanism can be represented by the following scheme :

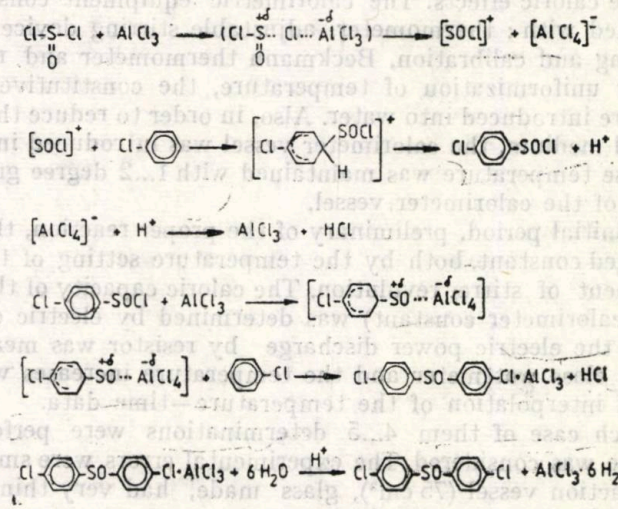

Under the catalytic action of $AlCl_3$ the cation $[SOCl]^+$ is generated and, by electrophyle substitution at monochlorobenzene, leads to formation of *p*-chlorobenzenesulphoxide. This forms an intermediary complex with aluminium chloride, and, by electrophyle substitution at monochlorobenzene, leads to a stable complex : 4,4′-dichlorodiphenylsulphoxide. $AlCl_3$. This is an enough slabe molecular combination so that the catalytic action of $AlCl_3$ is entirely destroyed by the inclusion of this into the complex.

In order to react the whole quantity of $SOCl_2$ at least an equimolecular proportion of $AlCl_3$ and $SOCl_2$ is necessary.

For separation of 4,4′-dichlorodiphenylsulphoxide, the sulphoxide complex is destroyed by water, this leading to an irreversible loss of the catalyst. To avoid the $Al(OH)_3$ formation which is not separable from 4,4′-dichlorodiphenylsulphoxide, the complex destruction is carried out in acidified water [6].

The monochlorobenzene is taken out in a great excess versus $SOCl_2$, it being a reaction medium at the same time.

At usual temperatures, the considered reactions occurs with an appreciable rate, so that for an optimal achievement, the caloric effects are necessary to be known. Since the total caloric effect is not dependent on the intermediary stages, it can take into consideration only the following two distinct reactions : the formation of the molecular compound and its destruction by the water :

$$(I) \qquad 2C_6H_5Cl + SOCl_2 + AlCl_3 \rightarrow Cl-C_6H_4-SOC_6H_4-Cl.AlCl_3 + 2HCl$$

$$(II) \quad ClC_6H_4-SO-C_6H_4-Cl.AlCl_3 + 6H_2O \xrightarrow{H^+} Cl-C_6H_4-SO-C_6H_4-Cl + AlCl_3 \cdot 6H_2O$$

This paper reports the experimental results related to the caloric effects for the two main stages considered.

2. Experimental

An adiabatic calorimeter with isothermal mantle was used in order to determine the caloric effects. The calorimetric equipment consist of a Dewar vessel provided with : thermometer, adjustable stirring device, electric resistor for heating and calibration, Beckmann thermometer and reaction vessel. For a better uniformization of temperature, the constitutive pieces of the calorimeter are introduced into water. Also, in order to reduce the heat echange with external medium, the calorimeter vessel was introduced into an air thermostat, whose temperature was maintained with 1...2 degree greater than the temperature of the calorimeter vessel.

In the initial period, preliminary of the proper reaction, the temperature was maintained constant, both by the temperature setting of thermostat and the adjustement of stirrer revolution. The caloric capacity of the calorimetric system (the calorimeter constant) was determined by electric calibration. For this purpose the electric power discharge by resistor was measured with an 0.2 precision class wattmeter and the temperature increases was determined by graphical interpolation of the temperature—time data.

For each case of them 4...5 determinations were performed and the average value was considered. The experimental errors were smaller than 1%.

The reaction vessel (75 cm^3), glass made, had very thin walls in order to obtain the most favourable heat transfer.

In order to determine the caloric effect of the reaction (I), $AlCl_3$ and the corresponding quantity of monochlorobenzene were introduced in the reaction vessel and a stationary thermal regime was achieved. After this stage the thionyl chloride was added. The temperature variation due to the reaction

(ΔT_R) was determined also by graphical interpolation of the temperature—time data. The caloric effect was calculed with relationship :

$$\Delta_R H = - \frac{\bar{K} \Delta T_R}{n}, \quad (1)$$

where : $\bar{K}$ is the mean value of the calorimeter constant ; ΔT_R — the temperature variation in the reaction vessel ; n — number of moles of $SOCl_2$ used in a given experiment.

In order to determine the caloric effect for the destruction of the sulphoxide $AlCl_3$ complex (reaction (II)), the experimental measurements were achieved in an analogous manner, introducing acidified water (3% HCl) in the reaction mixture obtained in the first stage and measuring the temperature increase in the calorimetric vessel. All the measurements were carried out at a 25° ± 0.5°C temperature.

The monochlorobenzene was dried on the $CaCl_2$ and distilled before use. After distillation the water content was determined by Carl-Fisher method, this being of 0.07%. The thionyl chloride, technical grade, was fresh distilled before use. The aluminium chloride has 99% purity.

3. Results and Discussions

3. 1. The Caloric Effect for the Formation Reaction of the 4,4'-Dichlorodiphenylsulphoxide. $AlCl_3$ Complex (Reaction I)

For the first stage of the reaction three series of measurements were performed, the quantity of $AlCl_3$ being modified for each run. The monochlorobenzene/thionyl chloride molar ratio was kept constant at the value of 6.75, while for $n(AlCl_3) / n(SOCl_2)$ ratio the 1.00, 1.25 and 1.53 values were taken. The quantity of $SOCl_2$ was of 0.01379 moles (1 cm³). The experimental results are presented in Table 1.

Table 1

The Caloric Effects for the Synthesis of $Cl-C_6H_4-SO-C_6H_4-Cl.AlCl_3$ *Complex, at 25°C*

No. Det.	Molar ratio $SOCl_2 : AlCl_3 : C_6H_5Cl$	$\bar{K}$ J/K	ΔT_R °C	$10^{-4} \times \Delta_R H$ J/mole
1	1 : 1.00 : 6.75	980.21	0.990	−7.042
2		972.07	1.000	−7.054
3		979.40	0.996	−7.079
4		977.23	0.991	−7.028
5	1 : 1.25 : 6.75	991.84	1.154	−8.306
6		990.40	1.158	−8.322
7		990.45	1.150	−8.266
8	1 : 1.53 : 6.75	984.68	1.162	−8.300
9		991.98	1.138	−8.193
10		993.39	1.150	−8.290

The results obtained in the first four measurements, in wich the equimolecular quantity of $AlCl_3$ and $SOCl_2$ were used, are very close, so that for this series of measurements the following mean value of the caloric effect can be considered :

$$\Delta_R H = -(7.051 \pm 0.019) \times 10^4, \quad [\text{J mole}^{-1}]. \tag{2}$$

In the case of the last six determinations (5...10), in which the experiments were performed with excess of $AlCl_3$, the caloric effect value is approximately 15% greater than in the first series of measurements and it is practical independent on the $AlCl_3$ excess. The mean value for these measurements is :

$$\Delta_R H(I) = -(8.280 \pm 0.042) \times 10^4, \quad [\text{J mole}^{-1}]. \tag{3}$$

The difference can be explained by the fact that $AlCl_3$ quantitative participates in reaction. In the measurements where equimolecular quantities of $AlCl_3$ and $SOCl_2$ were used a certain part of $SOCl_2$ remain unreactioned, probably due to an inactive part of $AlCl_3$. This behaviour of aluminium trichloride can be attributed either to the purity of reagent or by water traces from monochlorobenzene.

Therefore, taking into account the above mentioned aspects, only the mean value of the obtained results in the experiments (runs 5...10) can be admitted for the caloric effect of complex formation.

Another important aspect emphasized by the performed measurements is related to the reaction rate. This can be analysed on the basis of Fig. 1, where the time dependence of the temperature in the calorimeter vessel, for different $AlCl_3$: $SOCl_2$ molar ratios, was plotted. It can be noticed that reaction time decrease as the excess of $AlCl_3$ increases, so that for the ratio $n(AlCl_3) : n(SOCl_2) = 1.5$ the reaction is practically instantaneous.

3.2. The Caloric Effect for the Reaction (II)

For the second stage of 4,4'-dichlorodiphenysulphoxide synthesis the same molar ratios between reactants were considered as in the first stage. The decomposition of the complex was carried out with acidified water, using 20 cm^3 HCl solution (3%) for each cm^3 of $SOCl_2$ taken in the first stage of the reaction. The experimental results are presented in Table 2, where the caloric effect

Table 2

The Caloric Effect for the Destruction of the $Cl-C_6H_4-C_6H_4-Cl.AlCl_3$ *Complex with Water, at 25°C*

No. Det.	Molar ratio $SOCl_2 : AlCl_3 : C_6H_5Cl$	$\overline{K}$ J/K	$10^{-5} \times \Delta_R H(II)$ J/mole $SOCl_2$	$10^{-5} \times \Delta_R H(II)$ J/mole $SOCl_2$	$10^{-5} \times \Delta_R H$ J/mole $AlCl_3$
1	1 : 1.00 : 6.75	1 018.93	−2.675		−2.675
2		1 016.76	−2.684		−2.684
3		1 063.00	−2.673	−2.677	−2.673
4		1 060.83	−2.676		−2.676
5	1 : 1.25 : 6.75	1 031.38	−3.279		−2.637
6		1 056.98	−3.257	−3.274	−2.606
7		1 076.31	−3.268		−2.614
8	1 : 1.53 : 6.75	1 068.28	−4.055		−2.650
9		1 075.58	−4.004	−4.027	−2.617
10		1 076.99	−4.023		−2.629

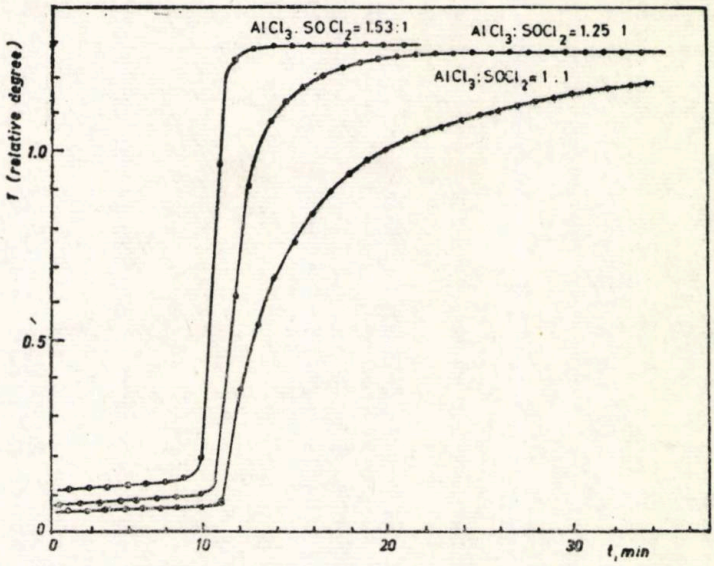

Fig. 1.—Time dependence of the temperature in the calorimeter vessel for different $AlCl_3/SOCl_2$ molar ratios.

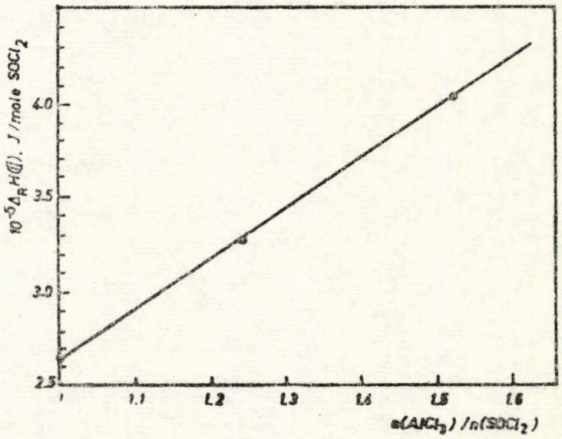

Fig. 2. — Variation of the caloric effect for the destruction process of the monomer. $AlCl_3$ complex versus the $AlCl_3/SOCl_2$ molar ratio.

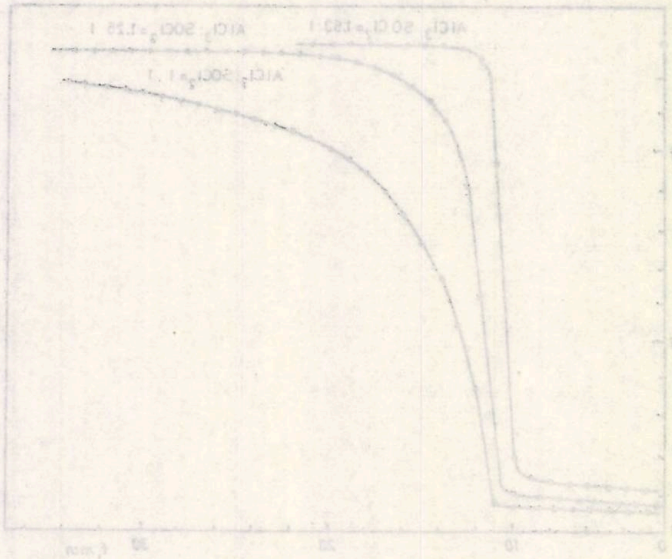

Fig. 1. — Time dependence of the temperature in the calorimeter vessel for different $AlCl_3/SOCl_2$ molar ratios.

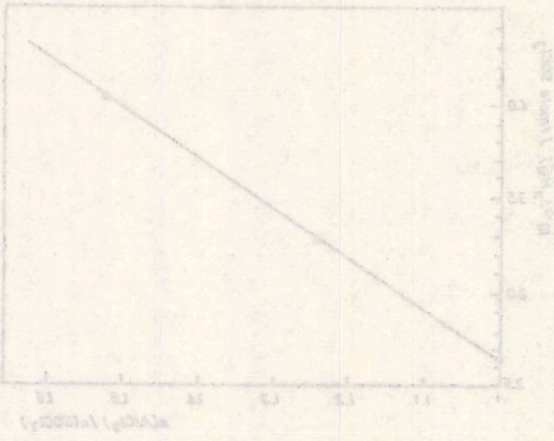

Fig. 2. — Variation of the caloric effect for the destruction process of the monomer, $AlCl_4^-$ complex versus the $AlCl_3/SOCl_2$ molar ratio.

values were calculated both, in relation to the $SOCl_2$ quantity used in the first stage (column 4 and 5) and in relation to the $AlCl_3$ quantity (column 6).

As it is expected, the total caloric effect for the second stage of the reaction considerable varies with the $AlCl_3/SOCl_2$ molar ratio, because the $AlCl_3$ excess reacts with water simultaneously with the complex destruction. The data from Fig. 2 indicate a linear dependence between the caloric effect and $AlCl_2/SOCl_2$ molar ratio.

When the caloric effect is calculated in relation to the $AlCl_3$ quantity it is practical independent on $AlCl_3/SOCl_2$ molar ratio, the mean value being:

$$\Delta_R H(II) = -(2.646 \pm 0.028) \times 10^5, \quad [J/\text{mole } AlCl_3]. \tag{4}$$

This value is with 2.8% smaller than the caloric effect for the hydration of $AlCl_3$:

$$AlCl_3 + 6H_2O = AlCl_3 \cdot 6H_2O. \tag{III}$$

The caloric effect for this reaction was calculated on the basis of the standard enthalpies of formation [7] and it is:

$$\Delta_R H(III) = -2.722 \times 10^5, \quad [J/\text{mole } AlCl_3].$$

The very small difference between the caloric effect of complex destruction reaction and the caloric effect of $AlCl_3$ hydration (about 7.6 KJ/mole) points out the fact that the delay energy of $AlCl_3$ into complex is small but enough to cancel the catalytic action of $AlCl_3$.

4. Conclusions

1. An adiabatic calorimeter with isothermal mantle was used for the determination of caloric effects for synthesis of 4,4'-dichlorodiphenysulphoxide monomer.

2. The process of monomer synthesis was achieved in two stages: (I) — the reaction between monochlorobenzene and thionyl chloride in the presence of anhydrous $AlCl_3$, obtaining a molecular complex and (II) — the destruction of formed complex by the acidified water. The caloric effects for the two stages are given by (3), respectively (4).

3. The caloric effect of the complex destruction process is only with 2.8% smaller than that of the $AlCl_3$ hydration process, this indicating a reduced stability of 4,4'-dichlorodiphenylsulphoxide.$AlCl_3$ complex.

Received, February 18, 1991

Polytechnic Institute, Jassy,
Department of Physical Chemistry
and
Macromolecular Chemistry
Institute „P. Poni",
Iași

REFERENCES

1. Johnson R.N., *Polysulphones.* In *Encyclopedia of Polymer Science and Technology.* Vol. **11**, Interscience Publ., John Wiley & Sons Inc., Ed. Bicales N. M., New York, 1969, 447.

2. Othwer K., *Encyclopedia of Chemical Technology*. Vol. **18**, John Wiley & Sons Inc., New York, 1982, 832.
3. МироновГ. С, ВетроваВ. В., ФарберовМ. И., ЖПХ, **43**, *12*, 2967 (1970).
4. * * * England Pat., *926 291* (1963).
5. * * * France Pat., *1 456 314* (1966).
6. Nenițescu C. D., *Chimie generală*. Editura Tehnică, București, 1963, 633.
7. Nenițescu C. D., Ioan V., *Manualul inginerului chimist*. Vol. II, Editura Tehnică, București, 1952.

UNELE ASPECTE TERMOCHIMICE ALE REACȚIEI DE OBȚINERE A MONOMERULUI 4,4'-DICLORDIFENILSULFOXID

(Rezumat)

Efectele calorice ale reacțiilor implicate în sinteza monomerului 4,4'-diclordifenilsulfoxid s-au determinat experimental cu ajutorul unui calorimetru adiabatic cu manta izotermă. Procesul chimic s-a realizat în două etape : obținerea combinației moleculare monomer. $AlCl_3$ ($Cl-C_6H_4-SO-C_6H_4-Cl.AlCl_3$), prin reacția dintre monoclorbenzen și clorură de tionil în prezență de $AlCl_3$ anhidră și distrucția complexului format cu apă acidulată. Pentru efectele calorice de reacție în cele două etape s-au găsit valorile date de (3) și respectiv (4).

BULETINUL INSTITUTULUI POLITEHNIC DIN IAŞI
Tomul XXXVII (XLI), Fasc. 1—4, 1991
Secţia II
CHIMIE ŞI INGINERIE CHIMICĂ

D.K. 544.17 ; 678. 746. 22 — 136. 22 ; 547, 315. 2

KINETISCHES STUDIUM DER ANIONEN-KOPOLYMERISATION DES ε-KAPROLAKTAM MITS ISOPREN

VON

N. HURDUC und NATALIA HURDUC

1. Einleitung

Vorherig wurde die Möglichkeit der Herstellung von Kopolymeren aufgrund des ε-Kaprolaktams und des Isoprens, durch anionisch eingeleitete Massenpolymerisation mit metallischem Natrium [1], [2], erwähnt. Jedoch, bis jetzt, kann man nicht präzisieren, ob die erhaltenen Produkte Block- oder Statistik-Kopolymere sind, ihre Struktur beanstandet nachträgliche Untersuchungen. Was den Mechanismus anbelangt, nimmt man an, daß die Polymerisation mittels einiger Verbindungen vom Typ Chelat, die sich zwischen dem katalytischen System und dem Isopren bilden [3], verläuft.

Die vorliegende Arbeit verfolgt die Durchführung eines kinetischen Studiums des Verfahrens der Kopolymerisation des ε-Kaprolaktams mit Isopren, zwecks Erläuterung des Mechanismus dieser Reaktion.

Zur Berechnung der Ausbeute und zum Aufzeichnen der entsprechenden Kurven wurde ein unkonventionelles Verfahren angewendet und zwar die thermodifferentiale Analyse. Dieses war möglich, da die Differenz zwischen den Zerfallstemperaturen des Monomers und des Polymers größer als 200°C ist.

2. Experimenteller Teil

Das ε-Kaprolaktam wurde aus Benzol rekristallisiert, getrocknet und im Vakuum aufbewahrt. Das metallische Natrium und das Toluylendiisozyanat wurden nicht zusätzlich gereinigt, die Reagenzien stammten von den Firmen Riedel de Haën AG bzw. Aldrich. Das Isopren wurde nach der Destillation auf Molekularsieben getrocknet.

Die Synthesen wurden identisch, mit jenen aus [1], durchgeführt.

Nach der Synthese wurden die Proben plötzlich in einem Gemisch Wasser —Eis gekühlt.

Zur Berechnung der Ausbeute entnahm man dann Proben, die der thermodifferentialen Analyse unterworfen wurden.

Die thermodifferentiale Analyse wurde auf einem Apparat vom Typ MOM Budapest, in Platintiegeln, unter normalen Luftverhältnissen und mit einer Heizgeschwindigkeit von 12°C/Min, durchgeführt. Es wurde bis auf 600°C

geheizt und als Referenzsubstanz wurde bei 1 000°C kalziniertes Aluminiumoxyd verwendet.

3. Ergebnisse und Diskussion

Wie aus Abb. 1 ersichtlich ist, weist das Derivatogramm des ε-Kaprolaktams das Zerfallsmaximum bei 240°C auf. Gleichzeitig mit der Bildung des Polymers treten entsprechende Zerfallsmaxima bei 240°C und 400°C auf (Abb. 2); das Maximum bei 400°C ist charakteristisch für den Zerfall des Polymers.

Allmählich, je weiter die Reaktion fortschreitet, bemerkt man die Verminderung des ersten und die Betonung des zweiten, dem Polymer entsprechenden Maximum.

Die Korrelation der DTG- und TG-Kurven hat die Berechnung des Umwandlungsgrades erlaubt.

Das kinetische Studium wurde bei drei Temperaturen und zwar bei 185°C, 190°C und 195°C durchgeführt.

Die Bearbeitung der thermogravimetrischen Daten hat die Aufzeichnung der kinetischen Kurven Umformung—Zeit (Abb. 3) erlaubt.

Im Vergleich zu der schneller verlaufenden Homopolymerisationsreaktion des ε-Kaprolaktams, bei der die Umwandlungsmaxima nach 5...10 Min. erreicht werden [4], verlauft diese Kopolymerisationsreaktion langsamer, die Umwandlungsmaxima werden nach 35... 40 Min. erreicht. Bei der Temperatur von 185°C wird sogar eine Induktionsperiode der Reaktion beobachtet.

Um die Reaktionsordnung zu bestimmen, wurde die differentialgraphische Methode angewandt, die zur Geraden aus Abb. 4 führte.

Somit wurde die Reaktionsordnung von 1,6 erhalten, ein Wert, der die Komplexität des Reaktionsmechanismus andeutet.

Die Geschwindigkeitskonstanten wurden mittels der integralen graphischen Methode berechnet. Die für die drei Temperaturen erhaltenen Geraden sind in Abb. 5 dargestellt.

Das Arrhenius-Diagramm aus Abb. 6 hat die Berechnung der Aktivierungsenergie erlaubt, die zu einem Wert von 71,01 KJ/mol führte.

Tabelle 1

Kinetische Parameter der Anionen-Kopolymerisation des ε-Kaprolaktams mit Isopren

Arbeitsemperatur, [°C]	n	k $mol^{-0,6}l^{-0,6}s^{-1}$	E KJ/mol	A
185	1,6	0,180	71,01	$3,54.10^7$
190	1,6	0,275	71,01	$3,54.10^7$
195	1,6	0,393	71,01	$3,54.10^7$

Die bewerteten kinetischen Parameter sind aus Tabelle 1 ersichtlich.

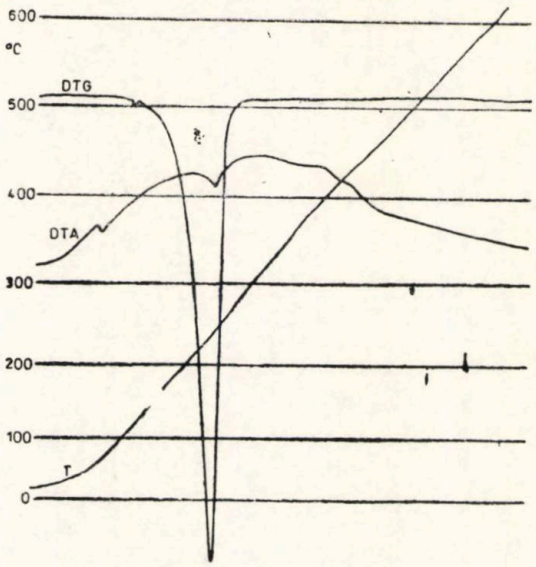

Abb. 1. — Derivatogramm des ε-Kaprolaktams.

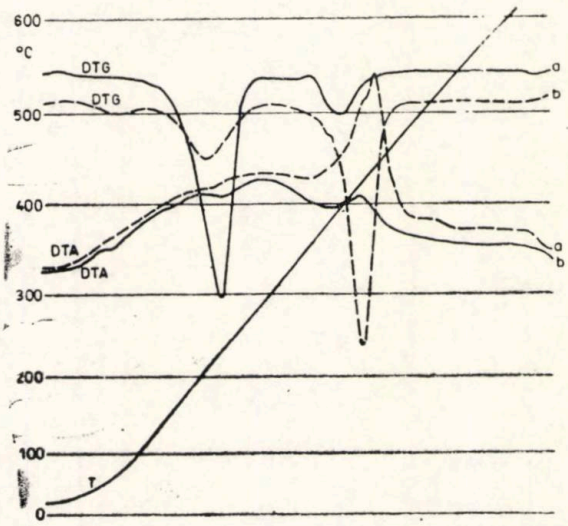

Abb. 2. — Derivatogramme der Polymere mit verschiedenen Umwandlungsgraden: *a* — nach 20 Min.; *b* — nach 40 Min.

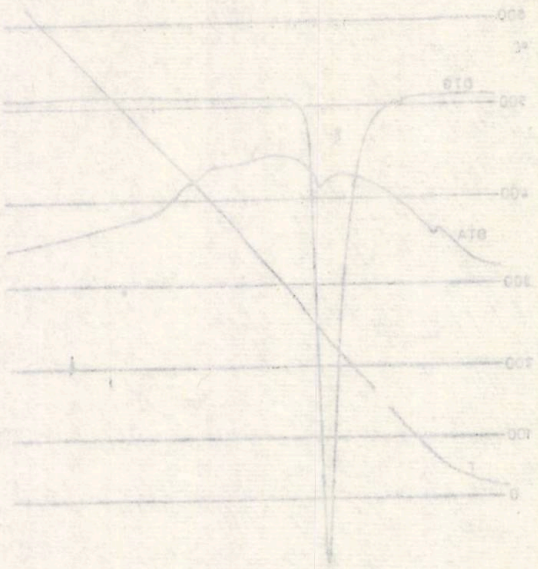

Abb. 1. — Derivatogramm des e-Kaprolaktams.

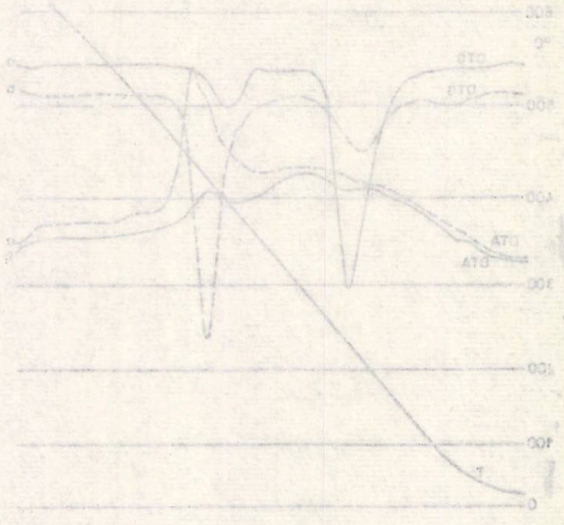

Abb. 2. — Derivatogramme der Polymere mit verschiedenen Umwandlungsgraden: a – nach 20 Min.; b – nach 40 Min.

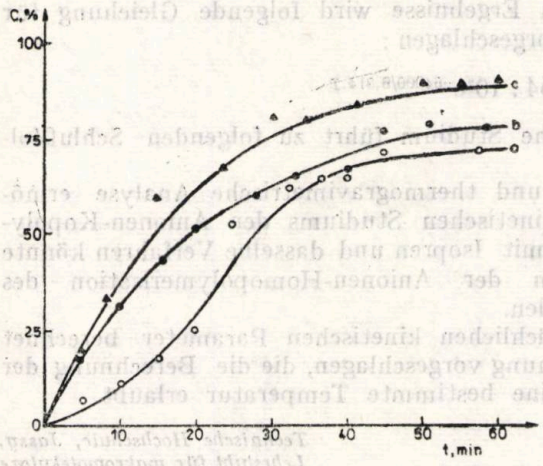

Abb. 3.—Die Kurven Umformung — Zeit entsprechend der Kopolymerisation des ε-Kaprolaktams mit Isopren bei: *a* — 185°C; *b* — 190°C; *c* — 195°C.

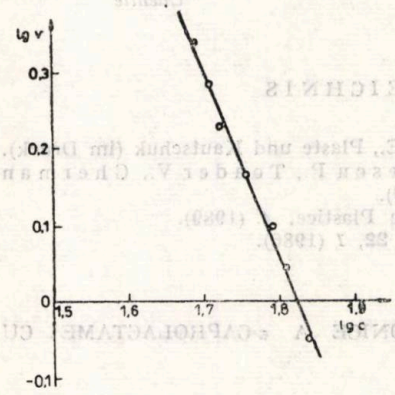

Abb. 4.—Die graphische Darstellung lg *v* in Abhängigkeit von lg *c* für die Synthesetemperatur von 190°C.

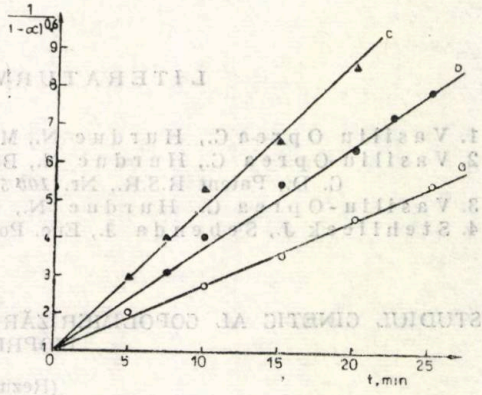

Abb. 5 — Die graphische Darstellung $1/(1-\alpha)^{0,6}$ in Abhängigkeit von der Zeit für die Synthesetemperaturen von: *a* — 185°C; *b* — 190°C; *c* — 195°C.

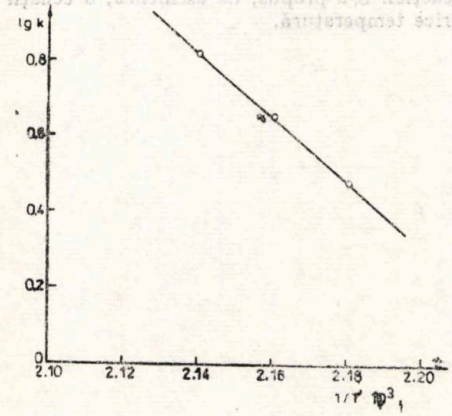

Abb. 6.—Das Arrhenius Diagramm.

Aufgrund der dargestellten Ergebnisse wird folgende Gleichung für die Geschwindigkeitskonstante vorgeschlagen :

$$k=3{,}54 \cdot 10^{7} e^{-64000/8{,}314\,T}$$

Das durchgeführte kinetische Studium führt zu folgenden Schlußfolgerungen :

1. Die thermodifferentiale und thermogravimetrische Analyse ermöglicht die Durchführung eines kinetischen Studiums der Anionen-Kopolymerisation des ε-Kaprolaktams mit Isopren und dasselbe Verfahren könnte auch zum kinetischen Studium der Anionen-Homopolymerisation des ε-Kaprolaktams verwendet werden.

2. Es wurden die hauptsächlichen kinetischen Parameter berechnet und es wurde die kinetische Gleichung vorgeschlagen, die die Berechnung der Geschwindigkeitskonstante für eine bestimmte Temperatur erlaubt.

Eingegangen am 17. Mai 1990

Technische Hochschule, Jassy,
Lehrstuhl für makromolekulare Chemie

LITERATURVERZEICHNIS

1. Vasiliu Oprea C., Hurduc N., Moisii E., Plaste und Kautschuk (im Druck).
2. Vasiliu-Oprea C., Hurduc N., Bîrsănescu P., Toader V., Gherman C. D., Patent R.S.R., Nr. *100 579* (1990).
3. Vasiliu-Oprea C., Hurduc N., Materiale Plastice, *4* (1989).
4. Stehlicek J., Sebenda J., Enc. Polym. J., **22**, *1* (1986).

STUDIUL CINETIC AL COPOLIMERIZĂRII ANIONICE A ε-CAPROLACTAMEI CU IZOPRENUL

(Rezumat)

Se prezintă rezultatele unui studiu cinetic al reacţiei de copolimerizare anionică a ε-caprolactamei cu izoprenul, calculele de conversie fiind efectuate prin analiză termică diferenţială. Acest studiu a permis calcularea ordinului de reacţie, a constantelor de viteză pentru diverse temperaturi, precum şi a energiei de activare a reacţiei. S-a propus, de asemenea, o ecuaţie care permite calcularea constantelor de viteză la orice temperatură.

BULETINUL INSTITUTULUI POLITEHNIC DIN IAȘI
Tomul XXXVII (XLI), Fasc. 1—4, 1991
Secția II
CHIMIE ȘI INGINERIE CHIMICĂ

D.C. 547. 538,241 ; 54.07 ; 66.095.2

CONTRIBUTIONS TO THE SYNTHESIS AND POLYMERIZATION OF SOME *p*-SUBSTITUTED PHENYLACETYLENES

BY

I. MAZILU, I. COCÎRLĂ, LUCIA TĂTARU, M. VÂȚĂ, D. SCUTARU and TATIANA LIXANDRU

1. Introduction

The substituents'influence on the polymerization of phenylacetylene monomers, as well as on the properties of the obtained polymers, has been studied, establishing the extent to which the electronic effects of the *p*-substituent do modify the monomer's reactivity and the properties of the products [1], [2].

The present paper deals with the synthesis and characterization of *p*-methoxy and *p*-ethoxy substituted phenylacetylene, the radicalic polymerization of these two new acetylenic monomers, along with the characterization of the products obtained in the reaction of polymerization.

The substituent's effect on the phenylacetylene rest has been analyzed by applying HMO method, i.e., by calculating the charge distribution, the bond orders, the indices of free valency, the resonance energy and the copolymerization constants.

2. Experimental

Monomers of the $X-C_6H_4-C\equiv CH$ type, $X=-OCH_3$, $-OC_2H_5$, have been synthesized from the corresponding chloroformilated vinylic derivatives, by heating in the presence of alkalies [3]...[5].

The reaction of radicalic polymerization has been performed in sealed glass vials, under argon atmosphere. Both insoluble and soluble fractions have been obtained in usual organic solvents. Purification of the soluble fractions has been performed through dissolution in benzene, filtration and precipitation with acidified methylic alcohol, while the insoluble fractions have been purified by repeated washings with solvent, for removing the monomer traces.

IR spectra were recorded, in KBr tablets, on a UR-20 Carl-Zeiss, Jena, spectrophotometer.

The thermal behaviour of monomers and polymers was established from the thermograms recorded on a MOM-type derivatograph, Budapest, J. Paulik, F. Paulik, L. Erdey.

The monomer's reactivity has been estimated by the HMO method.

3. Results and Discussion

3.1. Structure and Reactivity of Monomers

p-Substituted phenylacetylene monomers have been characterized by elemental analyses, IR spectra and thermogravimetry, the obtained experimental results agreeing with the calculated values.

In the IR spectra of both monomers are present bands characteristic for the benzenic nucleus (ν_{C-C}=1 610 cm^{-1}, ν_{C-H}=2 930, 2 970 cm^{-1}) and for the triple bond ($\nu_{C\equiv C}$=2 115 cm^{-1} and $\nu_{=C-H}$=3 300 cm^{-1}), while, at 1 275 cm^{-1} correspond the band characteristic for the etheric bond.

Thermogravimetric analysis has evidenced a good thermal stability for both monomers, up to 100°...110°C, when degradation occurs gradually, between 600°...650°C the monomers being completely decomposed.

The substituent's influence on the monomer's reactivity was established by molecular orbitals calculations in Hückel approximation, on employing — according to literature indications — the h_x and k_{C-X} parameters [6],...,[8].

Table 1 presents the molecular characteristics of the two monomers in comparison with literature data concerning other *p*-substituted acetylene derivatives.

Table 1

Molecular Characteristics of p-Substituted Phenylacetylene Monomers

No.	Monomer	Resonance energy (β)	F_1	P_{1-2}	Ref.
1.	Phenyl-acetylene	2.4242	0.6176	0.9334	[9]
2.	*p*-Ferrocenylphenyl-acetylene	4.3257	0.6232	0.9336	[9]
3.	*p*-Methoxyphenyl-acetylene	4.6425	0.6431	0.9352	
4.	*p*-Ethoxyphenyl-acetylene	4.6513	0.6436	0.9354	
5.	*p*-Chlorphenyl-acetylene	—	—	0.9318	[2]

F — index of free valency ; P — order of electronic π bond.

Taking into consideration the resonance energy for phenyl-acetylene and its *p*-substituted derivatives, it is to be observed that the substituents contribute to the increasing of the monomer's stability.

Calculation of the copolymerization constants was performed with the following relation :

$$-RT\ln K=(\Delta E_{rs})^1-(\Delta E_{rs})^2,$$

where $(\Delta E_{rs})^1$, $(\Delta E_{rs})^2$ represent the energies of stabilization through resonance of the transitions between the radical and its monomer and, respectively, between the same radical and comonomer [10] ; the (ΔE_{rs}) values

have been calculated according to the indications given in literature [11], being expressed in $-(\Delta\beta)^2/\beta$ units. In the expression of $(\Delta E_{r,s})$, indices r and s refer to the monomer's atom and, respectively, to the radical's atom, participating in the transition state.

The constants involved in the copolymerization of *p*-ferrocenyl-phenylacetylene (Table 2 *a*) and of *p*-methoxyphenylacetylene (Table 2 *b*) with phenylacetylene have been calculated, too.

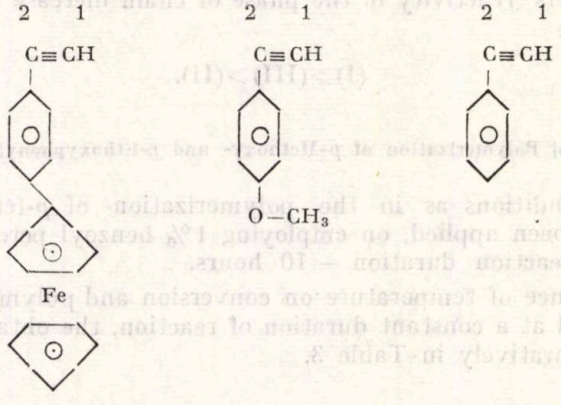

(I) (II) (III)

Monomers (I), (II) and (III) participate in the transition state with atom 1, the index of free valency, F, being maximum for this position, while the radicals are involved by the carbon atom 2.

Table 2 lists the values of copolymerization constants, r, calculated at 200°C (473°K).

Table 2

Copolymerization Constants of the Acetylene Monomers I, II and III

Macroradical		Monomer	E_{rs} $-(\Delta\beta)^2/\beta$	Difference $\Delta(\Delta E_{rs})$ $-(\Delta\beta)^2/\beta$	Calc. r
a	I	I	0.7978	+0.2260	2.30
	I	III	0.5718		
	III	III	0.6650	−0.0125	0.95
	III	I	0.6775		
b	II	II	0.5992	−0.0252	0.91
	II	III	0.6244		
	III	III	0.6650	+0.0533	1.21
	III	II	0.6117		

In both cases, regardless of the proportion in which the two monomers are employed, the copolymer will be enriched in *p*-ferrocenyl-phenylacetylene (*a*) and in phenylacetylene (*b*) ; finally, (II) and (III) remainder monomers will homopolymerize [12].

Analysis of the relative activities values, *r*, evidences that macroradical (I) links more quickly its own monomer ; in copolymerization (II)—(III), macroradical (III) reacts more rapidly with the same monomer. The conclusion to be drawn, from an energetic viewpoint, is that such processes are favourized and the monomers' reactivity in the phase of chain increase decreases in the following order :

$$(I) > (III) > (II).$$

3.2. Radical Polymerization of *p*-Methoxy- and *p*-Ethoxyphenyl-acetylene

Similar conditions as in the polymerization of *p*-ferrocenyl-phenylacetylene have been applied, on employing 1% benzoyl peroxide (B. P.) as initiator ; the reaction duration — 10 hours.

The influence of temperature on conversion and polymerization degree has been studied at a constant duration of reaction, the obtained data being presented comparatively in Table 3.

Table 3

Radicalic Polymerization of some p-Substituted Phenylacetylene Monomers, BP Initiator (1%), for a Reaction Time of 10 Hours

Monomer	Initiator	Temp. °C	Conv. %	M.p. °C	$\bar{p}^{a)}$	Ref.
p-Ferrocenylphenyl-acetylene	BP	140	16.00	350		[9]
	BP	200	19.90	350		
	BP	230	32.50	350		
	Thermic	200	63.50	350		
p-Methoxyphenyl-acetylene	BP	140	9.50$^{b)}$	160	5	
	BP	200	7.50$^{b)}$	162	7	
			10.00	210		
	BP	230	28.50	220		
	Thermic	200	57.20	220		
p-Ethoxyphenyl-acetylene	BP	140	8.00$^{b)}$		5	
	BP	200	6.00$^{b)}$		7	
			9.50	165		
	BP	230	25.00	220		
	Thermic	200	55.50	225		

a) osmometric method ; *b*) soluble fraction.

Data listed in Table 3 evidence that, for the same reaction time, conversion increases with temperature. At the same temperature and reaction

time, conversion deareases in the series : *p*-ferrocenyl-phenylacetylene > *p*-methoxyphenylacetylene > *p*-ethoxyphenylacetylene, which agrees with the calculated scale of monomer reactivity. The fact that at 200°C, in the absence of initiator, much higher conversions are obtained than in its presence, evidences that the initiator favours the formation of higher amounts of soluble oligomers, which are removed with ethylic ether.

3.3. Molecular Structure of Polymers

The structure of the products obtained by radicalic polymerization of *p*-methoxy- and *p*-ethoxyphenylacetylene has been estimated from data of elemental analysis, IR spectra and thermogravimetry.

A good agreement between the calculated values and the experimental data supplied by elemental analysis has to be mentioned.

The spectra of all products, synthesized at various temperatures, are identical, which leads to the conclusion that this element has no influence upon structure.

Fig. 1 plots graphically the IR spectra of *p*-methoxyphenylacetylene (*a*) and poly-*p*-methoxyphenylacetylene (*b*) obtained at 200°C as soluble fraction.

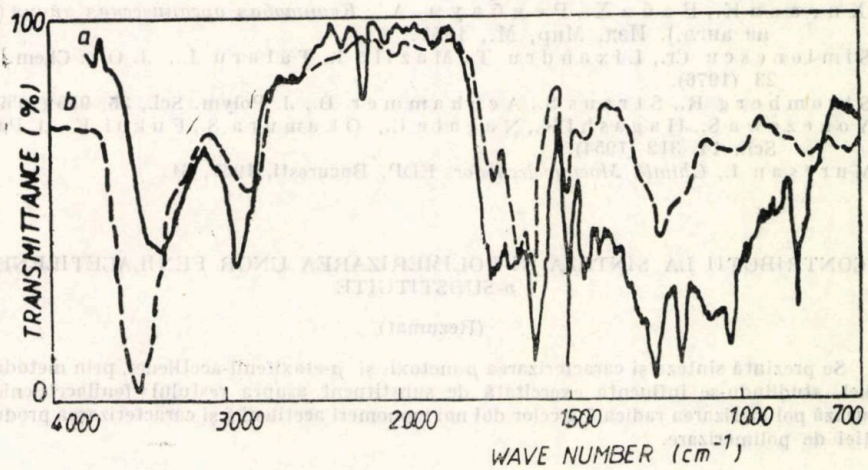

Fig. 1

Generally, the polymer's IR spectrum evidences all the absorption bands characteristic to the monomer, yet of a lower intensity. Thus, the valency vibrations for the aromatic nucleus at 1 610 cm^{-1} (λ_{C-C}) and ν_{C-O-C} at 1 275 cm^{-1} are maintained, simultaneously with the disappearance of the bands characteristic for the triple bond ; absorptions of the olephinic bond are superposed on those of the aromatic nucleus.

The polymers' thermal stability has been estimated from the data supplied by thermogravimetric analysis, which evidences a two step decomposition. Both poly-*p*-methoxyphenylacetylene and poly-*p*-ethoxyphenylacetylene

are thermally stable up to 180°C ; within the 180°..350°C interval, a slow weight loss occurs, followed by a rapid decomposition rate, so that at 600°C destruction is almost complete.

Received, February 2, 1991

Polytechnic Institute, Jassy,
Department of Organic Chemistry

REFERENCES

1. Simionescu Cr., Dumitrescu Sv., Lixandru T., Dăringă M., Simionescu B., Vâţă M., Eur. Polym. J., **8**, 719 (1972).
2. Симионеску К., Думитреску С., Ликсандру Т., Дэрынгэ М., Симионеску Б., Выцэ М., Сахини И., Вейнберг Ж. Высокомол. Соед., **XVI** (**A**), *7*, 1464 (1974).
3. Simionescu Cr., Lixandru T., Mazilu I., Tătaru L., Makromol. Chem., **147**, 69 (1971).
4. Simionescu Cr., Păstrăvanu M., Bull. Acad. Pol. Sci., Ser. Sci. Chem., **9**, 523 (1971).
5. Simionescu Cr., Lixandru T., Mazilu I., Tătaru L., Ghirvu C., Chem. Zvesti, **28**, 810 (1974).
6. Purcell P., Singel J., J. Chem. and Eng. Data, **12**, 235 (1967).
7. Стрейтвизер Э., *Теория молекулярных орбит для химиков—органиков*, (пер. из англ.). Изд. Мир, М., 1965.
8. Хигаси К., Баба Х., Рембаум А., *Квантобая органическая химия* (пер. из англ.). Изд. Мир, М., 1967.
9. Simionescu Cr., Lixandru T., Mazilu I., Tătaru L., J. Org. Chem., **113**, 23 (1976).
10. Stromberg R., Straus S., Achhammer B., J. Polym. Sci., **35**, 955 (1959).
11. Yonezowa S., Hagashi K., Nagata C., Okamura S., Fukui K., J. Polym. Sci., **14**, 312 (1954).
12. Mureşan I., *Chimia Macromoleculelor*. EDP, Bucureşti, 1967, 61.

CONTRIBUŢII LA SINTEZA ŞI POLIMERIZAREA UNOR FENILACETILENE *p*-SUBSTITUITE

(Rezumat)

Se prezintă sinteza şi caracterizarea *p*-metoxi- şi *p*-etoxifenil-acetilenei, prin metoda OM Hückel, studiindu-se influenţa exercitată de substituent asupra restului fenilacetilenic. Se abordează polimerizarea radicală a celor doi noi monomeri acetilenici şi caracterizarea produşilor reacţiei de polimerizare.

BULETINUL INSTITUTULUI POLITEHNIC DIN IAȘI
Tomul XXXVII (XLI), Fasc. 1—4, 1991
Secția II
CHIMIE ȘI INGINERIE CHIMICĂ

D.C. 54.07 ; 616.717.5 ; 621.1.016.7

NEW THERMODYNAMIC MODEL OF THE UREA SYNTHESIS PROCESS

BY

ILIE SIMINICEANU and CORNELIU PETRILĂ

1. Introduction

Having major applications in agriculture as well as in industry, urea is produced in very large quantities. The world's production capacity was about 10^8 tons (44×10^6 tons N) in 1989 [1]. The existing commercial processes are all based on the urea synthesis from ammonia and carbon dioxide. Although the urea production capacity has been dramatically increased in the last three decades, the theoretical bases of the urea synthesis process are not yet clearly defined. This because the urea synthesis is one of the most difficult chemical processes.

It is difficult, firstly, because of its complex stoichiometry implying the main reactions in the liquid phase:

(1) $CO_2 + 2NH_3 = NH_2COONH_4$, (2) $NH_2COONH_4 = (NH_2)_2CO + H_2O$,

the phase changes:

(3) $CO_{2(l)} = CO_{2(g)}$, (4) $NH_{3(l)} = NH_{3(g)}$, (5) $H_2O_{(l)} = H_2O_{(g)}$,

as well as the side transformations:

6) $2(NH_2)_2CO = NH_3 + NH(CONH_2)_2$, (7) $(NH_2)_2CO = HNCO + NH_3$,

(8) $(NH_2)_2CO_{(l)} = (NH_2)_2CO_{(g)}$.

Secondly, the operating conditions are rather severe: pressure of 14 to 20.0 MPa, temperature of 453 to 473 K, and high concentration („melt"). As a result, both liquid and vapour phases deviate from ideality.

In addition, the urea synthesis system has some peculiar properties: azeotropic points, extremal shape of the equilibrium conversion as a function of temperature, extremal dependance of equilibrium pressure on the excess of ammonia.

Last, but not least, is the impossibility of direct determination of the actual liquid—phase composition at equilibrium. Being measurable only urea, water, ammonia and a „total" carbon dioxide, the following global reaction is usually considered:

(9) $CO_2 + 2NH_3 = (NH_2)_2CO + H_2O$.

The equation (9) could be regarded as the sum of (1) and (2) when the reaction (2) could be considered complete. Practically, the dehydration reaction (2) does not go to completion (the conversion per pass of the carbamate into urea usually varies from 60 to 75 per cent) and the unconverted carbamate must be decomposed and recycled to the synthesis. Consequently, the equation (9) does not describe the process correctly.

2. Previous Work

The first method for the equilibrium liquid—phase composition determination of the urea system has been proposed by F r é j a c q u e s. By defining an euquilibrium constant of the reaction (9):

$$K_x = \frac{x_U x_{H_2O}}{x_{CO_2} x_{NH_3}^2}, \tag{10}$$

wherein the molar fractions of the „fictitious" components are substituted as functions of the carbon dioxide conversion degree [4],

$$x_{CO_2} = \frac{1-\eta_{CO_2}}{1+a+b-\eta_{CO_2}}, \quad x_{NH_3} = \frac{a-2\eta_{CO_2}}{1+a+b-\eta_{CO_2}},$$
$$X_U = \frac{\eta_{CO_2}}{1+a+b-\eta_{CO_2}}, \quad X_{H_2O} = \frac{b+\eta_{CO_2}}{1+a+b-\eta_{CO_2}}, \tag{11}$$

results:

$$K_x = \frac{\eta_{CO_2}(b+\eta_{CO_2})(1+a+b-\eta_{CO_2})}{(1-\eta_{CO_2})(a-2\eta_{CO_2})^2}, \tag{12}$$

where a and b are the input molar ratios:

$$a = \frac{n^0_{NH_3}}{n^0_{CO_2}}, \quad b = \frac{n^0_{H_2O}}{n^0_{CO_2}}. \tag{13}$$

Using the experimental values of K_x, F r é j a c q u e s has prepared a nomograph, based on the equation (12) [5]. This nomograph provides a means of evaluating the equilibrium yield of urea when the operating temperature and the feed molar ratios of reactants are known. But the theoretical yield obtained from this nomograph is always less than the actual yield calculated from industrial-scale data [4]. That is why, although improved by other authors [6], [7], the semiempirical method of F r é j a c q u e s is not recommended today.

Another semiempirical method consists of the direct correlation of the equilibrium experimental data by regression [8], [10], [11]. The most important empirical equations are presented below.

K u c h e r y a v y i [8], using experimental data very similar to those of K a w a s u m i [9], has obtained the equation:

$$\eta_{CO_2} = 0.3428a - 0.0177a^2 - 0.293b + 0.03699ab - 0.7428\times10^{-3}at + \\ + 0.9129\times10^{2}t - 0.53\times10^{-7}t^3 + 0.2293\times10^{-4}P - 1.121, \tag{14}$$

valid in the following ranges of parameters: $a=2.0 \ldots 6.0$, $b=0.0 \ldots 1.6$, $t=170° \ldots 230°C$, $P=100 \ldots 1.000$ atm.

I n o u e, K a n a i and O t s u k a [10] have proposed another regression equation based on their own experimental data:

$$\eta_{CO_2} = 0.2616a - 0.01945a^2 - 0.116b + 0.0382ab - 0.2732\times10^{-3}at + \\ + 1.64\times10^{-2}t - 1.394\times10^{-7}t^3 - 1.03\times10^{-3}bt - 1.869, \tag{15}$$

which is valid for: $a=3.0 \ldots 5.0$, $b=0.0 \ldots 1.0$, $t=170° \ldots 220°C$.

P i o t r o w s k i [11] derived a new equation:

$$\eta_{CO_2} = 0.46365a - 0.018998a^2 - 0.2315b + 0.02988ab - 1.329\times10^{-3}at + \\ + 1.1243\times10^{-2}t - 0.55339\times10^{-7}t^3 - 1.536, \tag{16}$$

based on laboratory measurements carried out in the following ranges of parameters: $a=2.0 \ldots 6.0$, $b=0.0 \ldots 1.2$, $t=170° \ldots 210°C$.

Table 1 presents the values of the carbon dioxide conversion at equilibrium resulting from the existing semiempirical models, for a commercial plant operated at $t=190°C$, $P=20.0$ MPa, $a=3.947$ and $b=0.642$. The corresponding actual value of conversion is also presented in the last column of the table. These results relieve that the industrial-scale data are not consistent with the Fréjacques' nomograph. The other semiempirical models give numerical values that differ considerably from each other. In addition, they do not allow the prediction of the complete liquid—phase composition (with carbamate), and give no information on the gas—phase composition.

Table 1

Comparision between the semiempirical methods under the operating conditions: $a=3.947$, $b=0.6418$, $t=190°C$, $P=20.0$ MPa

Method	Nomograph		Regression equations			Actual Plant-scale
	Frejacques	Cook	(14)	(15)	(16)	
CO_2	0.635	0.695	0.689	0.712	0.694	0.640

There are several attempts to describe the combined chemical and phase equilibria of the urea synthesis in the literature [12] ... [15], too. Some of them are formally correct [12], [15] but, because of their simplified assumptions (particularly concerning both phases of the system to be ideal), they do not permit a quantitative analysis of the urea synthesis process at equilibrium.

It is the aim of this paper to present a new thermodynamic model of the urea synthesis process. This model is theoretically substantiated by the recent progresses in the thermodynamics of non-ideal systems [16] ... [18], and experimentally verified with the new experimental data [19], [20].

3. The Model Development and Testing

While the existing semiempirical models were based on the total liquid—phase reaction (9) alone, the new model assumes that the urea synthesis process is described by the reactions (1) and (2), and the phase changes (3) ... (5). The side transformations (6) ... (8) are negligible under normal operating conditions. As a result, the process proceeds in a two-phase gas—liquid system, the liquid phase being composed of ammonia, carbon dioxide, water, urea (U), and ammonium carbamate (Cb). The gas phase is composed of ammonia, carbon dioxide and water. Both phases are non-ideal mixtures. According to the phase rule, such system has three degrees of freedom and three independent variables can be arbitrary chosen. It was found that temperature and two concentration variables (a and b) are the most suitable [11], [16].

On the bases of the fundamental assumptions above, the mathematical model is composed of the following equations:

a) The definitions of the equilibrium constants of the reactions (1) and (2):

$$(17)\quad K_1=\frac{(\alpha-\beta)(1+a+b-2\alpha+\beta)^2}{(a-2\alpha)^2(1-\alpha)},\qquad (18)\quad K_2=\frac{\beta(b+\beta)}{(\alpha-\beta)(1+a+b-2\alpha+\beta)}.$$

b) The mole fractions related to the conversion degrees α and β, and the molar ratios a and b;

$$x_{CO_2}=\frac{1-\alpha}{1+a+b-2\alpha+\beta},\quad x_{NH_3}=\frac{a-2\alpha}{1+a+b-2\alpha+\beta},\tag{19}$$

$$x_{H_2O}=\frac{b+\beta}{1+a+b-2\alpha+\beta};$$

$$x_U=\frac{\beta}{1+a+b-2\alpha+\beta},\quad x_{Cb}=\frac{\alpha-\beta}{1+a+b-2\alpha+\beta}.\tag{20}$$

c) The equations for the calculation of the equilibrium constants as functions of temperature:

(21) $\text{Log } K_1=993.162/T-2.444,$ (22) $\text{Log } K_2=-969.365/T+2.769.$

d) The equations of the modified activity coefficients:

$$\gamma_{NH_3}=4.7895-1.6679\,a-7.2034\times10^{-3}at+5.08\times10^{-1}a^2+\\+1.5361\times10^{-5}at^2-3.4357\times10^{-2}a^3,\tag{23}$$

$$\gamma_{CO_2}=2.5702-2.9456\times10^{-2}t+7.338\times10^{-5}t^2+1.4494\times10^{-1}b^2+\\+7.1914\times10^{-6}at^2-3.4036\times10^{-5}bt^2-2.3629\times10^{-4}a^2t+\\+3.355\times10^{3}abt+2.9826\times10^{-3}\,a^3-8.4403\times10^{-2}a^2b,\tag{24}$$

$$\alpha_{H_2O}=55.509-0.44264t-2.9217b+4.617\times10^{-6}t^3-1.107\times\\\times10^{-5}at^2+9.5049\times10^{-5}bt^2.\tag{25}$$

Starting from the equilibrium criterion in the transformation (3):

$$PY_if_i=p_0^ix_i\gamma_i',\tag{5}$$

the modified activity coefficients have been defined as $\gamma_i=\gamma_i'/f_i$ [16].

e) The equations of Clausius–Clapeyron type for the partial pressures p_i^0:

$$\ln p^0_{NH_3}=-25.0698/T+56.321\ln T-0.26246\,T+1.7525\times10^{-4}T^2-258.139,\tag{26}$$

$$\ln p^0_{CO_2}=-2\,370.26/T-0.5913\ln T-1.178\times10^{-2}T+\\+1.5977\times10^{-5}T^2+15.2721,\tag{27}$$

$$\ln p^0_{H_2O}=-5\,231.82/T-6.1668\times10^{-2}\ln T-3.2907\times10^{-3}T+\\+1.222\times10^{-6}T^2+13.1833.\tag{28}$$

The coefficients of Eqs. (26) ... (29) have been identified by regression, using the existing experimental data [17], [21].

f) The total pressure equation:

$$P=\sum_i p_0^ix_i\gamma_i,\quad i=CO_2,\ NH_3,\ H_2O.\tag{29}$$

g) The mole fractions of the components in the gas-phase :

$$(30) \qquad Y_{NH_3} = \frac{p^0_{NH_3} x_{NH_3} \gamma_{NH_3}}{\sum_i p^0_i x_i \gamma_i}, \qquad (31) \qquad Y_{CO_2} = \frac{p^0_{CO_2} x_{CO_2} \gamma_{CO_2}}{\sum_i p^0_i x_i \gamma_i},$$

$$(32) \qquad Y_{H_2O} = \frac{p_{H_2O} x_{H_2O} \gamma_{H_2O}}{\sum_i p^0_i x_i \gamma_i}.$$

The system (17) ... (32) correlates the composition of the liquid phase (α, β), the composition of the gas-phase (Y_i) as well as the total pressure (P) as functions of the three independent variables : a, b, and t.

The equations (17) ... (32) have been numerically solved by computer programming in PASCAL. The adequacy of the model has been tested by comparing the computed values of α, β, Y_i, P to those experimentally obtained by P i o t r o w s k i [4].

Table 2

Model Testing

Parameters			α		β		P, [MPa]		Y_{NH_3}		Y_{CO_2}	
t, [°C]	a	b	Exp.	Calc.	Exp.	Calc.	Exp.	Calc.	Exp.	Calc.	Exp.	Calc.
170	4.08	0.14	—	0.798	0.721	0.757	12.9	12.33	0.97	0.96	0.15	0.02
180	3.96	0.07	—	0.799	0.776	0.763	13.8	13.90	0.96	0.96	0.02	0.02
190	3.49	0.00	—	0.774	0.731	0.742	17.5	16.60	0.90	0.93	0.01	0.03
200	3.59	0.59	—	0.688	0.652	0.653	17.7	19.60	0.86	0.86	0.06	0.07
210	3.77	0.25	—	0.753	0.718	0.724	26.0	24.60	0.87	0.86	0.06	0.07

The data from Table 2 show a good agreement between the computed and the experimental values. The most important deviations presents the mole fraction of carbon dioxide in the gas-phase (Y_{CO_2}) because of its low value.

4. Process Simulations. Results

The agreement between the computed data and the experimental values for a number of sets of parameters may be considered only a necessary condition, but not sufficient, for the validity of the model. It must be further tested the capacity of the model to simulate the influence of the parameters on the composition and total pressure according to the general laws of the thermodynamic equilibrium. The results of this simulation are partly presented in Tables 3 ... 5.

The influence of the *temperature* on the dependent variables α, β, P, Y_{NH_3} and Y_{CO_2}, for a given input composition (a=4.0, b=0.6), is represented in Table 3. The variations are qualitatively in agreement with V a n ' t H o o f's rule, namely, the equilibrium conversion in the exothermic reaction (1) is

Table 3

Influence of the Temperature, at $a=4.0$ and $b=0.6$

Temperature, [K]	433	443	453	463	473	483
α	0.7302	0.7279	0.7259	0.7241	0.7226	0.7212
β	0.6771	0.6804	0.6832	0.6859	0.6876	0.6894
P, [MPa]	10.508	11.733	13.421	15.822	19.297	24.368
Y_{NH_3}	0.9445	0.9440	0.9323	0.9076	0.8708	0.8259
Y_{CO_2}	0.0212	0.0278	0.0392	0.0542	0.0709	0.0866
η_{CO_2} rel. (14)	0.6527	0.6649	0.6769	0.6831	0.6837	0.6766
η_{CO_2} rel. (15)	0.6675	0.7055	0.7193	0.7230	0.7109	0.6820
η_{CO_2} rel. (16)	0.6713	0.6828	0.6912	0.6936	0.6897	0.6793

Table 4

Influence of the Ammonia Excess, at $T=453$ K and $b=0.4$

a	2.0	3.0	4.0	5.0	6.0
α	0.5030	0.6568	0.7532	0.8135	0.8526
β	0.4694	0.6169	0.7126	0.7748	0.8167
P, [MPa]	14.831	13.932	13.589	14.979	15.802
Y_{NH_3}	1 0000	0.9412	0.9451	0.9735	0.9950
Y_{CO_2}	0.0000	0.0238	0.0299	0.0117	0.0000
η_{CO_2} rel. (14)	0.4773	0.6126	0.7125	0.7770	0.8061
η_{CO_2} rel. (15)	0.5270	0.6575	0.7491	0.8017	0.8155
η_{CO_2} rel. (16)	0.4718	0.6130	0.7162	0.7814	0.8086

Table 5

Influence of the Excess of Water (b), at $T=453$ K and $a=3.0$

b	0.0	0.2	0.4	0.6	0.8	1.0
α	0.7271	0.6904	0.6568	0.6258	0.5972	0.5705
β	0.6923	0.6526	0.6169	0.5844	0.5546	0.5273
P, [MPa]	14.393	14.125	13.932	13.827	13.819	13.909
Y_{NH_3}	0.9550	0.9507	0.9412	0.9258	0.9044	0.8774
Y_{CO_2}	0.0195	0.0189	0.0238	0.0348	0.0522	0.0757
η_{CO_2} rel. (14)	0.6856	0.6492	0.6128	0.5764	0.5410	0.5036
η_{CO_2} rel. (15)	0.7322	0.6948	0.6575	0.6202	0.5828	0.5454
η_{CO_2} rel. (16)	0.6345	0.6070	0.5787	0.5503	0.5219	0.4935

negatively influenced by the temperature. On the other hand, because of the inequality $\eta_{Cb} > \eta_{CO_2}$, the global conversion monotonously increases with the temperature without any extreme point in the studied range. This is in contrast with the variations predicted by the regression equations (14) ... (16). May be our model must be improved in order to increase the sensibility of the two equilibrium constants in the temperature range 170° ... 210°C. The other variables normally depend on the temperature: the total pressure increases with the temperature, while ammonia concentration in the gas-phase decreases.

The influence of the *ammonia excess* is presented in Table 4. The two conversions continuously increases with the excess of ammonia. This is consistent with the law of mass action. Similar variation are predicted by the semiempirical equations (14) ... (16). The equilibrium pressure has a minimum. The study of the curves $P=f(a)$ for other values of t and b has shown that the position of minimum point (a_{min}) shifts with the increase of temperature and water excess to higher values of a. The curves $Y_{NH_3}=f(a)$ have an extreme shape, too, the position of the minimum point being almost the same.

The influence of the *excess of water* (b) is ilustrated in the Table 5. The predicted dependence of the conversions is still in agreement with the law of mass action. The effect of the excess water on the equilibrium pressure is dependent on the values of the parameter a. For values $a>2.0$, usually applied in industry, the excess of water reduces the value the equilibrium pressure (as we can see in Table 5). The excess of water has a small influence on the composition of the gas-phase.

5. Conclusions

a) The semiempirical methods, available in the literature, permit only the evaluation of a fictitious liquid—phase composition of the urea system at equilibrium.

b) A new thermodynamic model of the urea synthesis process has been proposed in this paper, based on the two main reactions in liquid—phase and three gas—liquid equilibria. The model can predict the complete composition of the two phases, as well as the total pressure, the only independent variables being the operating temperature and two input molar ratios.

c) The new model complies with the experimental data, as well as with the equilibrium thermodynamic laws.

Notations

a — molar ratio NH_3/CO_2 in the liquid phase;
b — molar ratio H_2O/CO_2 in the liquid phase;
Cb — ammonium carbamate;
f_i — fugacity coefficient;
K_1, K_2, K_x — approximate equilibrium constants of the reactions (1), (2), and (9) respectively;
n_i^0 — mole number of component i, in the feed;
P — total equilibrium pressure, [MPa];
p_i^0 — partial pressure of pure component;

t — temperature, [°C]; T — absolute temperature, [K];
x_i — mole fraction of component i, in liquid phase;
Y_i — mole fraction of component i, in gas phase;
α — conversion degree of CO_2 in the reaction (1);
$\beta = \eta_{CO_2}$ — conversion degree of CO_2 in the global reaction;
$\gamma_i = \gamma_i/f_i$;
η_{Cb} — conversion degree of the carbamate in the reaction (2).

Received, November 30, 1991

Polytechnic Institute, Jassy,
Faculty of Chemical
Engineering

REFERENCES

1. * * * Informations Chimie, *202*, 107 (1989).
2. Dürich W., Chimie, **31**, 8 (1977).
3. Ruf A., Müller W., Buck A., Swiss. Chem., **6**, *9*, 129 (1984).
4. Calistru C., Leonte C., Siminiceanu I., Hagiu C., *Technology of Mineral Fertilizers* (in Romanian)., Vol. **I**, Ed. Tehn., Bucharest, 1984, 293.
5. Fréjacques M., Chimie et Industrie, **60**, *1*, 22 (1948).
6. Cook L., Hydrocarbon Processing, **45**, *2*, 129 (1966).
7. Mavrovič I., Chem. Eng. Progress, **70**, *2*, 69 (1974).
8. Кучерявий В. И., Горловский Д. М., Хим. Пром, *11*, 836 (1966).
9. Kawasumi S., Bull. Chem. Soc. Japan, **25**, 227 (1952); Ibid., **26**, 218 (1953); Ibid., **27**, 254 (1954).
10. Inoue S., Kanai K., Otsuka E., Bull. Chem. Soc. Japan, **45**, 1 339 (1972).
11. Piotrowski J., Chem. Stosowana, **28**, *2*, 239 (1984); Ibid., **29**, *1–2*, 41 (1985).
12. Lembowitz S.M., de Cooker M., Van der Berg P., J. Appl. Chem. Biotechnol., **23**, 63 (1973).
13. Vičar S., Brit. Chem. Eng., **8**, *12*, 828 (1963).
14. Кучерявий В. М., Зиновьев Г., Хим пром., *5*, 354, (1969).
15. Ефремова Г. Д., Леонтьева Г. Г., Хим. пром., *10*, 742, (1962).
16. Szaravara J., Gawdik A., Chem. Eng. Sci., **44**, *7*, 1 489 (1989).
17. Sandler S. I., *Chemical Engineering Thermodynamics*. J. Wiley, New York, 1989.
18. Siminiceanu I., *The Backgrounds of Inorganic Technology*, (in Romanian), Polyt. Inst., Iași, 1987.
19. Piotrowski J., Ph. D., Diss., Silesian Techn. Univ., 1976.
20. Szarawara J., Piotrowski, J., Chem. Stosowana, **31**, *1*, 73 (1987).
21. Reid R. C., Sherwood T. K., *The Properties of Gases and Liquids*. Mc Graw-Hill, New York, 1966.

UN NOU MODEL TERMODINAMIC PENTRU PROCESUL DE SINTEZĂ A UREEI

(Rezumat)

Se stabilește un nou model matematic al procesului de sinteză a ureei la echilibru, care ia în considerație două reacții chimice în faza lichidă:

$$CO_2 + 2NH_3 = NH_2COONH_4, \qquad NH_2COONH_4 = CO(NH_2)_2 + H_2O$$

precum și trei transformări de fază lichid – gaz:

$$NH_{3(l)} = NH_{3(g)}, \qquad CO_{2(l)} = CO_{2(g)}, \qquad H_2O_{(l)} = H_2O_{(g)}.$$

Modelul permite precizarea compoziției complete a fazei lichide (x_U, x_{Cb}, x_{NH_3}, x_{CO_2}, x_{H_2O}) și a celei gazoase (Y_{NH_3}, Y_{CO_2}, Y_{H_2O}) precum și a presiunii totale (P) în funcție de numai, trei variabile independente: temperatura (T) și rapoartele molare ale reactanților NH_3/CO_2 (a), H_2O/CO_2 (b). Adecvanța modelului este testată cu date experimentale de echilibru (Piotrowski, Szarawara) precum și cu mărimi măsurate pe o instalație industrială. Simularea procesului a confirmat capacitatea modelului de a descrie corect influența celor trei parametri asupra compoziției și presiunii de echilibru în următoarele intervale ale variabilelor independente: $T = 443 \ldots 483$ K, $a = 2{,}0 \ldots 6{,}0$ și $b = 0{,}0 \ldots 1{,}2$.

BULETINUL INSTITUTULUI POLITEHNIC DIN IAŞI
Tomul XXXVII (XLI), Fasc. 1—4, 1991
Secţia II
CHIMIE ŞI INGINERIE CHIMICĂ

D.C. 552.54 ; 541.11

ON KINETICS OF THE MAGNESITE THERMAL DECOMPOSITION

BY

AL. SZÉP, GH. MIHĂILĂ, RODICA ŞMOCOT and MARIA IVANIGIUC

1. Introduction

The process of the magnesite thermal decomposition belongs to the unitary process group „adsorption—formation and growing of germs" [1]. This is of great interest in both magnesium salts manufacture and metallurgical industry. The experimental data available [2] ... [4], concerning with thermogravimetrical studies of different micronized particles of natural magnesite and synthetic magnesium carbonate, point out that the process develops according with the classical dissociation mechanism in the temperature range of 633 ... 1 073 K.

The aim of the present work was to provide a consistent set of experimental data on thermal decomposition of a Greek magnesite, in crushed form, having granula size from 0.125 up to 7.6 mm in diameter, in a wide temperature range.

2. Experimental

A Greek magnesite, having 96.7% $MgCO_3$, 2.3% $CaCO_3$ and 2.0% insolubles in hydrochloric acid, was investigated.

The thermal decomposition of magnesite samples was carried out on a thermoanalyzer fully described in a previous paper [5]. This device allowed either a single macrostructural element or more granules, in fixed-bed of different heights, to be studied. The magnesite pellets, having 7.6 mm in diameter and 2.5 mm in height, were fashioned mechanically from raw mineral. To determine how the decomposition mechanism depends on the granula size, three different granulometrical classes of crushed magnesite, namely $0.40 \leqslant \varnothing \leqslant 0.63$, $0.315 \leqslant \varnothing \leqslant 0.40$ and $0.125 \leqslant \varnothing \leqslant 0.160$ mm, have been also investigated. All experiments were carried out under isothermal conditions within the temperature range of 673...1123 K and a constant flowrate of carrier gas of 20 l/h.

3. Results, Modelling and Discussion

The quantitative development of the process vs. time was studied by means of the decarbonation degree, η, defined by the relation

$$\eta = \frac{m^0 - m}{m^0 \bar{X}^0_{CO_2}} \tag{1}$$

where : m^0 is the initial mass of the sample, m — its mass at any instant and $\bar{X}^0_{CO_2}$ — the mass fraction of carbon dioxide in the initial sample.

The experimental measurements allowed to establish the dependence of decarbonation degree on time, τ, temperature and granula size (Figs. 1...3).

Under the conditions considered above, as shown in Figs. 1... 3, the temperature and granula size influence greatly on the rate of over-all process, especially in the low temperature range and big granula size.

To find out what is the rate controlling step of the process (chemical reaction, phase transformation, transfer of CO_2 through crust, etc.) the kinetical data set out in Figs. 1...3 were processed in proper co-ordinates, namely $\ln\tau^{-1}$ vs. T^{-1} (Figs. 4 and 5). The data represented in these figures show that the process is kinetically controlled ($E_a = 110{,}000$ J.mol^{-1}), but, as granula size increases from micronized ones up to 7.6 mm in diameter ones, the apparent activation energy becomes lower ($E_a = 51{,}170$ J.mol^{-1}). This fact illustrates a modification in the mechanism, i.e. the diffusional processes as well as formation and growing of germs become important.

In order to select the mathematical model of the real development of the process, the obtained kinetical data were plotted in the co-ordinates specific to each kinetical equations summarized in Table 1. As in the case of thermal decomposition of dolomite [6], ..., [8], the mathematical model which describes with enough precision the real process kinetics is the topochemical equation :

$$\eta = 1 - e^{K^*\tau^n}. \tag{2}$$

In fact, the linear dependence obtained by plotting the experimental data in the co-ordinates proper to the topochemical equation (2), represented in Fig. 6, allowed the determination of the exponential factor n and the $K = f(T)$ dependence.

Table 1

Modells of the Macrostructural Element

Nr.	Controlling step of the process	Equation	
		Differential form	Integral form
1.	Thermal dissociation	$\frac{\rho^* H d\eta}{2d\tau} = k(1-\eta)^n$	$\tau = \frac{\rho^* H}{2k}\eta$ for $n=0$ $\tau = -\frac{\rho^* H}{2k}\ln(1-\eta)$ for $n=1$ $\tau = \frac{\rho^* H}{2(1-u)k}\left[1 - \frac{1}{(1-\eta)^{n-1}}\right]$ for $n>1$
2.	Phase transformation	$\frac{\rho^* H d\eta}{2d\tau} = k(1-\eta)^n \tau^m$	$\eta = 1 - \exp[-2k\,\tau^{m-1}/\rho^* H(m+1)]$
3.	Transfer through crust	$-q = D f_{CO_2} \frac{dC_{CO_2}}{d\delta}$	$1 - 3(1-\eta)^{2/3} + 2(1-\eta) = K^*_G \tau$ $[1-(1-\eta)^{1/3}]^2 = K^*_G \tau$ $\left(1 - \frac{2}{3}\eta\right) - (1-\eta)^{2/3} = K^*_G \tau$

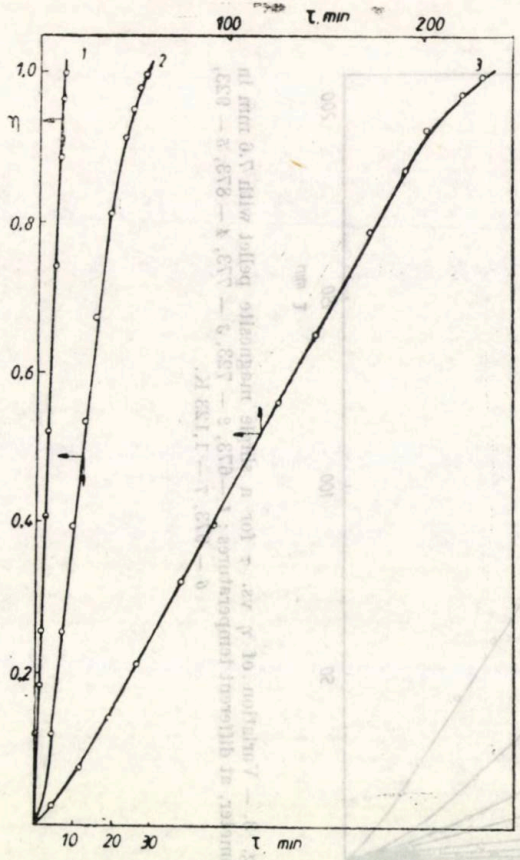

Fig. 1. — Variation of η vs. τ for magnesite particles of 0.315 ... 0.400 mm in diameter, in a fixed-bed of 2 mm in height, at different temperatures : *1*—773, *2*—873, *3*—973 K.

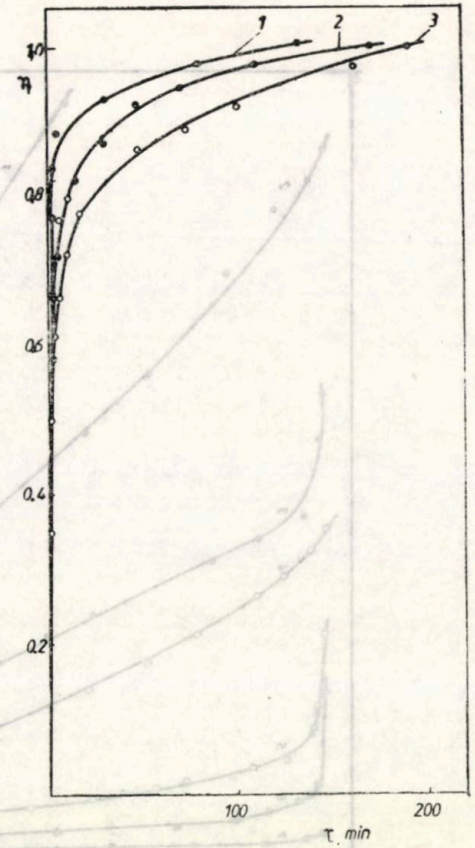

Fig. 2. — Variation of η vs. τ for magnesite particles of different diameter, in a fixed-bed of 2 mm in height, at 673 K: *1*—0.125< Ø<0.160, *2*—0.315< Ø<0.400, *3*—0.400< Ø<0.630 mm.

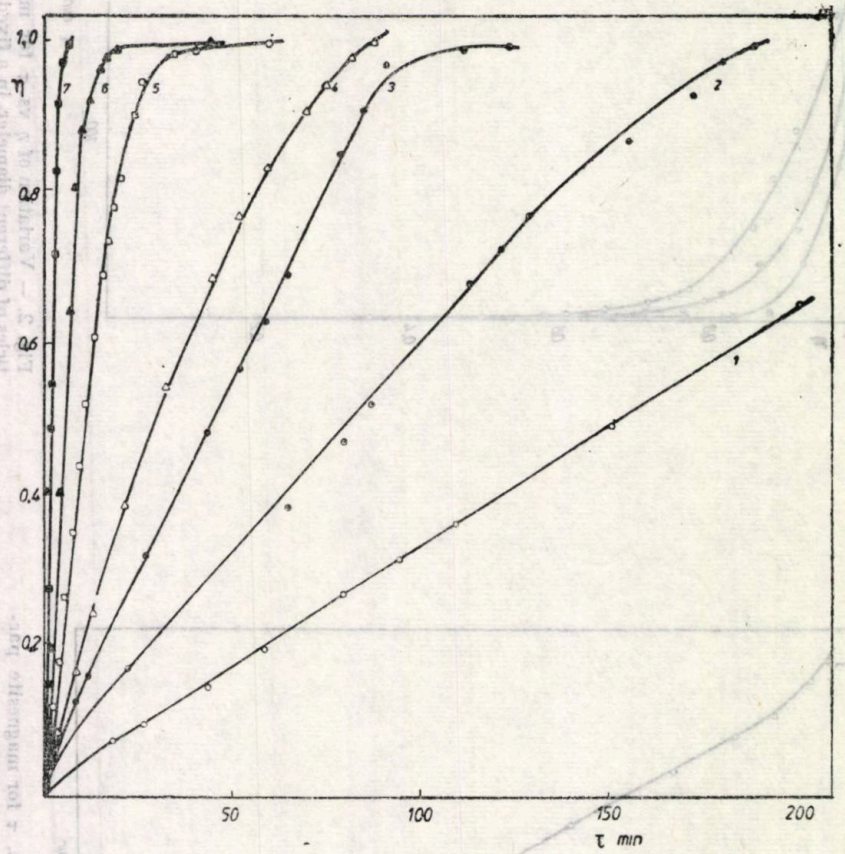

Fig. 3. — Variation of η vs. τ for a single magnesite pellet with 7.6 mm in diameter, at different temperatures : *1* — 673, *2* — 723, *3* — 773, *4* — 873, *5* — 923, *6* — 973, *7* — 1,123 K.

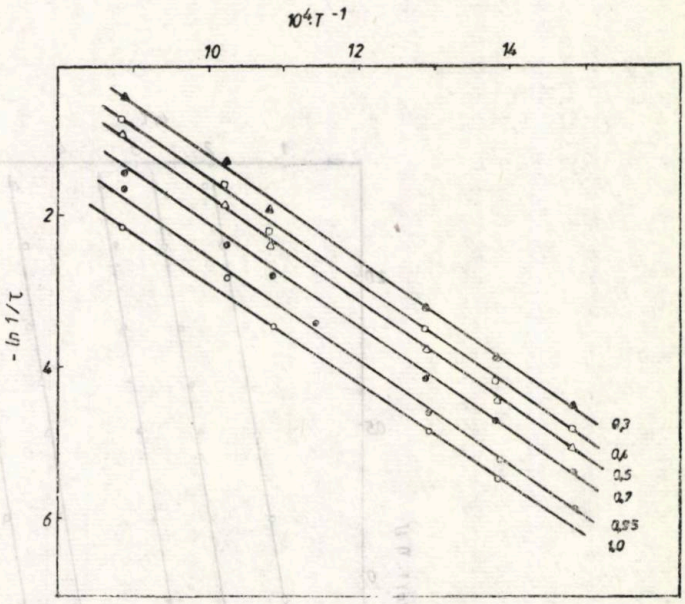

Fig. 4. — Dependence of $\ln \tau^{-1}$ vs. T^{-1} for different values of decarbonation degree of magnesite particles of 0.315 ... 0.400 mm in diameter, decomposed in a fixed-bed of 2 mm in height.

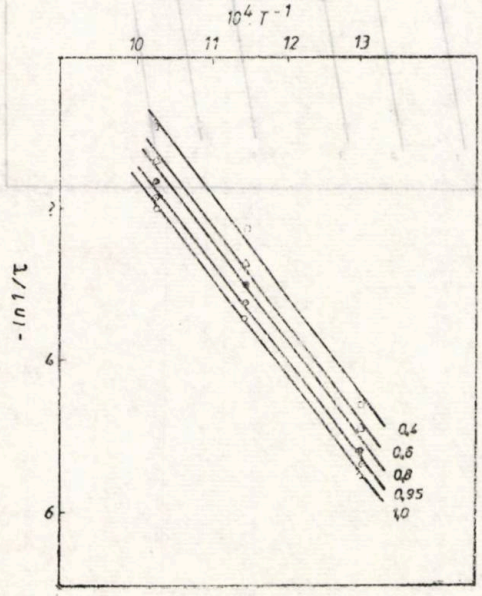

Fig. 5. — Dependence of $\ln \tau^{-1}$ vs. T^{-1} for different values of decarbonation degree of a single magnesite pellet with 7.6 mm in diameter.

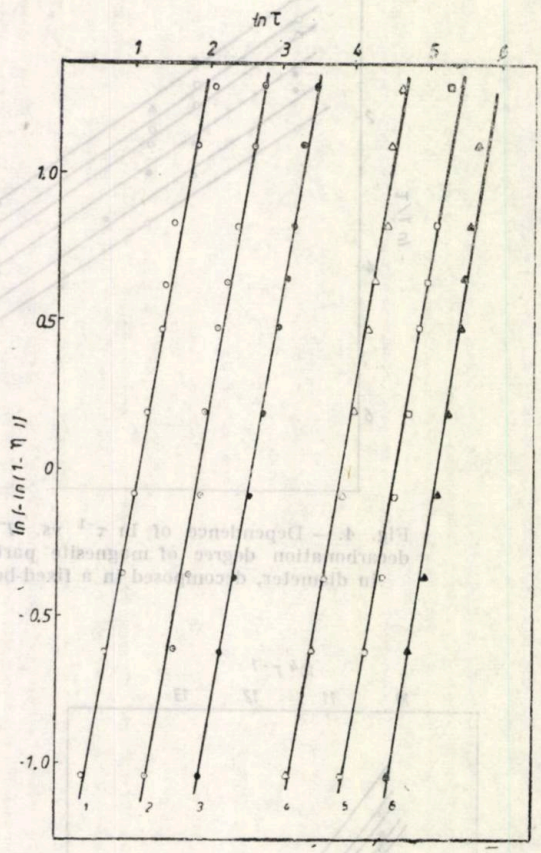

Fig. 6. — Plot of $\ln[-\ln(1-\eta)]$ vs. $\ln \tau$ at different temperatures for the pellets with 7.6 mm in diameter: *1* — 1 123, *2* — 973, *3* — 923, *4* — 773, *5* — 723, *6* — 673 K.

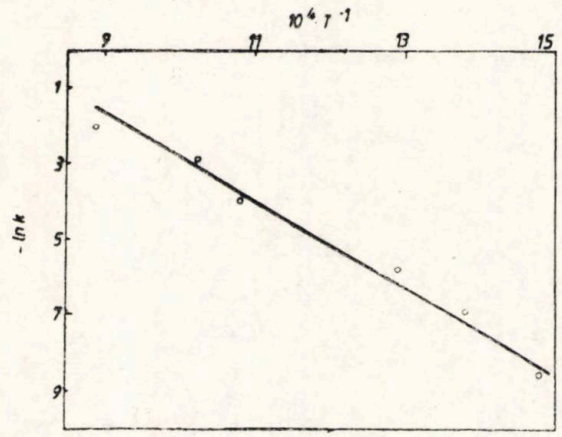

Fig. 7. — Arrhenius' plot for magnesite pellets with 7.6 mm in diameter.

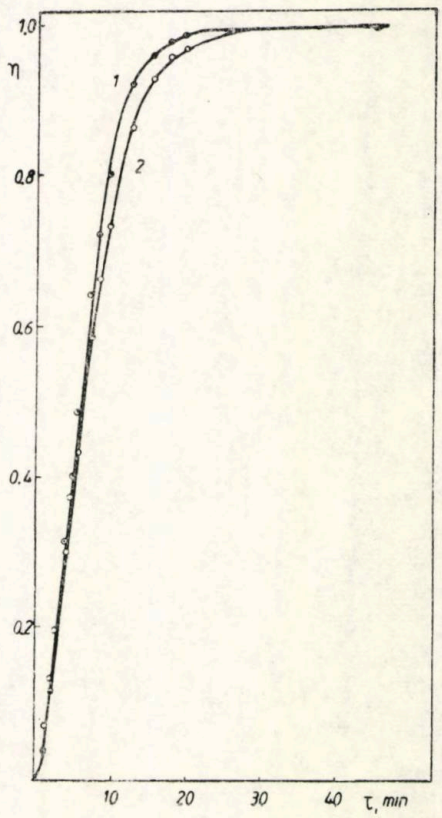

Fig. 8. — Comparison of the experimental and calculated kinetical data : *1* — experimental ; *2* — calculated.

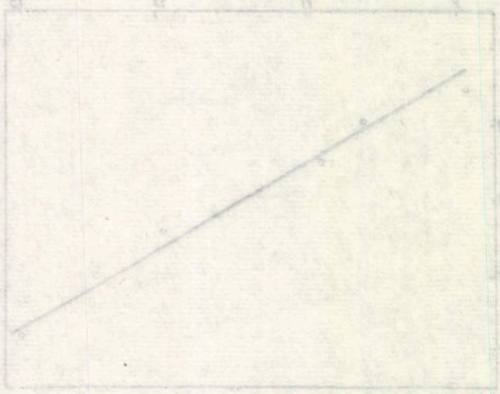

The Arrhenius' plot (Fig. 7), where the six values obtained are situated more or less on a straight line, points out that the process develops according with one single mechanism within the temperature range investigated.

The mathematical model of the process is the topochemical equation:

$$\eta = 1 - e^{K^* \tau^{3/2}}, \tag{3}$$

where

$$K^* = 5113.81 e^{-\frac{94,477.22}{RT}} \quad \text{for } d_p = 7.6 \text{ mm}. \tag{4}$$

As shown in Fig. 8, where both experimental and calculated kinetical curves were plotted, the model fits satisfactorily the experimental data.

4. Conclusions

Our results may be summarized as follows:

1. The thermal decomposition of one high $MgCO_3$ content Greek magnesite, in crushed form, under isothermal conditions, was investigated thermogravimetrically.

2. The macrokinetic and mathematical modells of the process for a macrostructural element have been reported.

3. A careful analysis of the kinetical experimental data, taking into account the modells elaborated, pointed out that the proces develops according with a transformation mechanism only, whose mathematical model is given by (3), where, for $d_p = 7.6$ mm, K^* has the value (4).

Notations

p^* — molal density of the particle, [Kmol/m^3];
H — height of the magnesite pellet, [m];
k — rate constant of the dissociation process, [Kmol/m^2·s];
K_G — over-all constant of the diffusion process, [s^{-1}];
k^* — rate constant of the transformation process, [s$^{-5/3}$];
n, m — reaction order, exponential coefficient;
Df_{CO_2} — molecular diffusion coefficient of CO_2, [m/s];
C_{CO_2} — concentration of CO_2, [Kmol/m^3];
d_p — diameter of the particles, [mm].

Received, November 22, 1990

Polytechnic Institute, Jassy,
Department of Anorganic Chemical Technology

REFERENCES

1. Calistru C., Leonte C., C. R. du XXXVI-ème Congrès Intern. de Ch. Industrielle, Bruxelles, 1967, 756.
2. Rostovțiev V. S., *Teoria proceselor metalurgice* (trad. du russe). Ed. Tehnică, București, 1959.
3. Позин М. Е., *Технология минеральных солей*, Гос. научно-техн. изд. хим. литер., Ленинград, 1961, 168.

4. Позин М. Е., Зинюк Р. Ю., *Физико-химические основы неорганической технологий*. Изд. Химия, Ленинград, 1985, 209.
5. Calistru C., Mihăilă Gh., An. Șt. Univ. „Al. I. Cuza", Iași, **18**, 97 (1972).
6. Leonte C., Szép Al., Calistru C., Ifrim L., Rev. Chim. (Bucharest), **34**, 894 (1983).
7. Szép Al., Mihăilă Gh., Leonte C., Vuță Gh., Rev. Chim. (Bucharest), **39**, 32 (1988).
8. Leonte C., Szép Al., Bilbă N., Calistru C., Ifrim L., Mihăilă Gh., Rev. Roum. Chim., **35**, 41 (1990).

STUDIUL PROCESULUI DE DESCOMPUNERE TERMICĂ A MAGNEZITEI

(Rezumat)

S-a cercetat descompunerea termică a unei magnezite cu conținut ridicat de $MgCO_3$, din Grecia, sub formă mărunțită, în condiții izoterme, folosind metoda termogravimetrică. S-au elaborat modelele macrocinetice și matematice ale procesului într-un element macrostructural și, printr-o analiză atentă a datelor cinetice experimentale, prin reprezentări grafice specifice modelelor elaborate, s-a găsit că procesul se desfășoară după un singur mecanism de transformare, al cărui model matematic este dat de ecuația topochimică (3), în care, pentru d_p = =7.6 mm, K este dat de (4).

BULETINUL INSTITUTULUI POLITEHNIC DIN IAȘI
Tomul XXXVII (XLI), Fasc. 1—4, 1991
Secția II
CHIMIE ȘI INGINERIE CHIMICĂ

C.D. 631.859.12

ANALYSE DE L'INSTALLATION NORSK-HYDRO POUR L'OBTENTION DES NITRO-PHOSPHATES

I. LE PROCESSUS TECHNOLOGIQUE DE DÉSAGRÉGATION NITRIQUE

PAR

CAROLINA HAGIU, RODICA DIACONESCU et ADRIANA MĂRGINEAN

1. Introduction

Les technologies d'obtention des engrais N—P et N—P—K se sont développées et ont été appliquées à l'échelle industrielle sous différentes variantes parmi lesquelles le procédé Norsk-Hydro occupe une place importante [1] ... [3]. Le procédé Norsk-Hydro consiste dans la décomposition nitrique des matières premières à base de phosphates, suivie par la séparation partielle du $Ca(NO_3)_2 \cdot 4H_2O$ par cristallisation, refroidissement, filtrage et lavage. La solution phospho-nitrique obtenue, appellée „solution-mère", est transformée par ammonisation, concentration et granulation avec ou sans supplément de KCl ; on en obtient des engrais N—P—K ou N—P.

Le produit secondaire, le $Ca(NO_3)_2 \cdot 4H_2O$, est soumis à la conversion avec des solutions de bicarbonate et de carbonate d'ammonium ; on en obtient des solutions de NH_4NO_3 dont une partie est utilisée à la carbo-ammonisation et à l'ammonisation et une autre partie à l'obtention du nitrocalcaire.

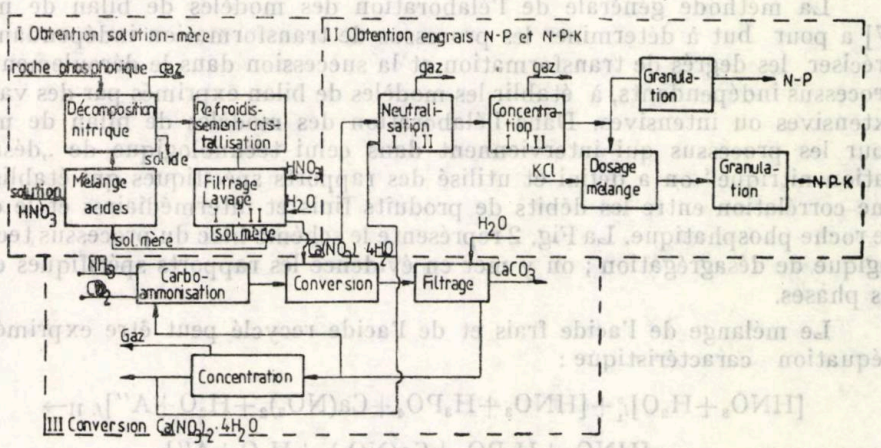

Fig. 1. — Schéma des opérations du procédé Norsk-Hydro.

Le schéma des opérations du procédé Norsk-Hydro est représenté par la Fig. 1. L'analyse technologique de l'installation sur ordinateur et l'utilisation des modèles de bilan de masse exigent qu'on considère le processus global comme étant formé de trois processus technologiques composants à savoir : I. processus technologique de „désagrégation nitrique". II. processus

technologique de l'„obtention des engrais N—P et N—P—K"; III. processus technologique de „conversion du $Ca(NO_3)_2 \cdot 4H_2O$".

Pour obtenir des engrais d'une qualité bien déterminée il faut rigoureusement maintenir les paramètres de fonctionnement tout au long du flux technologique surtout pendant le processus technologique de désagrégation afin qu'on obtienne des „solutions-mère" ayant une composition chimique constante et un rapport Ca/P imposé. C'est la qualité de la matière première phosphatique qui représente le facteur principal perturbateur du fonctionnement normal de l'installation. La composition chimique de cette matière première varie selon la nature des gisements et selon la zone géographique [1] ... [6].

On remarque une variation entre des limites larges du contenu en phosphore, en calcium et en fluor, éléments chimiques de base et en impuretés, les plus fréquentes étant le Fe, l'Al, le K, le Na, le Mg, le Si. Une partie de ces impuretés réagissent avec l'acide azotique pendant le processus de décomposition nitrique et se solubilisent, d'autres, telles le Si, le Sr, se comportent comme inertes.

Si l'on change la variété des matières premierès, déterminée dans l'actuelle conjoncture économique par les offres des partenaires étrangers, se produit un déréglement des paramètres technologiques et, d'une façon implicite, la modification de la qualité des produits ainsi que la diminution de la capacité de production causée par le temps nécessaire à faire revenir les paramètres à leurs valeurs optima. Pour réduire au minimum les effets défavorables causés par la modification de la qualité des matières premières il est nécessaire d'élaborer une documentation de génie chimique adéquate et d'utiliser l'ordinateur pour contrôler le fonctionnement des installations industrielles. La solution rigoureusement scientifique des problèmes technologiques implique, premièrement, l'élaboration des modèles de bilan de masse et leur utilisation dans le calcul du bilan de masse et des consommations spécifiques.

2. Modèles de bilan de masse

La méthode générale de l'élaboration des modèles de bilan de masse [7] a pour but à déterminer les processus de transformation indépendants, à préciser les degrés de transformation et la succession dans le déroulement des processus indépendants, à établir les modèles de bilan exprimés par des valeurs extensives ou intensives. Dans l'élaboration des modèles de bilan de masse pour les processus qui interviennent dans celui technologique de „désagrégation nitrique" on a défini et utilisé des rapports spécifiques qui établissent une corrélation entre les débits de produits finis et intermédiaires et le débit de roche phosphatique. La Fig. 2 représente le schéma bloc du processus technologique de désagrégation ; on y met en évidence les rapports spécifiques entre les phases.

Le mélange de l'acide frais et de l'acide recyclé peut être exprimé par l'équation caractéristique :

$$[HNO_3 + H_2O]_{l_1^0} + [HNO_3 + H_3PO_4 + Ca(NO_3)_2 + H_2O + A'']_{f.\,II} \rightarrow$$

$$\rightarrow [HNO_3 + H_3PO_4 + Ca(NO_3)_2 + H_2O + A'']_{l^0}.$$

Les équations de bilan de masse, les valeurs nécessaires et les relations pour leur calcul sont présentées dans le Tableau 1. Les relations de définition et de calcul des rapports spécifiques entre les phases sont présentées dans le Tableau 5.

Tableau 1

Mélange des acides

Entrée			Sortie			Valeurs nécessaires
Phase	Composant	Équations de bilan, [Kg/h]	Phase	Composant	Équations de bilan, [Kg/h]	
Solution de HNO_3 $[]^0_{l_1}$	HNO_3	$m_{HNO_3[]^0_{l_1}} = m_{[]^0_{l_1}} \bar{X}_{HNO_3[]^0_{l_1}}$	Mélange des solutions acides $[]^0_l$	HNO_3	$m_{HNO_3[]^0_l} = 4{,}5 m_{[]^0_l} (\bar{X}_{N[]^0_l} - 0{,}7 \bar{X}_{Ca[]^0_l})$	$m^0_{[]_s}$; $\bar{X}_{HNO_3[]^0_1}$; $\bar{X}_{N_{fII}}$; $\bar{X}_{P_{fII}}$; $\bar{X}_{Ca_{fII}}$; $\bar{X}_{A''_{fII}}$; $\bar{X}_{H_2O_{fII}} = \bar{X}_{N[]^0_l} = \bar{X}_{N[]^0_l} = \bar{X}_{N_{fII}} + R^0_L (0{,}2222 \times \bar{X}_{HNO_3[]^0_l} - \bar{X}_{N_{fII}})$ $\bar{X}_{P[]^0_l} = (1 - R^0_L) \bar{X}_{P_{fII}}$ $\bar{X}_{Ca[]^0_l} = (1 - R^0_L) \bar{X}_{Ca_{fII}}$ $\bar{X}_{A''[]^0_l} = (1 - R^0_L) \bar{X}_{A''_{fII}}$ $\bar{X}_{H_2O[]^0_l} = \bar{X}_{H_2O_{fII}} + R^0_L (1 - \bar{X}_{N_{fII}} - \bar{X}_{HNO_3[]^0_l})$ R^0_L, R_D, F
	H_2O	$m_{H_2O[]^0_{l_1}} = m_{[]^0_{l_1}} (1 - \bar{X}_{HNO_3[]^0_{l_1}})$		H_3PO_4	$m_{H_3PO_4[]^0_l} = 3{,}161 m_{[]^0_l} \bar{X}_{P[]^0_l}$	
	Total	$m_{[]^0_{l_1}} = R_L R^0_L m_{[]^0_s}$		$Ca(NO_3)_2$	$m_{Ca(NO_3)_2[]^0_l} = 4{,}1 m_{[]^0_l} X_{Ca[]^0_l}$	
Filtré II recyclé $[]^0_{fII}$	HNO_3	$m_{HNO_3 fII} = 4{,}5 m_{fII} (\bar{X}_{N fII} - 0{,}7 \bar{X}_{Ca fII})$		Inerte	$m_{A''[]^0_l} = m_{[]^0_l} \bar{X}_{A''[]^0_l}$	
	H_3PO_4	$m_{H_3PO_4 fII} = 3{,}161 m_{fII} \bar{X}_{P fII}$		H_2O	$m_{H_2O[]^0_l} = m_{[]^0_l} \bar{X}_{H_2O[]^0_l}$	
	$Ca(NO_3)_2$	$m_{Ca(NO_3)_2 fII} = 4{,}1 m_{fII} \bar{X}_{Ca fII}$				
	Inerte	$m_{A''fII} = m_{fII} \bar{X}_{A''fII}$		Total	$m_{[]^0_l} = m_{[]^0_{l_1}} + m_{fII} = R_D m_{[]^0_s}$	
	H_2O	$m_{H_2O fII} = m_{fII} \bar{X}_{HO_2 fII}$				
	Total	$m_{F II} = F m^0_{[]_s} = R_D (1 - R^0_L) m^0_{[]_s}$				

Le processus de „désagrégation nitrique" est exprimé par l'équation caractéristique :

$$[Ca_3(PO_4)_2+CaF_2+CaCO_3+A'']_{s^\circ}+[HNO_3+H_3PO_4+Ca(NO_3)_2+H_2O+$$
$$+A'']_{l^\circ}\rightarrow[H_3PO_4+HNO_3+Ca(NO_3)_2+HF+CO_2+H_2O+A]_{l_2}+[A'']_{s_2}+$$
$$+[CO_2+HF+H_2O+HNO_3]_{g_2}.$$

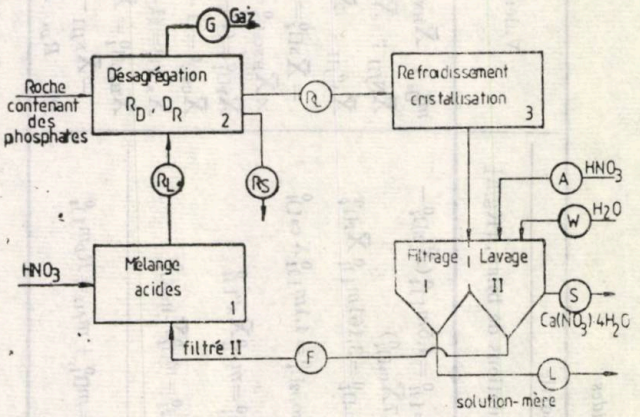

Fig. 2. — Schéma bloc du processus technologique de désagrégation.

La matière première phosphatique s'exprime par des composants réels, car pour la plupart des variétés de roche phosphatique le rapport CaO/P_2O_5 diffère par rapport à celui qui correspond aux fluorapatites. On considère que les impuretés de la roche phosphatique sont formées par des impuretés solubles qui réagissent avec les acides et passent en phase liquide ($[\ ]_{l_2}$) et des impuretés insolubles qui restent sous forme de solides ($[\ ]_{s_2}$) (SiO_2, silicates, alumino-silicates). Les composants contenant de l'azote (HNO_3, NO_x) qui passent en phase gazeuse ne sont exprimés que par le HNO_3. Les processus de transformation indépendents sont :

(1) $$Ca_3(PO_4)_2+6HNO_3=2H_3PO_4+3Ca(NO_3)_2,$$

(2) $$CaF_2+2HNO_3=2HF+Ca(NO_3)_2,$$

(3) $$CaCO_3+2HNO_3=Ca(NO_3)_2+CO_2+H_2O,$$

(4) $HF_{[]l}\rightleftarrows HF_{[]g}$, (5) $CO_{2[]l}\rightleftarrows CO_{2[]g}$,

(6) $H_2O_{[]l}\rightleftarrows H_2O_{[]g}$, (7) $HNO_{3[]l}\rightleftarrows HNO_{3[]g}$.

Outre les réactions chimique (1)...(3), des réactions secondaires peuvent avoir lieu entre le HNO_3 et les impuretés de la matière première, réactions qui exercent une influence sur la norme de HNO_3. La norme stoechiométrique d'acide azotique, calculée selon les réactions chimiques possibles entre le HNO_3 et les composants de la roche phosphatique, est calculée à l'aide de l'équation présentée dans le Tableau 5.

Tableau 4

Filtrage — lavage du $Ca(NO_3)_2.4H_2O$

Entrée			Sortie			Valeurs nécessaires
Phase	Composant	Équations de bilan, [Kg/h]	Phase	Composant	Équations de bilan, [Kg/h]	
Solide, $[]_{s_3}$	$Ca(NO_3)_2.4H_2O$	$m_{Ca(NO_3)_2\cdot 4H_2O}=\dfrac{5{,}9m_{[]l_2}(\bar{X}_{Ca[]l_2}-\bar{X}_{Ca[]l_3})}{1-5{,}9\bar{X}_{Ca[]l_3}}$	Liquide, $[]_1$	H_3PO_4	$m_{H_3PO_4[]_l^I}=3{,}161m_{[]_l^I}\bar{X}_{P[]_l^I}$	$m_{[]_s^0}$; $\bar{X}_{P[]l_2}$; $\bar{X}_{N[]l_2}$; $\bar{X}_{Ca[]l_3}$; $\bar{X}_{Ca[]l_2}$; $\bar{X}_{F[]l_2}$; $\bar{X}_{CO_2[]l_2}$; $\bar{X}_{H_2O[]l_2}$; $\bar{X}_{A''[]l_2}$ (Tableau 2)
	Total	$m_{[]s_3}=m_{Ca(NO_3)_2\cdot 4H_2O}$		$Ca(NO_3)_2$	$m_{Ca(NO_3)_2}=4{,}1m_{[]_l^I}\bar{X}_{Ca[]_l^I}$	
Liquide, $[]_{l_3}$	H_3PO_4	$m_{H_3PO_4[]l}=3{,}161m_{[]l_2}\bar{X}_{P[]l_2}$		HNO_3	$m_{HNO_3[]_l^I}=4{,}5m_{[]_l^I}(\bar{X}_{N[]_l^I}-0{,}7\bar{X}_{Ca[]_l^I})$	
	$Ca(NO_3)_2$	$m_{Ca(NO_3)_2[]l_3}=4{,}1m_{[]l_3}\bar{X}_{Ca[]l_3}$		HF	$m_{HF[]_l^I}=1{,}052m_{[]_l^I}\bar{X}_{F[]_l^I}$	$\bar{X}_{HNO_3[]_{l_2}^0}$
	HNO_3	$m_{HNO_3[]l_3}=4{,}5m_{[]l_2}(\bar{X}_{N[]l_2}-0{,}7\bar{X}_{Ca[]l_2})$		CO_2	$m_{CO_2[]_l^I}=m_{[]_l^I}\bar{X}_{CO_2[]_l^I}$	
	HF	$m_{HF[]l_3}=1{,}052m_{[]l_2}\bar{X}_{F[]l_2}$		H_2	$m_{H_2O[]_l^I}=m_{[]_l^I}\bar{X}_{H_2O[]_l^I}$	$\bar{X}_{P_{fII}}$; $\bar{X}_{N_{fII}}$; $\bar{X}_{Ca_{fII}}$; $\bar{X}_{A''_{fII}}$; $\bar{X}_{H_2O_{fII}}$
	CO_2	$m_{CO_2[]l_3}=m_{[]l_2}\bar{X}_{CO_2[]l_2}$		Inerte	$m_{A''[]_l^I}=m_{[]_l^I}\bar{X}_{A''[]_l^I}$	
	H_2O	$m_{H_2O[]l_3}=m_{[]l_2}(\bar{X}_{H_2O[]l_2}-1{,}8\bar{X}_{Ca[]l_2}+$ $+1{,}8m_{[]l_3}\bar{X}_{Ca[]l_3}$		Total	$m_{[]_l^I}=Lm_{[]_s^0}$	
	Inerte	$m_{A''[]l_3}=m_{[]l_2}\bar{X}_{A''[]l_2}$	Solide, $[]_{s^*}$	$Ca(NO_3)_2.4H_2O$	$m_{Ca(NO_3)_2\cdot 4H_2O}=5{,}9m_{[]_{s^*}^I}\bar{X}_{Ca[]_{s^*}^I}$	$\bar{X}_{P[]_l^I}$; $\bar{X}_{Ca[]_l^I}=0{,}35\bar{X}_{P[]_l^I}$; $\bar{X}_{N[]_l^I}=(R_L\bar{X}_{N[]l_2}+0{,}2222A\bar{X}_{HNO_3[]_{l_1}^0}-S\bar{X}_{N[]_s^*}-F\bar{X}_{N_{fII}})/L$; $\bar{X}_{P[]_l^I}=R_L\bar{X}_{F[]l_2}/L$; $\bar{X}_{CO_2[]_l^I}=R_L\bar{X}_{[]_2[]l_2}/L$; $\bar{X}_{A''[]_l^I}=0{,}935\bar{X}_{A''[]_s^0}/L$; $\bar{X}_{H_2O[]_l^I}=1-4{,}5\bar{X}_{N[]_l^I}-0{,}85\bar{X}_{Ca[]_l^I}-3{,}161\bar{X}_{P[]_l^I}-$ $-1{,}052\bar{X}_{F[]_l^I}-\bar{X}_{CO_2[]_l^I}-\bar{X}_{A''[]_l^I}$
	Total	$m_{[]l_3}=m_{[]l_2}(1-5{,}9\bar{X}_{Ca[]l_2})/(1-5{,}9\bar{X}_{Ca[]l_3})$		$4H_2O$		
Liquide, $[]_{l_2^0}$	HNO_3	$m_{HNO_3[]l_2^0}=m_{[]l_2^0}\bar{X}_{HNO_3[]l_2^0}$		HNO_3	$m_{NHO_3[]_{s^*}^I}=4{,}5m_{[]_{s^*}^I}(\bar{X}_{N[]_{s^*}^I}-0{,}7\bar{X}_{Ca[]_{s^*}^I})$	
	H_2O	$m_{H_2O[]l_2^0}=m_{[]l_2^0}(1-\bar{X}_{HNO_3[]l_2^0}$		H_2O	$m_{H_2O[]_{s^*}^I}=m_{[]_{s^*}^I}(\bar{X}_{H_2O[]_{s^*}^I}-1{,}25\bar{X}_{Ca[]_{s^*}^I})$	
	Total	$m_{[]l_2^0}=Am_{[]_s^0}$		Total	$m_{[]_{s^*}^I}=Sm_{[]_s^0}$	
Liquide, $[]_{l_3^0}$	H_2O	$m_{H_2O[]l_2^0}=m_{[]l_3^0}$	Filtré, $[]_{fII}$	H_3PO_4	$m_{H_3PO_4f_{II}}=3{,}161m_{f_{II}}\bar{X}_{P_{f_{II}}}$	
	Total	$m_{[]_3^0}=Wm_{[]_s^0}$		$Ca(NO_3)_2$	$m_{Ca(NO_3)_2f_{II}}=4{,}1m_{f_{II}}\bar{X}_{Ca_{f_{II}}}$	
				HNO_3	$m_{NNO_3f_{II}}=4{,}5m_{f_{II}}(X_{N_{f_{II}}}-0{,}7\bar{X}_{Ca_{f_{II}}})$	
				H_2O	$m_{H_2O_{f_{II}}}=m_{f_{II}}\bar{X}_{H_2O_{f_{II}}}$	
				Inerte	$m_{A''_{f_{II}}}=m_{f_{II}}\bar{X}_{A''_{f_{II}}}$	
				Total	$m_{f_{II}}=Fm_{[]_s^0}$	R_L, L, A, W, S, F

Tableau 2

Désagrégation nitrique

Entrée			Sortie			Valeurs nécessaires
Phase	Composant	Équations de bilan, [Kg/h]	Phase	Composant	Équations de bilan, [Kg/h]	
Solide, $[]_s^0$	$Ca_3(PO_4)_2$	$m_{Ca_2(PO_4)_2[]_s^0} = 2{,}183 m_{[]_s^0} \bar{X}_{P_2O_5[]_s^0}$	Liquide, $[]_{l_2}$	H_3PO_4	$m_{H_3PO_4[]_l^2} = 3{,}161 m_{[]l_2} \bar{X}_{P[]l_2}$	$m_{[]_s}^0$; $\bar{X}_{P_2O_3[]_s^0}$; $\bar{X}_{CaO[]_s^0}$; $\bar{X}_{CaO[]_s^0}$; $\bar{X}_{F[]_s^0}$; $\bar{X}_{CO_2[]_s^0}$; $\bar{X}_{H_2O[]_s^0}$; $\bar{X}_{Fe_2O_3[]_s^0}$; $\bar{X}_{Al_2O_3[]_s^0}$; $\bar{X}_{K_2O[]_s^0}$; $\bar{X}_{A''[]_s^0}$
	CaF_2	$m_{CaF_2[]_s^0} = 2{,}052 m_{[]_s^0[]} \bar{X}_{F_s^0}$		$Ca(NO_3)_2$	$m_{Ca(NO_3)_2[]l_2} = 4{,}1 m_{[]l_2} \bar{X}_{Ca[]l_2}$	
	$CaCO_3$	$m_{CaCO_3[]_s^0} = 2{,}272 m_{[]_s^0} \bar{X}_{CO_2[]_s^0}$		HNO_3	$m_{HNO_3[]l_2} = 4{,}5 m_{[]l_2} (\bar{X}_{N[]l_2} - 0{,}7 \bar{X}_{Ca[]l_2})$	$\bar{X}_{N[]_l^0}$; $\bar{X}_{P[]_l^0}$; $\bar{X}_{Ca[]_l^0}$; $\bar{X}_{H_2O[]_l^0}$; $\bar{X}_{A''[]_l^0}$; (Tableau 1)
	CaO*	$m_{CaC_3[]_s^0} = m_{[]_s^0} (1 - \bar{X}^*_{CaO[]_s^0} - X_{H_2O[]_s^0} - X_{A''[]_s^0})$		HF	$m_{HF[]l_2} = 1{,}052 m_{[]l_2} \bar{X}_{F[]l_2}$	$\bar{X}_{F[]_{g2}}$; $\bar{X}_{N[]_{g2}}$; $X_{CO_2[]_{g2}}$; $\bar{X}_{H_2O[]_{g2}}$
	H_2O	$m_{H_2O[]_s^0} = m_{[]_1^0} \bar{X}_{H_2O[]_s^0}$		H_2O	$m_{H_2O[]l_2} = m_{[]l_2} \bar{X}_{H_2O[]l_2}$	$\bar{X}_{P[]l_2} = \dfrac{0{,}4366 \bar{X}_{P_2O_5[]_s^0} + F \bar{X}_{PfII}}{R_L}$
	Inerte	$m_{A''[]_s^0} = m_{[]_s^0} \bar{X}_{A''[]_s^0}$		CO_2	$m_{CO_2[]l_2} = m_{[]l_2} \bar{X}_{CO_2[]l_2}$	$\bar{X}_{N[]l_2} = \dfrac{R_D \bar{X}_{N[]_l^0} - G \bar{X}_{N[]_{g2}}}{R_D}$
	Total	$m_{[]_s^0} = \Sigma m_{A[]_s^0}$		Inerte	$m_{A''[]l} = m_{[]l_2} \bar{X}_{A''[]l_2}$	$\bar{X}_{Ca[]l_2} = \dfrac{0{,}7142 \bar{X}_{CaO[]_s^0} + F \bar{X}_{CafII}}{R_L}$
	Obs. CaO*—CaO non lié du P, F et CO_2 $X_{CaO^*[]_s^0}$ — fraction de CaO lié du P, F et CO_2			Total	$m_{[]l_2} = R_L m_{[]_s^0}$	$\bar{X}_{F[]l_2} = \dfrac{\bar{X}_{N[]_s^0} - G \bar{X}_{P[]_{g_2}}}{R_L}$
Liquide, $[]_l^0$	HNO_3	$m_{HNO_3[]_l^0} = 4{,}5 m_{[]_l^0} (\bar{X}_{N[]_l^0} - 0{,}7 \bar{X}_{Ca[]_l^0})$	Gaz, $[]_{g_2}$	HF	$m_{HF[]_{g2}} = 1{,}052 m_{[]_{g2}} \bar{X}_{F[]_{g2}}$	$\bar{X}_{CO_2[]l_2} = \dfrac{\bar{X}_{CO_2[]_s^0} - G \bar{X}_{CO_2[]_{g_2}}}{R_L}$
	H_3PO_4	$m_{H_3PO_4[]_l^0} = 3{,}161 m_{[]_l^0} \bar{X}_{P[]_l^0}$		CO_2	$m_{CO_2[]_{g2}} = m_{[]_{g2}} \bar{X}_{CO_2[]_{g_2}}$	$\bar{X}_{A''[]l_2} = \dfrac{\bar{X}_{A''[]_s^0} + F \bar{X}_{A''fII} - R_s \bar{X}_{A''[]_s^0}}{R_L}$
	$Ca(NO_3)_2$	$m_{Ca(NO_3)_2[]_l^0} = 4{,}1 m_{[]_l^0} X_{Ca[]_l^0}$		H_2O	$m_{H_2O[]_{g2}} = m_{[]_{g2}} \bar{X}_{H_2O[]_{g_2}}$	$\bar{X}_{H_2O[]l_2} = 1 - 4{,}5 \bar{X}_{N[]l_2} - 0{,}95 \bar{X}_{Ca[]l_2} - 3{,}16 \bar{X}_{P[]l_2} - 1{,}052 \bar{X}_{P[]l_2} - \bar{X}_{CO_2[]l_2} - \bar{X}_{A''[]l_2}$
	H_2	$m_{H_2O[]_l^0} = m_{[]_l^0} \bar{X}_{H_2O[]_l^0}$		HNO_3	$m_{HNO_3[]_{g_2}} = 4{,}5 m_{[]_{g2}} \bar{X}_{N[]_{g2}}$	R_D, R_L, R_s, G, F
	Inerte	$m_{A''[]_l^0} = m_{[]_l^0} \bar{X}_{A''[]_l^0}$		Total	$m_{[]_{g2}} = G m_{[]_s^0}$	
	Total	$m_{[]_l^0} = R_D m_{[]_s^0}$	Solide, $[]_{s_2}$	Inerte	$m_{A''[]_{s2}} = m_{[]_{s2}} \bar{X}_{A''[]_{s_2}}$	
				Total	$m_{[]_{s2}} = R_S m_{[]_s^0}$	

La dépense spécifique d'acide azotique, D_R, appelée frequemment „taux de digestion", comprend également l'excès d'acide azotique (E) et s'exprime par l'équation :

$$D_R = N + E.$$

Le Tableau 2 présente les équations de bilan de masse, les valeurs nécessaires et les relations pour leur calcul. Les relations de définition et de calcul pour les rapports spécifiques entre les phases sont présentées dans le Tableau 5.

Le processus de cristallisation du $Ca(NO_3)_2 \cdot 4H_2O$ est réalisé on refroidissant indirectement la solution avec de la soude dans les conditions spécifiques du processus Norsk-Hydro établies selon l'analyse de l'équilibre dans le système de double change [9], [10] :

$$Ca_3(PO_4)_2 + H_6(NO_3)_6 \rightleftarrows H_6(PO_4)_2 + Ca_3(NO_3)_6.$$

L'équation caractéristique du processus est :

$$[H_3PO_4 + HNO_3 + Ca(NO_3)_2 + HF + CO_2 + H_2O + A'']_{l_2} \rightarrow \{[Ca(NO_3)_2 \cdot 4H_2O]_{s_3} +$$
$$+ [H_3PO_4 + HNO_3 + Ca(NO_3)_2 + HF + CO_2 + H_2O + A''']_{l_1}\}^*_{s_3}.$$

Le processus de transformation indépendant est :

$$Ca(NO_3)_2 + 4H_2O = Ca(NO_3)_2 \cdot 4H_2O.$$

Les équations de bilan de masse et les valeurs nécessaires sont présentées dans le Tableau 3.

Le processus de filtrage — lavage se réalise en deux étapes : I. séparation du solide humide non-lavé qui contient encore du HNO_3, du H_3PO_4, de l'eau et d'autres composants ; II. lavage du solide humide tout d'abord avec de l'acide azotique frais pour faire disparaître l'acide phosphorique et ensuite avec de l'eau pour récupérer l'acide azotique retenu par le solide. Après la I-ère étape de filtrage on obtient la solution mère, $[\ ]_{l^I}$, dirigée vers l'installation de neutralisation.

Après la II-ème étape il résulte de l'acide de recyclage (f_{II}) et du $Ca(NO_3)_2 \cdot 4H_2O$ dirigé vers l'installation de conversion.

Les équations caractéristiques du processus de filtrage—lavage sont :

I-ère étape :

$$\{[Ca(NO_3)_2 \cdot 4H_2O]_{s_3} + [H_3PO_4 + HNO_3 + Ca(NO_3)_2 + HF + CO_2 +$$
$$+ H_2O + A'']_{l_3}\}_{susp_3} \rightarrow$$
$$\rightarrow \{[Ca(NO_3)_2 \cdot 4H_2O]_{s_4} + H_3[PO_4 + HNO_3 + Ca(NO_3)_2 + H_2O + A'']_{l_4}\}^*_{s_4} +$$
$$+ [H_3PO_4 + HNO_3 + Ca(NO_3)_2 + HF + CO_2 + H_2O + A'']_{l^I}.$$

II-ème étape :

$$\{[Ca(NO_3)_2 \cdot 4H_2O]_{s_4} + [H_3PO_4 + HNO_3 + Ca(NO_3)_2 + H_2O + A'']_{l_4}\}^*_{s_4} +$$
$$+ [HNO_3 + H_2O]^0_{l_2} + [H_2O]^0_{l_3} \rightarrow \{[Ca(NO_3)_2 \cdot 4H_2O]_{s^I} +$$
$$+ [H_2O + HNO_3]_{l^*}\}_{s^{I^*}} + [H_3PO_4 + HNO_3 + Ca(NO_3)_2 + H_2O + A'']_{f\,II}.$$

Tableau 3

Cristallisation du $Ca(NO_3)_2.4H_2O$

Entrée			Sortie			Valeurs nécessaires
Phase	Composant	Équations de bilan, [Kg/h]	Phase	Composant	Équations de bilan, [Kg/h]	
Liquide $[]l_2$	H_3PO	$m_{H_3FO_4[]l_2}=3,161m_{[]l_2}\bar{X}_{P[]l_2}$	Solide $[]s_3$	$Ca(NO_3)_2.4H_2O$	$m_{Ca(NO_3)_2\cdot 4H_2O[]s_2}=5,9m_{[]l_2}\times$ $\times\left(\bar{X}_{Ca[]l_2}-\frac{1-5,9\bar{X}_{Ca[]l_2}}{1-5,9\bar{X}_{Ca[]l_3}}\bar{X}_{Ca[]l_3}\right)$	$m^0_{[]s}$
	$Ca(NO_3)_2$	$m_{Ca(NO_3)_2[]l_2}=4,1m_{[]l_2}\bar{X}_{Ca[]l_2}$				$\bar{X}_{Ca[]l_3}$
	HNO_3	$m_{HNO_3[]l_2}=4,5m_{[]l_2}(\bar{X}_{N[]l_2}-0,7\bar{X}_{Ca[]l_2})$				$\bar{X}_{P[]l_2}$
	HF	$m_{HF[]l_3}=1,052m_{[]l_2}\bar{X}_{F[]l_2}$				$\bar{X}_{N[]l_2}$
	CO_2	$m_{CO_2[]l_2}=m_{[]l_2}\bar{X}_{CO_2[]l_2}$		Total	$m_{[]s_3}=5,9\frac{m_{[]l_2}(\bar{X}_{Ca[]l_2}-\bar{X}_{Ca[]l_2})}{1-5,9\bar{X}_{Ca[]l_3}}$	$\bar{X}_{Ca[]l_2}$
	Inerte	$m_{A''[]l_2}=m_{[]l_2}\bar{X}_{A''[]l_2}$				$\bar{X}_{F[]l_2}$
	Total	$m_{[]l_2}=R_Lm^0_{[]s}$	Liquide $[]l_3$	H_3PO_4	$m_{H_3PO_4[]l_3}=3,161m_{[]l_2}\bar{X}_{P[]l_2}$	$\bar{X}_{CO_2[]l_2}$
				$Ca(NO_3)_2$	$m_{Ca(NO_3)_2[]l_3}=4,1m_{[]l_2}\bar{X}_{Ca[]l_3}$	$\bar{X}_{A''[]l_2}$
				HNO_3	$m_{HNO_3[]l_3}=4,5m_{[]l_2}(\bar{X}_{N[]l_2}-0,7\bar{X}_{Ca[]l_2})$	$\bar{X}_{H_2O[]l_2}$
				HF	$m_{HF[]l_3}=1,052m_{[]l_2}\bar{X}_{F[]l_2}$	(Tableau 2)
				CO_2	$m_{CO_2[]l_3}=m_{[]l_2}\bar{X}_{CO_2[]l_2}$	. . . . .
				H_2O	$m_{H_2O[]l_3}=m_{[]l_2}(\bar{X}_{H_2O[]l_2}-1,8\bar{X}_{Ca[]l_2})+$ $+1,8m_{[]l_3}\bar{X}_{Ca[]l_3}$	R_L
				Inerte	$m_{A''[]l_3}=m_{[]l_2}\bar{X}_{A''[]l_2}$	
				Total	$m_{[]l_3}=\frac{m_{[]l_2}(1-5,9\bar{X}_{Ca[]l_2})}{1-5,9\bar{X}_{Ca[]l_3}}$	

Tableau 5

Rapports entre les phases spécifiques

No. crt.	Relations de définition	Relations de calcul
1	$R_L^{00}=m_{[]l_1}^0/(m_{[]l_1}^0+m_{fII})$	$R_L^0=(D_R-A\bar{X}^0_{HNO_3})/R_D\bar{X}^0_{HNO_3}$; $D_R=N+E$ $N=2{,}25\bar{X}_{CaO[]_s^0}+2{,}362\bar{X}_{Fe_2O_3[]_s^0}+3{,}706\bar{X}_{Al_2O_3[]_s^0}+1{,}340\bar{X}_{K_2O[]_s^0}$
2	$R_L=m_{[]l2}/m_{[]_s^0}$	$R_L=L(\bar{X}_{P[]l_I}-\bar{X}_{P[]s_I^*})/(\bar{X}_{P[]l2}-\bar{X}_{P[]s_4^*})$
3	$R_D=(m_{[]_{l_1}^0}+m_{FII})/m_{[]_s^0}$	$R_D=\dfrac{R_L\bar{X}_{N[]l2}\bar{X}_{PfII}+G\bar{X}_{N[]_{l2}}\bar{X}_{PfII}-(R_L\bar{X}_{P[]l2}-0{,}4366\bar{X}_{P_2O_5[]_s^0})(\bar{X}_{NfII}-0{,}222\bar{X}^0_{HNO_3})}{0{,}222\bar{X}^0_{HNO_3}\bar{X}_{PfII}}$
4	$G=m_{[]_{l_2}}/m_{[]_s^0}$	$G=1+R_D-R_L-R_S$
5	$L=m_{[]l}/m_{[]_s^0}$	$L=0{,}4366\bar{X}_{P_2O_5[]_s^0}/\bar{X}_{P[]l_I}$
6	$S=m_{[]_s^*}/m_{[]_s^0}$	$S=(0{,}7143\bar{X}_{CaO[]_s^0}-L\bar{X}_{Ca[]_l^I}/\bar{X}_{Ca[]_s^*I}$
7	$F=m_{FII}/m_{[]_s^0}$	$F=\bar{X}_{P[]_{s_4}^*}(R_L-L)/\bar{X}_{PfII}$
8	$A=m_{[]l_2^0}/m_{[]_s^0}$	$A=\dfrac{4{,}5}{\bar{X}^0_{HNO_3}}[F(\bar{X}_{NFII}-0{,}7\bar{X}_{Ca_fII})+S(\bar{X}_{N[]_s^*I}-0{,}7\bar{X}_{Ca[]_s^*I})-R_L(\bar{X}_{N[]l2}-0{,}7\bar{X}_{Ca[]l2})+$ $+L(\bar{X}_{N[]l_I}-0{,}7\bar{X}_{Ca[]l_I})]$
9	$W=m_{[]l_3^0}/m_{[]_s^0}$	$W=L+S+F-R_L-A$
10	$R_S=m_{[]s2}/m_{[]_s^0}$	$R_S=0{,}065\bar{X}_{A''[]_s^0}$

Lorsqu'on a établi les équations de bilan de masse on a eu également en vue la dissolution partielle du $Ca(NO_3)_2$ pendant le processus de lavage. Le Tableau 4 présente les équations de bilan de masse pour le processus de filtrage — lavage, les valeurs nécessaires et les relations de définition et de calcul des rapports entre les phases.

3. Vérification des modèles de bilan de masse

Les modèles de bilan de masse pour les processus qui interviennent dans celui technologique de „désagrégation nitrique" sont utilisés pour calculer le bilan de masse théorique et réel.

Pour vérifier les modèles de bilan on a calculé le bilan de masse dans les conditions où l'on utilise la phosphatite de Maroc dont la composition est :

$$\bar{X}_{P_2O_5[]_s^0} = 0{,}3579\,; \quad \bar{X}_{F[]_s^0} = 0{,}03698\,; \quad \bar{X}_{CO_2[]_s^0} = 0{,}009\,;$$

$$\bar{X}_{CaO[]_s^0} = 0{,}547\,; \quad \bar{X}_{CaO[]_s^0} \text{ lié au P, F et } CO_2 = 0{,}4894\,;$$

$$\bar{X}_{H_2O[]_s^0} = 0{,}005\,; \quad \bar{X}_{A'[]_s^0} = 0{,}0596.$$

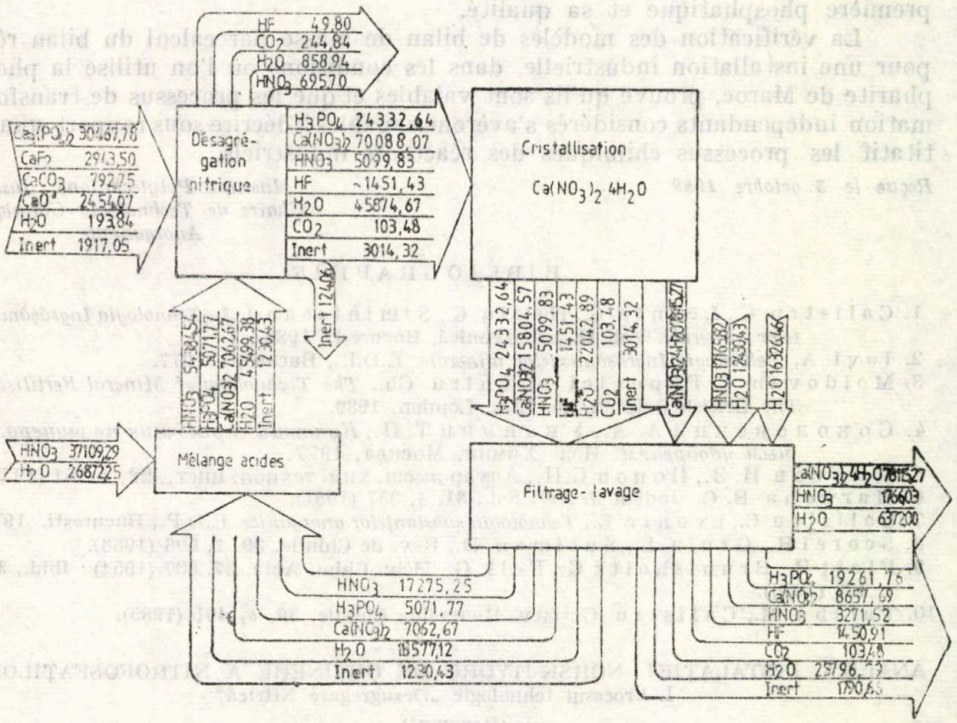

Fig. 3. — Bilan de masse pour le processus technologique de désagrégation nitrique.

Le débit de masse de la roche phosphatique est $m[]_s^0 = 38\,769$ Kg/h; les valeurs nécessaires ont été extraites des données pratiques ; on utilise de

l'acide azotique de 58%, la norme stoechiometrique d'acide azotique est $N=1{,}266$, $D_R=1{,}4$, ce qui correspond à un excès de HNO_3, $E=13{,}4\%$.

En utilisant les modèles de bilan de masse présentés dans les Tableaux 1...4 on calcule le bilan réel pour les processus composants et pour le processus global de „désagrégation" ; les résultats sont présentés sous la forme de schéma du bilan dans la Fig. 3.

Les résultats du calcul permettent de constater que le bilan de masse est confirmé tant pour les processus composants que pour celui global, ce qui prouve que les équations de bilan sont correctes et que les processus de transformation indépendants considérés caractérisent du point de vue quantitatif les processus chimiques des réacteurs industriels.

4. Conclusions

La solution rigoureusement scientifique des problèmes technologiques de l'installation Norsk-Hydro pour l'obtention des engrais complexes suppose l'élaboration et l'utilisation des modèles de bilan de masse. On a élaboré les modèles de bilan de masse pour les processus composants et pour celui technologique de „désagrégation nitrique", en corrélant, par des rapports spécifiques, les débits de produits finis et intermédiaires avec le débit de matière première phosphatique et sa qualité.

La vérification des modèles de bilan de masse par calcul du bilan réel pour une installation industrielle, dans les conditions où l'on utilise la phospharite de Maroc, prouve qu'ils sont valables et que les processus de transformation indépendants considérés s'avèrent capables à décrire sous rapport quantitatif les processus chimiques des réacteurs industriels.

Reçue le 3 octobre 1989

Institut Polytechnique, Jassy,
Chaire de Technologie Chimique Anorganique

BIBLIOGRAPHIE

1. Calistru C., Leonte C., Hagiu C., Siminiceanu I., *Tehnologia îngrășămintelor minerale*. Vol. II, Ed. Tehnică, București, 1984.
2. Iovi A, *Tehnologia îngrășămintelor minerale*. E.D.P., București, 1977.
3. Moldovan I., Popovici N., Chiru Gh., *The Technology of Mineral Fertilisers*. The British Sulphur Co. Ltd., London, 1989.
4. Соколовский А. А., Унанянц Т. П., *Краткий справочник по минеральным удобрениям*. Изд. Химия, Москва, 1977.
5. Кирсев И. З., Попов С.Н., Ануар высш. хим. технол. инст., **22**, *3*, 161 (1977).
6. Marwaha B. C., Indian J. Agr. Sci., **51**, *5*, 357 (1981).
7. Calistru C., Leonte C., *Tehnologia substanțelor anorganice*. E.D.P., București, 1972.
8. Scorei R., Gruia L., Sutiman D., Rev. de Chimie, **39**, *7*, 606 (1988).
9. Flatt R., Brunisholtz G., Fell G., Helv. Chim. Acta, **37**, 607 (1954) ; Ibid., **39**, 473 (1956).
10. Talabă M., Calistru C., Rev. Roumaine Chimie, **30**, *6*, 491 (1985).

ANALIZA INSTALAȚIEI NORSK-HYDRO DE OBȚINERE A NITROFOSFAȚILOR
I. Procesul tehnologic „Dezagregare Nitrică"

(Rezumat)

Analiza instalației de obținere a nitrofosfaților implică cunoașterea și utilizarea documentației de inginerie chimică pe baza căreia se pot evidenția posibilitățile de perfecționare a tehnologiei. Se elaborează și se verifică modelele de bilanț de masă pentru procesele de dezagregare nitrică, amestecare acizi, răcire—cristalizare $Ca(NO_3)_2 \cdot 4H_2O$ și filtrare—spălare, precum și pentru procesul tehnologic „dezagregare nitrică", într-o formă adecvată analizei pe calculator.

BULETINUL INSTITUTULUI POLITEHNIC DIN IAŞI
Tomul XXXVII (XLI), Fasc. 1—4, 1991
Secţia II
CHIMIE ŞI INGINERIE CHIMICĂ

D.C. 546.284.287 ; 54.07

THE MODELLING OF PHENYLCHLOROSILANE SYNTHESIS

BY

GH. CRISTIAN, N. VOICULESCU, MARIANA PINTEALĂ, RADU OGHINĂ, DANIELA CRISTIAN and RODINEL ARDELEANU

1. Introduction

The phenylchlorosilane synthesis is one of the fluid—solid reactions, well known in chemical and metalurgical industry. Among the industrial processes which imply these reactions are known ; sulphide oxidation, metal oxide reduction, combustions, coal gazeification, catalyst regeneration, thermal decomposition of some organic or inorganic substances, etc. These reactions are accompanied by mass and heat transfer.

At the reaction basis between a solid and a component in fluid phase the following elementary processes can be mentioned : the reactant diffusion from the fluid phase through the external limit layer to solid surface, the diffusion inside the solid when this is porous one and the chemical reaction. Each of these elementary processes is characterised with specifical coefficients, namely: a) external diffusion with the individual coefficient of mass transfer; b) internal diffusion with the effective diffusion coefficient ; c) chemical reaction with the constant of reaction velocity and the reaction order.

If the chemical reaction is accompanied by a thermal effect, then the heat transfer must be added to the above mentioned elementary processes. In many cases the mass and heat transfer are the determinant steps of the process, influencing significantly the velocity of chemical reaction.

A great number of fluid—solid reactions take place according to the following scheme ;

$$aA(g) + B(s) \rightarrow \text{products} \pm \Delta H_r . \tag{1}$$

The mechanism of these reactions can be described by some models presented in the literature on which basis an unitary theory has been established [1] ... [6].

If the solid particle is porous, then there are three models for the chemical reactions : heterogeneous, homogeneous and general. The fundamental criterion to establish the model of the chemical reaction is the non-dimensional thickness of the reaction zone, λ_p, which is the ratio between the thickness of the reaction zone and the granule radius. Depending on the ratio between the rates of elementary processes, the thickness of reaction zone has a value between zero and granule radius, and the non-dimensional thickness varies between zero and one.

When the chemical reaction velocity is much higher than the diffusion velocity of the reactant in pores of the solid, the chemical reaction takes places on a surface which is moving inside the granule leaving an ash layer. The model of this process is named *heterogeneous*.

If the chemical reaction velocity is much smaller than the diffusion velocity of the reactant in the pores of the solid, then the reactant of the gaseous phase will diffuse in all the granule volume. In this case it can be considered that the chemical reaction takes place in all the granules and the model which describes a such reaction is *homogeneous*.

In practice, there are cases in which the chemical reaction velocity is of the same order with the diffusion velocity inside the granule. The chemical reaction takes place in a zone of certain thickness and the model is general or with a limited zone of reaction.

Differences between these models are given by the number of steps and by the existing zones in each step.

The fluid—solid reactions may take place with or without modifications of the solid dimensions during the chemical process.

The solid granules do not modify their dimensions if in the granule there are large quantities of impurities which remains as nonbreakable ash, or after the reaction a hard solid product results. The solid particles modify their dimensions when the granule is pure and fluid products result from reaction.

This paper presents a physical model of the silicon granule and establish the mathematical model for the reaction velocity as a function of the resistance of elementary processes which are implied in the global one.

2. The Physical Model

The study regarding organohalogenosilane synthesis shows that during the reaction, the solid phase is consumed, which leads to the decrease of the dimensions of spherical particles [7]...[10]. The contact mixture Si — Cu is considered nonporous so that the reaction takes place on a surface and will go on according to the heterogeneous model. It is possible that a part of silicon granules are composed a microparticle agglomeration, known in the literature under the name granule-microparticle model [1]. In this paper we consider the solid as being a compact and continuous phase whose dimensions modify in time due to the chemical reaction (Fig. 1).

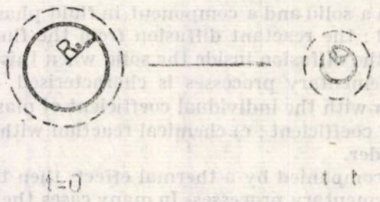

Fig. 1. — The variation of solid particle dimension in time.

Generally the chemical reaction between monochlorobenzene and silicon could be represented as follows:

$$(2) \qquad a C_6H_5Cl + Si \xrightarrow[\text{promotors}]{Cu} \text{fluid products.}$$

In connection with the mechanism of phenylchlorosilane synhesis it was shown that in the absence of catalyst the reaction between Si and organic halide takes place by adding hydrochloric acid or by increasing of the temperature and the organic halide decomposed yielding hydrochloric acid. The transfer of chlorine to Si is essential for the phenylchlorosilane formation [7]. Also the catalytic efect of certain metals particularly of copper, has been evidenced. Using the contact mixture Si — Cu it seems that the highest probability for the reaction process in organic halide — Si — Cu sistem is the alloy surface. It is assumed that the organic halide is adsorbed on the contact mixture simultaneously with the C — Cl bond breaking and the formation of a Si — Cu bond. The catalytic activity of copper has been evidenced by the increase of the reaction velocity and the selectivity. The composition of the reaction products is determined by the following factors: temperature, util-

ized procedure, process duration, composition and preparation method of contact mixture.

The elementary processes are the follows:

a) the monochlorobenzene diffusion through gas layer around the granule ;

b) the adsorption on external surface of contact mixture ;

c) the chemical reaction ;

d) the diffusion of reaction products through external limit layer to the principal mass of gas.

The determinant steps of the process could be the chemical reaction and the diffusion through the external limit layer.

3. The Mathematical Model

In order to construct the theoretical model of the phenylchlorosilane reaction progress we need the next simplyfing hypotheses: a) the quasi-stationary regime for reactant in gaseous phase; b) the solid particles have spherical shape ; c) the temperature gradient in the granule are neglected ; d) the solid reactant is uniformly distributed in granule ; e) activation energy, gas diffusion, densities, specific heats and reaction heat are considered constant and at the medium values of the temperature inside reactor.

In these conditions the reaction (2) can be considered of the first order towards the gaseous reactant and the reaction velocity is direct proportional to the reaction surface.

The experimental studies of the phenylchlorosilane synthesis show that the diffusion through the gas layer and the chemical reaction influence the process [12]. In these conditions the concentration variation of monochlorobenzene through external limit layer is linear according to the two layer model (Fig. 2).

The reaction velocity can be described as a function of the external surface of the granule for a given time by taken into account the two elemental resistances : gas layer resistance and the resistance due to the chemical reaction.

In order to obtain the reaction velocity equation it is necessary to write the reactant flux which diffuses through the external limit layer :

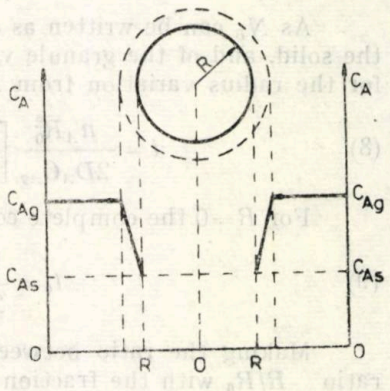

Fig. 2. — The variation of reactant concentration from gaseous phase.

$$-r_A = -r_B = -\frac{1}{S_{ext}} \cdot \frac{dN_B}{dt} = k_{Ag}(C_{Ag} - C_{As}). \tag{3}$$

This flux is equal to the one of surface granule :

$$-r_A = -r_B = -\frac{1}{S_{ext}} \cdot \frac{dN_B}{dt} = k_s C_{As}. \tag{4}$$

By elimination of the surface concentration from Eqs. (3) and (4), the reaction velocity equation is obtained as follows:

$$(5) \qquad -r_A = -r_B = -\frac{1}{S_{ext}} \cdot \frac{dN_B}{dt} = \frac{1}{1/k_{Ag} + 1/k_s} C_{Ag}.$$

The gas layer resistances and the resistance due to the chemical reaction varies during the process because of the modifications of the solid particle dimensions. To prove this fact it is necessary to write the reaction velocity equation as a function of initial external surface of the granule:

$$(6) \qquad -r_B = -\frac{1}{S_{ext}} \cdot \frac{dN_B}{dt} = \frac{1}{\frac{R_0^2}{R^2}\left(\frac{1}{k_{Ag}} + \frac{1}{k_s}\right)} C_{Ag}.$$

In the same time with the decrease of the solid particle dimensions the gas layer resistance and the resistance due to the chemical reaction increase. The gas layer resistance is a function both of the granule dimension and the relative velocity between particle and fluid and of the fluid properties. These factors has been correlated using an experimental data basis by the semiempirical nondimensional equations. The variation of the individual mass transfer coefficient can be expressed by the following relation, when the particles fall down in Stokes domain [11]:

$$(7) \qquad k_{Ag} = \frac{D_A}{Rn_A}.$$

As N_B can be written as a function of molar density of reactant B from the solid, and of the granule volume from Eqs. (5) and (7), the reaction time for the radius variation from R_0 to R can be calculated;

$$(8) \qquad t = \frac{n_A R_0^2}{2D_A C_{Ag}} \left[\left(1 - \frac{R^2}{R_0^2}\right) + \frac{2D_A}{n_A R_0 k_s}\left(1 - \frac{R}{R_0}\right)\right].$$

For $R=0$ the complete conversion time of the particle is obtained:

$$(9) \qquad t_0 = \frac{n_A R_0^2}{2D_A C_{Ag}}\left(1 + \frac{2D_A}{n_A R_0 k_s}\right).$$

Making the ratio between equations (8) and (9) and substituting the ratio R/R_0 with the fraction of nonconverted solid-reactant, the following equation is obtained:

$$(10) \qquad \frac{t}{t_0} = 1 - \frac{1}{1+k'}(1-X_B)^{2/3} - \frac{k'}{1+k'}(1-X_B)^{1/3},$$

where

$$k' = \frac{2D_A}{n_A R_0 k_s}.$$

This equation allows a graphical representation of $1-X_B$ vs. t/t_0 for different values of k' (Fig. 3). Theoretically the k' values varies between zero and

infinite. For $k'=0$ chemical reaction does not oppose any resistance to the progress of the chemical process and Eq. (10) becomes:

$$\frac{t}{t_0} = 1-(1-X_B)^{2/3}. \tag{11}$$

For $k' \to \infty$ the diffusion through the gas layer does not oppose any resistance to transfer and Eq. (10) becomes:

$$\frac{t}{t_0} = 1-(1-X_B)^{1/3}. \tag{12}$$

From the Fig. 3 it can be seen that the domain of variation of k' is practically comprised between 0 and 10. When $k>10$ it can be considered that the gas layer doesn't oppose any resistance to the chemical process. Big values for k' are obtained either during a rapid diffusion of the reactant from the gaseous phase through the exterior limit layer or in the case of reaction which goes with slow rate or when the solid particles are of big sizes.

According to Fig. 3 the value of the conversion of solid can be calculated in every moment if the size of particles and their complete conversion time is known.

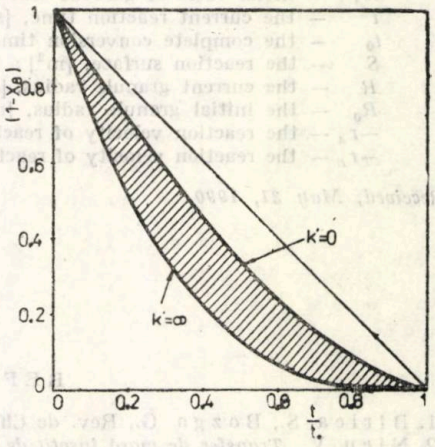

Fig. 3. — Variation of the fractions of non-reacted solid reactant as a function of the ratio t/t_0.

Experimental studies regarding the synthesis of phenylchlorosilanes have showed that the reaction velocity decreases much in the final step of the process, although the optimal conditions of this process has been established [12]. That can be explained by the fact that at the reaction temperature of about 450°C the decomposition of certain organic compounds takes place giving rise to coal which covers the contact mixture Si — Cu. This phenomenon leads to supplementary resistance towards the diffusion of the reactant from gaseous phase to the reaction surface and this resistance must be considered when selecting and designing the reactor for the synthesis of phenylchlorosilanes.

4. Conclusions

The synthesis of phenylchlorosilanes consists of a heterogeneous fluid — solid reaction which goes according to the heterogeneous model on the contact surface between the two phases. For the solid phase a physical model has been proposed and the equation of the reaction velocity has been obtained on its basis. An equation for the conversion as a function of reaction time has been established.

Notations

a — stoechiometric coefficient ;
A — the reactant in gaseous phase ;
B — the reactant in solid phase ;
C_{As} — the reactant concentration in gaseous phase on the solid surface, [mol/m^3] ;
C_{Ag} — the reactant concentration in gaseous phase, [mol/m^3] ;
C_{B0} — the reactant concentration in solid phase, [mol/m^3] ;
D_A — the reactant A diffusion coefficient, [m^2/s] ;
k_{Ag} — the individual mass transfer coefficient through the gas layer, [m/s] ;
k_s — the reaction velocity constant versus surface, [m/s] ;
n_A — molar ratio of gaseous reactant ;
t — the current reaction time, [s] ;
t_0 — the complete conversion time of the solid, [s] ;
S — the reaction surface, [m^2] ;
R — the current granule radius, [m] ;
R_0 — the initial granule radius, [m] ;
$-r_A$ — the reaction velocity of reactant A, [mol/m^2·s] ;
$-r_B$ — the reaction velocity of reactant B, [mol/m^2·s].

Received, May 31, 1990

Polytechnic Institute, Jassy,
Department of Chemical Engineering
and
Macromolecular Chemistry Institute,
„P. Poni", Jassy

REFERENCES

1. Bîrlea S., Bozga G., Rev. de Chimie, **40**, *12*, 989 (1989).
2. Nicu V., *Transfer de masă însoţit de reacţie chimică necatalitică în sisteme solid—fluid.* Ph. D. Diss., Polyt. Inst., Jassy, 1984.
3. Tudose R. Z., Bul. Inst. polit., Iaşi, **XVI** (**XX**), *1—2*, 241 (1970).
4. Yagi S., Kunii D., Fifth Symposium (International) on Combustion. Reinhold, New-York, 1955.
5. Wen C. Y., Ind. Eng. Chem., **60**, *9*, 34 (1968).
6. Ishida M., Wen C. Y., A. I. Ch. E. J., **14**, *2*, 311 (1968).
7. Voiculescu N., Rev. de Chimie, **40**, *12*, 962 (1989).
8. Trambouze P., Bull. Soc. Chim. Fr., 1 756 (1956).
9. Noll W., *Chimia şi tehnologia siliconilor* (transl. from German). Ed. Tehnică, Bucureşti, 1969.
10. Woorhoeve R. J. H., Vlugter J. C., J. Catal., **4**, 220 (1965).
11. Levenspiel O., *Chemical Reaction Engeneering.* John Wiley, NY, 1972.
12. Pinteală M., Săcărescu L., Oghină R., Voiculescu N., Dominte L., Ardeleanu R., Cristian Gh., *An Optimization Study of the Direct Synthesis of Phenylchlorosilane.* CHISA'90, Praga, August 26—31, 1990.

MODELAREA REACŢIEI DE OBŢINERE A FENILCLORSILANILOR

(Rezumat)

Reacţia de obţinere a fenilclorsilanilor este de tip fluid—solid, care are loc pe suprafaţa solidului. Această observaţie a condus la concluzia că reacţia se desfăşoară după modelul heterogen. Pentru faza solidă s-a propus un model fizic şi s-a efectuat modelarea matematică. S-a obţinut ecuaţia vitezei de reacţie şi s-a stabilit o ecuaţie de calcul pentru conversia solidului funcţie de timpul de reacţie.

BULETINUL INSTITUTULUI POLITEHNIC DIN IAȘI
Tomul XXXVII (XLI), Fasc. 1—4, 1991
Secția II
CHIMIE ȘI INGINERIE CHIMICĂ

D.C. 66.061.6

MASS TRANSFER AT SOLID—LIQUID DISSOLUTION

BY

STELIAN PETRESCU

1. Introduction

Few references may be found about solid dissolution by means of sedimentation technique [1]...[3], although this technique provides easy prevailing of data for mass transfer study.

This paper presents a mathematical model using the sedimentation technique which makes possible the computation of the dissolution rate and the individual mass transfer coefficient at solid dissolution. The mathematical model is in good agreement with the experimental data obtained by experiences which use spherical urea particles and water.

2. The Mathematical Model

In order to describe analytically the dissolution of a spherical solid particle sedimenting in a liquid, a physical model was established (Fig. 1), consisting of an imobile particle sorrounded by a liquid moving upwards with the speed of the sedimenting particle.

The solute diffusion is convective in direction θ and molecular in direction r. Owing to the symmetry:

$$\frac{\partial C}{\partial \varphi}=0\,;\quad \frac{\partial^2 C}{\partial \varphi^2}=0.$$

We assume that the process is stationary so that $\partial C/\partial t=0$. With these assumption the equation for convective diffusion (in spherical coordinates) [4], [5]:

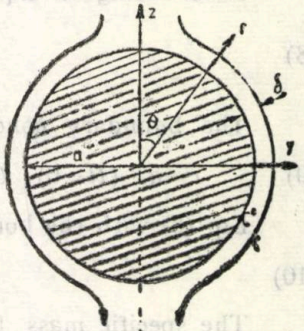

Fig. 1.—Physical model.

$$\frac{\partial C}{\partial t}+v_r\frac{\partial C}{\partial r}+\frac{v_\theta}{r}\cdot\frac{\partial C}{\partial \theta}+\frac{v_\varphi}{r\sin\theta}\cdot\frac{\partial C}{\partial \varphi}=D\left[\frac{1}{r^2}\cdot\frac{\partial}{\partial r}\left(r^2\frac{\partial C}{\partial r}\right)+\right.$$

$$\left.+\frac{1}{r^2\sin\theta}\cdot\frac{\partial C}{\partial \theta}\left(\sin\theta\frac{\partial C}{\partial \theta}\right)+\frac{1}{r^2\sin^2\theta}\cdot\frac{\partial^2 C}{\partial \varphi^2}\right] \tag{1}$$

becomes :

$$\frac{v_\theta}{r}\cdot\frac{\partial C}{\partial\theta}=\frac{2D}{r}\cdot\frac{\partial C}{\partial r}+\frac{D\partial^2 C}{\partial r^2}+\frac{D\cos\theta}{r^2\sin\theta}\cdot\frac{\partial C}{\partial\theta}. \tag{2}$$

As $D/r\simeq 0$, Eq. (2) leads to :

$$\frac{v_\theta}{r}\cdot\frac{\partial C}{\partial\theta}=D\frac{\partial^2 C}{\partial r^2}. \tag{3}$$

The azimuthal component of the liquid's speed is [4] :

$$v_\theta=-v_0\left(1+0.5\frac{a^3}{r^2}\right)\sin\theta. \tag{4}$$

For a particle with radius a :

$$v_\theta=-\frac{3}{2}v_0\sin\theta \tag{5}$$

and the mean speed is given by :

$$\bar{v}_\theta=\frac{3v_0}{4\pi}\int_0^{2\pi}\sin\theta\ d\theta=\frac{3v_0}{\pi}. \tag{6}$$

Puting $b=Da/v_\theta$, Eq. (3) becomes :

$$\frac{\partial C}{\partial\theta}=b\frac{\partial^2 C}{\partial r^2}. \tag{7}$$

Substituting in Eq. (7) $R=r-a$, we obtain :

$$\frac{\partial C}{\partial\theta}=b\frac{\partial^2 C}{\partial R^2}. \tag{8}$$

The boundary conditions are :

$$r=a,\ (R=0),\ C=C^e,\ \theta>0\ ;\ r>a,\ (R>0),\ C=0,\ \theta=0. \tag{9}$$

Eq. (8) with the boundary conditions (9), has the solution [4]:

$$C=C^e[1-R(\pi b\theta)^{-1/2}]. \tag{10}$$

The specific mass flux is given by :

$$n_A=-D\left.\frac{\partial C}{\partial R}\right|_{R=0(r=a)}=C^e\sqrt{\frac{\bar{v}_\theta D}{\pi a\theta}} \tag{11}$$

and the mean specific flux is :

$$\bar{n}_A=\sqrt{\frac{6v_0 D}{\pi^3 a}}\,C^e. \tag{12}$$

Table 2

The Sedimentation Rate versus Time

d_0, mm	1.92	t, [s]	1.5	6.75	16.25	26.5
		v_0, [m/s]	0.0999	0.0533	0.0260	0.0222
	2.05	t, [s]	1.45	6.20	14.30	22.80
		v_0, [m/s]	0.1034	0.0606	0.0312	0.0270
	2.16	t, [s]	1.38	5.78	13.30	21.15
		v_0, [m/s]	0.1086	0.0662	0.0333	0.0298

Table 3

The Variation of the Urea Particles Diameter versus Time

d_0, mm	1.92	t, [s]	1.5	6.75	16.25	26.25
		d_p, [mm]	1.8133	1.0405	0.5584	0.4863
	2.05	t, [s]	1.45	6.2	14.3	22.8
		d_p, [mm]	1.8688	1.1709	0.6550	0.5771
	2.16	t, [s]	1.38	5.78	13.3	21.15
		d_p, [mm]	1.9507	1.2650	0.6934	0.6292

Table 4

Verification of the Mathematical Model

d_0, [mm]	v_0, [m/s]	$10^3 . v_D$ kg/m^2.s	$10^4 K_1$, [m/s]	
			Experimental	Theoretical
1.92	0.0765	82.32	1.4000	1.4959
2.05	0.0820	88.99	1.5134	1.5024
2.16	0.0874	97.34	1.6554	1.5084

Substituting a from the sedimentation rate equation in (12) and using :

$$\bar{n}_A = K_1 C^e \tag{13}$$

it result :

$$K_1 = \left(\frac{6D}{\pi^3}\right)^{1/2} \cdot \left(\frac{2^{3+n} g \Delta\rho \, v_0^{2n-1}}{3m\rho^{1-n}\eta^n}\right)^{\frac{1}{2(n+1)}}, \tag{14}$$

where : K_1 is the individual mass transfer coefficient ; D — the diffusion coefficient ; g — gravitational acceleration ; $\Delta\rho = \rho_s - \rho$ — the difference between the solid and liquid density ; η — the dynamic viscosity of the liquid ; m, n — the hydrodynamic parameters ($\xi = m\mathcal{R}e^n$).

3. Experimental Determination of the Coefficient K_1. Verification of the Mathematical Model

Experimental determination of the individual mass transfer coefficient implies to establish first the experimental values of the sedimentation rate of the spherical particles. A simple installation was used for this purpose, consisting of a glass tube ($D = 0.045$ m and $L = 1.5$ m) with five marks A, B, C, D, E. In the experiment spherical urea particles with $d_0 = 1.92$; 2.05 ; 2.16 mm) and water were used at constant temperature ($T = 20°C$).

The time intervals in which the particles moved from A to B, A to C, C to D and C to E (Table 1), respectively, were determined, and the sedimentation rate was computed (Table 2). The particles diameter was computed for different moments (the sedimentation occurs in A l l e n 's field) using the equation for the sedimentation speed, and then the dissolution rate and K_1 using the relations

$$v_D = \frac{\rho_s \, d d_p}{2dt}, \tag{15}$$

$$K_1 = \frac{v_D}{C^e}. \tag{16}$$

Table 1

The Sedimentation Time for the Urea Particles

d_0, [mm]	1.92	2.06	2.16
$A-B$	3.0	2.9	2.7
$A-C$	10.5	9.5	8.8
$C-D$	11.5	9.6	9.0
$C-E$	20.5	17.0	15.7

K_1 was computed using the mathematical model (14). The results are given in Tables 3 and 4 and they clearly show the validity of the mathematical model solid dissolution.

4. Conclusions

A mathematical model for solid spherical particles dissolution in a liquid is presented. The proposed model makes possible to compute the coefficient K_1 and the solid dissolution rate.

In order to verify the mathematical model the coefficient K_1 was determined experimentally and analytically with Eq. (14), the two sets of values being approximatively the same. The model may be used in order to study the dissolution of other solids.

Notations

t — time, [s];
C, C^e — concentration at a given time, respectively mean concentration, [kg/m^3];
v_r, v_θ, v_φ — components of the liquid speed, [m/s];
v_0 — sedimentation rate, [m/s];
d_0, d_p — initial diameter of the particle, respectively diameter at a given time, [m];
ρ_s — solid density, [Kg/m^3];
ρ — liquid density, [Kg/m^3];
v_D — dissolution rate, [Kg/m^{2}s].

Received, October 9, 1990

Polytechnic Institute, Jassy,
Department of Chemical Engineerin,

REFERENCES

1. Левич В. Г., *Физико-химическая гидродинамика*. Гос. изд. физ.-матем. лит. Москва. 1959.
3. Rice R. G., Jones P. I., Chem. Eng. Sci., **34**, 847 (1979).
2. Petrescu S., *Cercetarea de inginerie chimică a procesului de obținere a sulfatului de potasiu prin valorificarea soluției de sulfat de amoniu rezultată la fabricarea caprolactamei*. Ph. D. Diss., Polyt. Inst., Jassy, 1987.
4. Iordache O., Smigelschi O., *Ecuațiile fenomenelor de transfer de masă și căldură*. Ed. Tehn., București, 1981.
5. Tudose R. Z. et al., *Procese, operații, utilaje în industria chimică*. EDP, București, 1977.

TRANSFERUL DE MASĂ SOLID—LICHID LA DIZOLVARE

(Rezumat)

Se studiază modelarea matematică a transferului de masă la dizolvarea unor granule solide de material, de formă sferică, care se deplasează prin cădere liberă. Rezultatele experimentale obținute cu granule de uree de dimensiuni diferite confirmă valabilitatea modelului matematic propus.

BULETINUL INSTITUTULUI POLITEHNIC DIN IAŞI
Tomul XXXVII (XLI), Fasc. 1—4, 1991
Secţia II
CHIMIE ŞI INGINERIE CHIMICĂ

D.C. 547. 556.5 ; 547. 283.3

HYDRAZIDES AND HYDRAZONES OF MORPHOLINO-SULPHONYL-PHENOXYACETIC ACIDS

BY

CAMELIA ŞOLDEA and CORNELIU ONISCU

1. Introduction

The employment in therapeutics of some compounds very active in tuberculosis treatments, such as the isonicotinic acid hydrazide, is rather difficult due to the high toxicity, rapid elimination from the organism and to the chemioresistance phenomenon of the bacili. These shortcomings can be overcame by using some derivatives of these drugs [1].

Shcziukina and coworkers [2] have studied a series of hydrazones resulting from the condensation of the isonicotinic acid hydrazide with aromatic aldehydes. The isonicotinoyl hydrazone thus obtained with vanillin is well supported by the organism being more active then streptomycin and *p*-aminosalicylic acid.

Gheorghiu and coworkers [3] have synthesized isonicotinoyl hydrazones of some aromatic aldehydes containing nitro and halogen groups in the molecule which showed antituberculosis action.

During the same period Baltazzi [4] has obtained for the first time hydrazides and hydrazones of phenoxyacetic acids. Later, Botez and coworkers [5] have obtained new hydrazides and hydrazones derived from some sulphonamidated aryloxyalkylcarboxilic acids.

Numerous other studies are to be found in literature concerning the biologically active hydrazones among which the phenoxy derivatives with antibacterial action deserve mention [6].

2. Results and Discussions

Taking the above considerations into account and in continuation of our studies regarding the sulphonamidated aryloxy-alkylcarboxilix acids [7]...[11] we have synthesized, in the present paper, new hydrazides and hydrazones derived from morpholinosulphonyl-phenoxyacetic acids with potential antituberculosis action and no toxicity [12].

The reaction sequence is applied according to the scheme (I), started with the obtaining of the esters of the phenoxyacetic acids which were then submitted to the chlorosulphonation reaction by chlorosulphonic acid and amidation by morpholine followed by the condensation with hydrazine and conversion of the obtained hydrazides into the corresponding hydrazones with acetone, vanillin and *p*-dimethylamino-benzaldehyde.

The hydrazides were obtained by the condensation of the amidated esters with hydrazine hydrate in a boiling alcoholic medium when they pre-

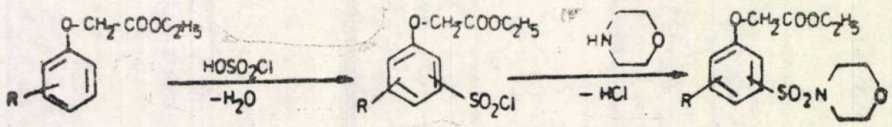

(I)

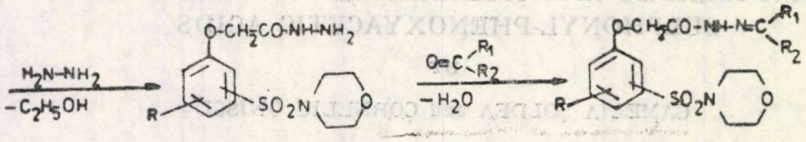

cipitated almost quantitatively. After allowing to stay for 12 hours the precipitate was filtered and purified by recristallization from ethanol. The obtained compounds are listed in Table 1.

Table 1

Hydrazides of Morpholinosulphonyl-phenoxyacetic Acids

No.	Compound	N, [%] Calculated	N, [%] Found	M. p. °C
I.	Hydrazide of 2-chloro-4-morpholino-sulphonyl-phenoxyacetic acid ($C_{12}H_{16}O_5N_3SCl$)	12.01	12.21	151
II.	Hydrazide of 3-chloro-4-morpholino-sulphonyl-phenoxyacetic-acid	12.01	11.84	163
III.	Hydrazide of 4-chloro-2-morpholino-sulphonyl-phenoxyacetic-acid	12.01	11.89	180
IV.	Hydrazide of 2-chloro-4-methyl-6-morpholino-sulphonyl-phenoxyacetic acid ($C_{13}H_{18}O_5N_3SCl$)	11.55	11.38	172
V.	Hydrazide of 4-chloro-3-methyl-6-morpholino-sulphonyl-phenoxy-acetic acid	11.55	11.32	150
VI.	Hydrazide of 2-methoxy-5-morpholino-sulphonyl-phenoxyacetic acid ($C_{13}H_{18}O_6N_3S$)	12.20	12.00	120
VII.	Hydrazide of 3-methyl-6-isopropyl-4-morpholino-sulphonyl-phenoxyacetic acid ($C_{16}H_{25}O_5N_3S$)	11.32	11.12	112

The structure of the hydrazides thus obtained was elucidated by both elemental analysis and IR spectral measurements as well as on the chemical way by their transformation into hydrazones by the condensation with acetone, vanillin, *p*-dimethylamino-benzaldehyde. The above mentioned hydrazones were obtained in a hydroalcoholic medium slightly acidified by acetic acid [13]. They are listed in Table 2 with the corresponding elemental analysis data and melting points.

Table 2

Hydrazones Derived from Morpholinosulphonyl-phenoxy-acetic Acids

Hydrazide condensed with carboxylic compounds	Hydrazones with	N, [%]		M. p. °C
		Calculated	Found	
I.	Acetone ($C_{15}H_{20}O_5N_3SCl$)	10.77	10.48	193
	Vanillin ($C_{20}H_{22}O_7N_3SCl$)	8.68	8.31	208
	p-Dimethylamino-benzaldehyde ($C_{21}H_{25}O_5N_4SCl$)	11.65	11.49	225
II.	Acetone	10.77	10.52	151
	Vanillin	8.68	8.31	121
	p-Dimethylamino-benzaldehyde	11.65	11.39	148
III.	Acetone	10.77	10.58	149
	Vanillin	8.68	8.35	108
	p-Dimethylamino-benzaldehyde	11.65	11.41	170
IV.	Acetone ($C_{16}H_{22}O_5N_3SCl$)	10.40	10.25	220
	Vanillin ($C_{21}H_{24}O_7N_3SCl$)	8.44	8.21	206
	p-Dimethylamino-benzaldehyde ($C_{22}H_{27}O_5N_4SCl$)	11.32	11.50	162
V.	Acetone	10.40	10.12	181
	Vanillin	8.44	8.56	95
	p-Dimethylamino-benzaldehyde	11.32	11.12	222
VI.	Acetone ($C_{12}H_{23}O_6N_3S$)	10.90	10.71	101
	Vanillin ($C_{21}H_{25}O_8N_3S$)	8.76	8.54	189
	p-Dimethyl-amino-benzaldehyde ($C_{22}H_{28}O_6N_4S$)	11.76	11.42	126

The obtained hydrazones are solid, crystalline compounds of white colour (those with acetone) or yellow colour (those with vanillin and some of those with *p*-dimethylamino-benzaldehyde), soluble in hot ethylic alcohol.

The IR spectral analysis made evident the absorption bands characteristics of the principal groups and structural characteristics of the compounds under study as discussed by us in previous papers [7]...[11].

3. Experimental

3.1. Hydrazide of the 2-Chloro-4-methyl-6-morpholino-sulphonyl-phenoxyacetic Acid

3 g ethylic ester of the 2-chloro-4-methyl-6-morpholinosulphonyl-phenoxyacetic acid are solved in 20 ml of hot ethylic alcohol. A solution of 0.75 ml hydrazine hydrate in 10 ml

ethanol is then added. The mixture is refluxed for 2 min. and allowed to stay for 12 hours. The crystallized hydrazide is then filtered and purified from water. The pure product melting at 172°C is thus obtained in almost quantitatively yield.

Analyses		C, [%]	H, [%]	N, [%]
$C_{13}H_{18}O_5N_3SCl$	Calculated	42.91	4.95	11.55
	Found	42.78	4.90	11.38

3.2. Hydrazone of the 2-Chloro-4-methyl-6-morpholinosulphonyl-phenoxy-acetic Acid with Acetone

0.8 g of hydrazide previously prepared are treated with 2 ml water, 2 ml acetone, a drop of acetic acid and refluxed for 2...3 min. The hydrazone precipitated by cooling is finally filtered and purified from ethanol. An white, crystalline, pure product melting at 220°C is finaly obtained.

Analyses		C, [%]	H, [%]	N, [%]
$C_{16}H_{22}O_5N_3SCl$	Calculated	45.78	5.45	10.40
	Found	47.72	5.24	10.24

3.3. Hydrazone of the 2-Chloro-4-methyl-6-morpholinosulphonyl-phenoxy-acetic Acid with *p*-Dimethyl-amino-benzaldehyde

0.75 g hydrazide previously prepared are mixed with 0.3 g of dimethylamino-benzaldehyde and suspended into 5 ml water acidified by a drop of acetic acid and refluxed for 2 min. The precipitate is then filtered and purified from ethanol. A crystalline yellow product melting at 162°C is thus obtained.

Analyses		C, [%]	H, [%]	N, [%]
$C_{22}H_{27}O_5N_4SCl$	Calculated	53.38	5.46	11.32
	Found	53.09	5.60	11.50

3.4. Hydrazone of the 2-Chloro-4-methyl-6-morpholino-sulphonyl-phenoxy-acetic-Acid with Vanillin

0.75 g hydrazide of the title acid are mixed with 0.5 g vanillin and suspended into 5 ml ethanol (50%) acidified by a drop of acetic acid and refluxed for 2 ... 3 min. The hydrazone precipitated by cooling is filtered and washed with ethylic alcohol. The product is insoluble in water and in hot solvents, soluble in alkaline hydroxides. By neutralizing the alkaline solution a light-yellow product separates which melts at 206°C.

Analyses		C, [%]	H, [%]	N, [%]
$C_{21}H_{24}O_7N_3SCl$	Calculated	50.65	4.82	8.44
	Found	50.43	4.44	8.21

4. Conclusions

1. In continuation of our studies concerning the sulphonamidated aryl-oxylkylcarboxylic acids, new hydrazides and hydrazones of some morpholinosulphonyl-penoxyacetic acids have been prepared.

2. By applying the reaction scheme starting from the sulphochlorinate esters of the phenoxyacetic acids, as described in previous papers, new hydrazides and hydrazones with acetone, *p*-dimethyl-amino-benzaldehyde and vanillin have been obtained.

3. The obtained products might be used as antituberculosis drugs which requiers the continuation of the studies.

Received, June 5, 1990

Polytechnic Institute, Jassy,
Department of Organic Chemica Technology

REFERENCES

1. Oniscu C., *Chimia şi tehnologia medicamentelor*. Ed. Tehnică, Bucureşti, 1988.
2. Щюкина М. Н., Созонова Е. А., ЖОХ, **23**, *85*, 687 (1953).
3. Gheorghiu C. V., Budeanu C., Toma A., An. Şt. Univ. „Al. I. Cuza", Iaşi, **I**, *1—2*, s. I. 320 (1955).
4. Baltazzi M. E., C. R. Acad. Sci. Paris, **241**, 321 (1955).
5. Botez Gh., Tutoveanu M., Comăniţă E., Bul. Inst. polit., Iaşi, **VIII (XII)**, *3—4*, 149 (1962).
6. Cremlyn R. J., Cronje T., Goulding K., Austr. J. Chem., **32**, 445 (1979).
7. Botez Gh., Oniscu C., Merică E., Gorea C., Bul. Inst. polit., Iaşi, **XII (XVI)**, *1—2*, 179 (1966).
8. Botez Gh., Oniscu C., Merică E., Gorea C., Bul. Inst. polit., Iaşi, **XIII (XVII)**, *1—2*, 257 (1967).
9. Botez Gh., Gorea C., Merică E., Oniscu C., Bul. Inst. polit., Iaşi, **XV (XIX)**, *1—2*, 67 (1969).
10. Botez Gh., Gorea C., Oniscu C., Merică E., Bul. Inst. polit., Iaşi, **XVI (XX)**, *1—2*, 161 (1970).
11. Botez Gh., Merică E., Gorea C., Oniscu C., Bul. Inst. polit., Iaşi, **XX (XXIV)**, *1—2*, 75 (1974).
12. Brinzei P., Botez Gh., Rev. Medico-chirurgicală, Iaşi, **LXV**, *2*, 487 (1961).
13. Baltazzi E., Delavigne R., C. Z., **11**, 3 446 (1959).

HIDRAZIDE ŞI HIDRAZONE PROVENITE DIN ACIZII MORFOLINO-SULFONIL-FENOXIACETICI

(Rezumat)

Se continuă studiul acizilor ariloxialchilcarboxilici sulfonamidaţi prin sinteze de noi derivaţi ai acizilor morfolino-sulfonil-fenoxiacetici. Aplicînd o schemă de transformări descrisă de autori în lucrări anterioare s-au obţinut noi hidrazide şi hidrazone provenite din acizii morfolino-sulfonil-fenoxiacetici cu eventuală acţiune biologică.

BULETINUL INSTITUTULUI POLITEHNIC DIN IAŞI
Tomul XXXVII (XLI), Fasc. 1—4, 1991
Secţia II
CHIMIE ŞI INGINERIE CHIMICA

D.C. 54-92 ; 629.1

THE EVALUATION OF THE REAL STRENGTH OF THE TENSILE STRESSED POLYMERS

BY

MARCEL POPA, CLEOPATRA VASILIU-OPREA and EMIL-GHIOCEL IOANID

1. Introduction

The mechanical properties of any material are quantitatively appreciated by the term „mechanical strength" which express the maximum value of the stress corresponding to a certain type of load at which its macroscopical fracture takes place.

The mechanical strength, e. g. the tensile one, depends on many factors among which the chemical nature of the polymer, the size and shape of the macromolecules, the crosslinked degree, the loading rate. For the usual polymers, the value of the tensile strength ranges between 500 ... 1 000 Kgf/cm^2.

Nowadays it is well known and unanimously accepted the fact that the fracture process of the macromolecular compounds is based on the mechanochemical act consisting in the splitting of the covalent bonds from the basic chain. For an ideal elastic body, the tensile strength given by the resistance of its individual atomic bonds should be determined from the following expression :

$$\sigma_r = E\varepsilon_m, \tag{1}$$

where : E — Young modulus, characteristic for the considered solid body ; ε_m — deformation of the covalent chemical bonds, with values varying between 0.1 ... 0.2.

Thus, expression (1) is valid in the hypothesis of a continuously and uniformly loaded solid body, in which the stress is invariably distributed on all chemical bonds. The result of the fracture would be, in this case, a complete dissociation of the atoms, just like when a solid body passes in a vapour phase by sublimation at the critical temperature.

However, the polymers are not continuous and ideally elastic bodies, so that the experimentally determined resistance is far from the theoretical values, the proportionality factor varying between 10^{-2} ... 10^{-4}.

2. Theoretics

The discrepancies which might appear are due to the faults manifesting at all their levels of structural organization acting as stress concentration factors. Thus, it becomes possible that at a loading stress lower than that of the macroscopic fracture, the local stress concentrated on a chemical bond from a fault zone should attain extremely high values, exceeding the activation energy of its splitting and bringing about its breaking.

At the chemical structure level, the faults are represented by weaker bonds, where tertiary and quaternary atoms are implied, and by the bonds adjacent to the double bonds or to the some functional groups. At the level of its supramolecular structure, the faults are represented by amorphous zones, crystalline-amorphous boundary, macromolecules end zones both from the amorphous and crystalline domains, shorter connecting chains between the crystallites, etc.

Therefore, under the action of the mechanical stress, the chemical bonds from these fault areas are the first to take over the load and become overstressed. The mechanical energy has the role of increasing the energetic state of the molecule, thus reducing the energetic potential barrier which must be exceeded with a quantity $\beta\sigma$ in order that the fracture should take place ; here σ is the loading stress of the bond and β is a factor which is called „activating volume". On this basis, the strength of a polymer under load has been expressed by the term „durability" [1] (τ), defined as :

$$\tau = \tau_0 \exp(E_a - s\beta\sigma/kT), \tag{2}$$

where : s — factor taking values in the domain $0 \ldots \psi_r\sigma$, expressing the fact that due to the structural nonhomogeneities of the sample, the loading stress of the chemical bond differs from the macroscopic one ; k — Boltzmann's constant ; T — absolute temperature.

Thus the primary act of the polymer fracture consists of the chemical bond splitting by thermal fluctuations caused by the increase of its inner energy by mechanical stress.

The accumulation of a great number of broken chemical bonds in a microvolume determines the appearance of a discontinuity in the material ; this is called a microcrack. The difrence between the elastic energy of the initial overstressed state and that of equilibrium attained by the macromolecules after the opening of the microcrack is dissipated in the polymer as thermal and acoustic energy, thus developing a series of phenomena such as electronic emission, chemiluminiscence, thermal and sound effects, etc.

The acoustic emission has been noticed for the first time in polymers during the fracture experiences of the polystyrene [2]. The effect, known as „the Kaizer phenomenon", has been initially discovered in metals [3], being used nowadays for detecting the flow or the propagation of the crack through these materials.

The appearance of this effect in polymers is thus correlated with the formation of microcracks and subsequently with the formation and propagation of the main crack which determines the macroscopic fracture. But, however, the formation of the microcracks before the fracture has as effect the depreciation of the physico-mechanical properties of the polymer by interrupting its continuity. It is evident that at values of the loading stress corresponding to the formation of the microcracks, the polymer is no longer functional and moreover, it cannot be reused under the condition of a subsequent load of the same intensity. The described phenomenon can become useful for determining the stress and the deformation a polymer can stand without undergoing irreversible structural modifications. Thus, it is created the possibility of characterizing a macromolecular compound not so much by the breaking stress and deformation (currently used nowadays to estimate its mechanical properties), but by the stress and deformation corresponding to the formation of the microcraks which would define the real strenght under load. This is the way we could obtain some information concerning the more sensible and longer standing usage of the objects manufactured from macromolecular compounds.

Starting from these premises, this paper presents a method and a device for the evaluation of the stress and tensile deformation corresponding to the formation of microcracks at the bar-shaped, film-shaped and monofilament bundle shaped polymers with utilisations in the physico-mechanical testing laboratories as well as in researches on the molecular aspects of the polymers deformation and fracture process during dynamic loading.

The principle to be found at the basis of this paper is the recording of an acoustic vibration — deformation diagram, simultaneous with the stress — strain curve, so that by comparing these two diagrams the magnitudes characterizing the real resistance of the polymer could be established.

Our device allows the picking up and the recording of the acoustic vibrations developed in a sample subjected to a tensile stress in the moment of

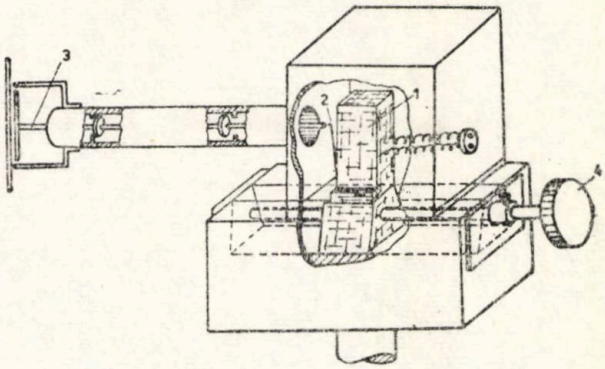

Fig. 1. — The schematic diagram of the sound test probe: *1.* — piezoelectric crystal ; *2* — elastic feeler ; *3* — rod for vibration take-over ; *4* — micrometrical screw.

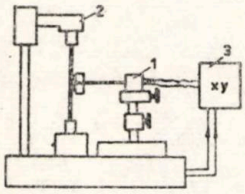

Fig. 2. — The location of the sound test probe *(1)* on a tensile stress dynamometer *(2)* ; *3* — tracer *XY*.

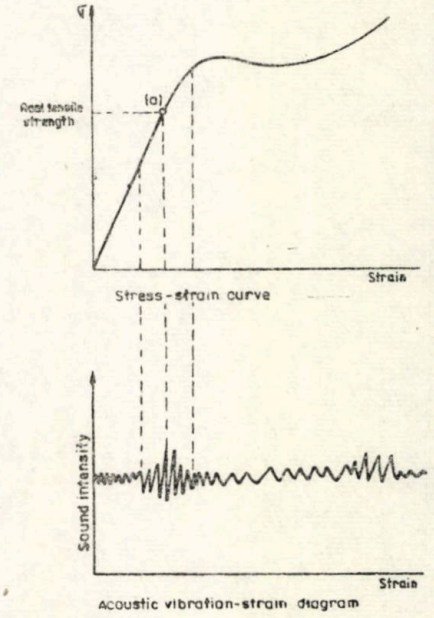

Fig. 3. — The correlation of the acoustic diagrame with the rheological stress —strain curve of a polymer.

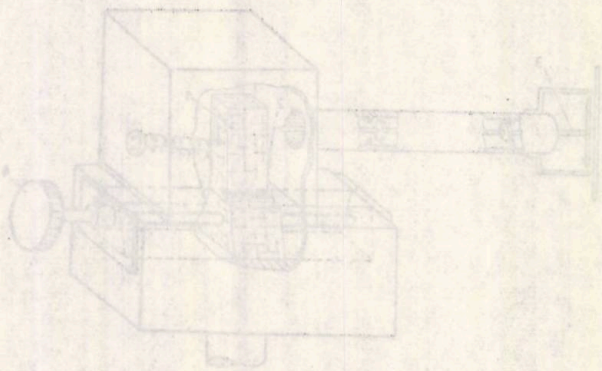

forming and opening of the microcracks; this device has the possibility of being adapted to any dynamometer.

The basic part is a sound test probe (Fig. 1) made up in the main from a piezoelectric crystal (*1*) provided with an elastic feeler (*2*) and a rod for vibration take-over (*3*) manufactured from a light material (aluminium). The sound test probe is mounted on a supporting — adjusting holder which allows its horizontal displacement by turning a micrometrical screw (*4*).

To obtain acoustic information from a tensioned polymer sample the rod for the vibration take over is brought near the sample in an active section area convenient for the measurements. The acoustic vibrations produced in the sample in the moment when the microcracks are formed by tensile stress, are converted in an electric signal by the piezoelectric transducer and introduced into a tracer *XY*.

The assembly sound test probe — dynamometer — recording system is presented in Fig. 2.

The above presented method and device have proved their utility for the study of the deformation and fracture of the MELANA-type monofilaments stressed as bundless [4].

This device has made us to obtain the acoustic diagram (shown in Fig. 3) which illustrates the number and amplitudes of vibrations in time. The comparison of this diagram with the rheological stress — strain curve (Fig. 3) simultaneously plotted by the dynamometer, has allowed that a point *a* corresponding to the area with a maximum number of acoustic impulses, should determine the value of the stress and deformation for which the microcracks have appeared in the polymer.

4. Conclusions

The advantages of the proposed method and device as resulting from the above mentioned facts, are the following:

1. They allow to establish the stress and the tensile deformation corresponding to the formation of the microcracks in polymers, characterizing more correctly their mechanical strength and thus allowing their rational use.

2. The device is easily adaptable to any type of dynamometer without any modification in its construction and service and can be used both in industry and laboratory researches concerning the fracture of the polymers.

Received, July 9, 1990

Polytechnic Institute, Jassy,
Department of Macromolecules
and
Institute of Macromolecular
Chemistry „P. Poni", Jassy

REFERENCES

1. Jurkov S. N., Vettegren V. I., Korsukov V. E., Novak I. I., Proc. 2nd Int. Conf. on Fracture, Brighton, Chapmann and Hall Ltd., London, 1969.
2. Sauer J. A., Hsiao J., Trans. ASME, **76**, 895 (1953).
3. Kaizer I., Archiv. für Eisenhüttenwesen, **34**, 43 (1953).

4. P o p a M., *Contribuţii la cunoaşterea unor reacţii mecanochimice privind sinteza, prelucrarea şi exploatarea copolimerului ternar pe bază de poliacrilonitrii* Ph. D. Diss., Polyt. Inst., Jassy, 1989.

EVALUAREA REZISTENŢEI REALE A POLIMERILOR SOLICITAŢI LA TRACŢIUNE

(Rezumat)

Se prezintă un procedeu şi un dispozitiv ce permit evaluarea rezistenţei reale la rupere a polimerilor solicitaţi la tracţiune. Valoarea acestei caracteristici mecanice este estimată prin compararea curbei reologice a polimerului cu o diagramă acustică, înregistrată cu ajutorul dispozitivului propus, pe baza vibraţiilor sonore produse în materialul solicitat la deschiderea microfisurilor, respectiv prin propagarea fisurii magistrale. Cele două înregistrări având ca bază comună timpul, zona de vibraţii cu frecvenţă şi amplitudine maximă din diagrama acustică identifică pe curba reologică valorile cercetate.

BULETINUL INSTITUTULUI POLITEHNIC DIN IAȘI
Tomul XXXVII (XLI) Fasc. 1—4, 1991
Secția II
CHIMIE ȘI INGINERIE CHIMICĂ

D.C. 547. 533 ; 66.097.3

THERMODYNAMIC AND KINETIC ASPECTS OF CATALYTIC DISPROPORTIONATION OF TOLUENE

BY

ABDELKRIM AZZOUZ, EMIL DUMITRIU and V. HULEA

1. Introduction

The complexity of the catalytic toluene disproportionation consists essentially in the process dependence on a high number of parameters and in their interdependences. The intervention of each reaction and therefore the process selectivity are justly function of each parameter. Among the latters, the reaction temperature and the catalyst nature play the main roles.

The most important aspect is indisputably the multitude of involved reactions [1]. Toluene disproportionation consists at least of fifty possible reactions among which the two first one were considered as principal whereas the seven or eight first reactions are the most probable (toluene disproportionation, xylenes isomerisation, xylenes disproportionation and trimethylbenzenes isomerisation). As we will examinate it later, the number of implied reactions in the overall process is proportional to the temperature increase.

In the other hand, the very specifical activities initiated by the catalysts modification are not taken into consideration in the equilibrium constants. In a theoretical process, the reactions occur according to their probabilities. In a real process, the order of the decreasing values of the equilibrium constants is often not respected. For example, on less selective catalysts demethylation take place simultaneously with the main process. For more selective catalysts, nondesired reactions are involved only after reaching a certain temperature. Anyway, pyrolysis can not be avoided but only minimized by a suitable choice of operating conditions.

It is obvious that the number and the nature of implied reactions depend on the kind and strenghth of active sites. So it is required to involve additive kinetic considerations to get a better approach to the real process.

2. Experimental

The disproportionation process was carried out in a tubular reactor made of pyrex. The particle size of the fixed bed of catalyst is about 1...2 mm. The catalyst were Y-faujasite ion-echanged by lanthanum, cerium, cobalt or strontium. The spatial velocities of the gaseous flow varied in the range 0.5... 15 h^{-1}. The samples of the reaction products were analysed by gas chromatography (8 500 Perkin Elmer apparatus) in a 4 mm × 2 m column of (bentone and dinonylphthalate) / chromosorb using a FID detector.

The calculations were achieved by Basic language using a VAX computer and a VT240 terminal.

3. Results and Discussions

3.1. Thermodynamic Considerations

The thermodynamical calculations were achieved by computing data in the temperature range 300°...500°C. The results permitted to put in evidence the most probable reactions and their contributions, according to the temperature, in the global process. Hence, as shown in Table 1, for conversions less than 40% and for ratio $B/X = 1$ ($T < 380$°C), this process is limited to the only disproportionation—isomerisation reactions (model *1* (I)...(IV)) :

(I) $2T \rightarrow p\text{-X} + \text{B}$, (II) $2T \rightarrow o\text{-X} + \text{B}$, (III) $o\text{-X} \rightarrow m\text{-X}$, (IV) $p\text{-X} \rightarrow m\text{-X}$.

In the range temperature of 300°...360°C, the isomerisation plays a secondary role, and the distribution of the three xylenes is very different from those at the thermodynamic equilibrium. At a temperature close to 440°C, the conversion attains the equilibrium (50... 57% mole) as shown in the Table 1.

Table 1

Applicability Field of Proposed Models

T, [°C]	300 ... 360	360 ... 435	440	440 ... 500
Model	*1*	intermediate	*2*	global model [1]
Reactions	1*a* – 2*b*	—	1*a* – 4*c*	all reactions
B/X	1	1 ... 1.5	1.5	>1.5
Conv., [% mol]	40	56	60	60

Exactly, at this point, model *1* should be completed by xylenes disproportionation and TMB's isomerization. Therefore, model *2* will include in addition to the reaction (I)...(IV) the transformations :

(V) $2p\text{-X} \rightarrow T + 1,2,4\text{-TMB}$, (VI) $o\text{-X} + m\text{-X} \rightarrow \text{T} + 1,2,4\text{-TMB}$,

(VII) $2m\text{-X} \rightarrow \text{T} + 1,2,3\text{-TMB}$, (VIII) $o\text{-X} + p\text{-X} \rightarrow \text{T} + 1,2,4\text{-TMB}$, (IX) $2p\text{-X} \rightarrow \text{T} + 1,2,3\text{-TMB}$,

(X) $m\text{-X} + p\text{-X} \rightarrow 1,2,4\text{-TMB}$, (XI) $o\text{-X} + m\text{-X} \rightarrow 1,3,5\text{-TMB}$,

(XII) $1,2,3\text{-TMB} \rightarrow 1,2,4\text{-TMB}$, (XIII) $1,2,3\text{-TMB} \rightarrow 1,3,5\text{-TMB}$,

(XIV) $1,2,4\text{-TMB} \rightarrow 1,3,5\text{-TMB}$.

The succession of these reactions is based on decreasing values of equilibrium constants which determines in someway their probabilities. It clearly appears that *m*-xylene (on the analogy) to mesitylene (1,3,5-TMB) can be obtained only by conversion of the two other isomers.

The formation of coke occurs even at B/X or B (X+2TMB) molar ratios equal to unity. This proves that, before the TMB formation, toluene and especially xylenes, contribute to coke deposit on the catalytic surface (except benzene which is theoretically the most stable). The substances stability in pyrolysis process is inversly proportional to their molecular weight.

These reactions are mainly favourised by the L e w i s sites which are the first poisoned. Coke yielding, if it is controlled (short contact times, low conversion rates for elevated temperatures), can occur without affecting the rearrangement process. Indeed, the liberated hydrogen by pyrolysis can favour the demethylation reactions ($K=0.0000001$), and the most probable are those presenting one methyl cleavage. The probability to loose one methyl group varies for the alkylbenzenes as follows :

(1) $$TMB > Xylenes > Toluene.$$

Demethylation reactions occur mainly in presence of large amounts of hydrogen. In any way these dissociation processes are depending each other. Whereas, the demethylation is less probable and occurs only in special conditions, the pyrolysis is unavoidable and takes place even spontaneously and the experience proves that.

Between 380° and 400°C, B/X ratio varies from 1 to 1.55 and the process is rather complex and intermediate limited at the extreme by the two models.

Pyrolysis reactions can be involved in the proposed models only by taking into account additive data. These data are based mainly on kinetic considerations and related to the selectivity and the specificity of each catalyst. Indeed, although the equilibrium constants values of pyrolysis reactions are relatively high, only a part (3...5%) of each alkylated hydrocarbon is converted to coke. Moreover, among these hydrocarbons only TMB's contribute really to coke formation, because these are more strongly retained on the catalyst than others.

According to these considerations model *2* be completed by the most probable reactions dissociation which are the following :

(XV) $1,2,3\text{-TMB} \rightarrow 9C + 6H_2$, (XVI) $1,2,4\text{-TMB} \rightarrow 9C \rightarrow 6H_2$,

(XVII) $1,2,3\text{-TMB} \rightarrow 9C + 6H_2$,

with constants values varying from 0.25×10^{23} to 0.29×10^{24}, and whose constants have an approximative value of 10^{-7}.

(XVIII) (XIX) (XX) $$1,2,4\text{-TMB} \begin{cases} \rightarrow p\text{-X} + CH_4 \\ \rightarrow m\text{-X} + CH_4 \\ \rightarrow o\text{-X} + CH_4 \end{cases}$$

(XXI) $$1,3,5\text{-TMB} \rightarrow m\text{-X} + CH_4.$$

(XXII) (XXIII) $$1,2,3\text{-TMB} \begin{cases} \rightarrow m\text{-X} + CH_4 \\ \rightarrow o\text{-X} + CH_4. \end{cases}$$

The six last reactions can be neglected because of their small contributions. Otherwise, because of their steric effect, TMB's are more retained in catalyst pores than less alkylated aromatic hydrocarbons. So, their further conversions are more probable.

3.2. Kinetic Aspects

All intramolecular rearrangement processes occur according to L a n g m u i r—H i n s h e l w o o d [7]...[9]. The intervention of all these reactions strongly depends on toluene conversion rate which at the same time is function

of many factors. Thus, the kinetic study of such a complex process can not be achieved only by insulating the principal reactions systeme (model *1*) from the side-chain reactions which do not present any interest in this case. The main process follows L a n g m u i r kinetics presenting fractionary reaction order (0.4 for NaCoY and 0.5 for NaLaY) [3].

The amount of yielding coke is proportional to that of heavy compound formed but still remains limited by the number of the pyrolysis sites (L e wi s). This number, in turn, depends on the nature and the amount of substitution cations and, of course, on the temperature (dehydration rate).

At the beginning of the process, the fresh catalyst contacted with evaporated reagent will first crack toluene until poisoning the most active sites. This occurs even at relatively low temperatures. Then, toluene will disproportionate into *para* (in preponderance) and *ortho*-xylene. Isomerisation and disproportionation of xylenes involve very strong acidic sites. When the reaction temperature increases, isomerization reactions become predominant because they need relatively less acidic sites and xylenes distribution reaches equilibrium. The rates of the different isomerisation reactions vary as follows [4]:

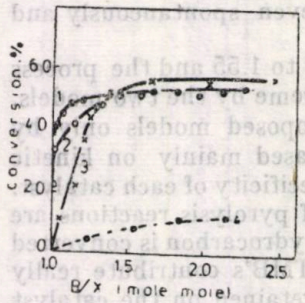

Fig. 1. — Dependence of B/X molar ratio on conversion: *1* — NaLaY with Na^+ substitution degree about 7 %; *2* — NaCeY with Na^+ substitution degree about 70 %; *3* — NaLaY with Na^+ substitution degree about 73 %; *4* — NaSrY with Na^+ substitution degree about 70 %.

$$(2)\quad (p\rightarrow m)\gg(o\rightarrow m)>(m\rightarrow p)>(m-o)>(p\rightarrow o)=(o\rightarrow p)=0.$$

This confirms the fact the *p*- and *o*-xylenes have more chances to be the starting point of the *m*-xylene formation. An excessive temperature increase permits to convert by dehydration a considerable number of B r o n s t e d sites in order to compensate coke centers blocking. Thus increasing conversion rate will enhance the side-chain reactions affecting the process selectivity for all the catalysts tested as shown in Fig. 1.

In such catalysts (except NaSrY), for temperatures less than 440°... 450°C, the required acidity force for different reactions varies in the following order :

Table 2

Experimental Data on Disproportionation and Isomerization of Alkylbenzenes (Catalyst — NaCeY with Na^+ substitution of 71 %; WHSV = 0.8 h^{-1})

Reagent	Temperature °C	Conversion, [%]		B/X mol/mol
		Disproportionation	Isomerization	
Toluene	400	23.1	—	1.4
	450	30.4	—	3.4
	500	46.7	—	3.8
p-Xylene	450	54.3	32.0	—
m-Xylene	450	60.2	21.1	—
o-Xylene	450	43.8	36.2	—

(3) Xylenes disp. > Xylenes isomer. > Toluene disp.

This assertion is clearly illustrated by the experimental data presented in Table 2. For example, at 450°C the above mentioned order is given by the values of the conversion occuring in the three reactions.

The three types of reactions coexist in the intermediate range 380°... 440°C (model *I*) but toluene disproportionation is still preponderant. Above 440°C, dehydration phenomenon is important and the Bronsted centers number will considerably decrease by yielding new aprotonic centers [6]. Therefore, in this field, reactions such as xylenes isomerization and disproportionation (which require respectively moderated and elevated acidities), and cracking, are preponderant. For example, at 440°C, disproportionation velocity is the same for NaCoY and NaLaY. Hence, the hydration avoid the behaviour differences between the catalyst. Therefore, these differences will be resulting from the nature of the sites formed by hydrated cations and the zeolitic surface.

4. Conclusion

Is is obvious that these results depend on the catalyst nature and its selectivity, but they mainly permit to give an idea about the selectivity of the tested catalysts and the applicability of the proposed model.

The comparison of thermodynamical simulation with experimental data shows clearly that the good adaptation of these models required to associate additive kinetic considerations. Therefore, this model remain applicable for catalysts presenting a good selectivity for toluene disproportionation, as in the case of NaCeY, NaLaY and to a less extend NaCoY.

The value 440°C seems to be an optimal temperature to improve selective disproportionation process over such catalysts. Above this value, the cation nature do not play any preponderant role.

Received, March 21, 1990

Polytechnic Institute, Jassy,
Department of Organic Chemical Technology
and
Haut Commissariat à la Rechercher
Organic Synthesis Division, Algie,

REFERENCES

1. Oprea S., Azzouz A., Dumitriu E., Constantinescu M., Bull. Soc. Chim. Belg., **92**, *3*, 289 (1983).
2. Mikhail S., Ayoub S. M., Barakat Y., Zeolites, **7**, 231 (1987).
3. Oprea S., Azzouz A., Dumitriu E., Bilbă N., Rev. Roum. Chim., **29**, *11—12*, 887 (1984).
4. Becker K., Chem. Tech., **18**, *8*, 455 (1966).
5. Raşeev S., Olteanu B., Rev. Chim. (Bucharest), **28**, *4*, 319 (1977).
6. Azzouz A., Fourar M., Berrak A., Bull. Soc. Chim. Belg., **95**, *12*, 1 059 (1986).
7. Миначев Н. М., Усашев Н. И., Исаков И. И., Богомолов В. И., ИАН СССР, сер. хим., *6*, 1395 (1973).
8. Беренцвейг В. В., Руденко А. П., Нефтехимия, **3**, *2*, 185 (1973).
9. Nicolescu I. V., Şerban O., Săndulescu I., Stoicescu L., Rev. Roum. Chim., **22**, *1*, 97 (1977).

ASPECTE TERMODINAMICE ȘI CINETICE PRIVITOARE LA DISPROPORȚIONAREA CATALITICĂ A TOLUENULUI

(Rezumat)

S-a studiat, sub aspect termodinamic și cinetic, procesul de disproporționare a toluenului pe catalizator Y schimbat cu lantanide. S-a analizat din punct de vedere al competitivității setul de douăzeci și trei de reacții implicate în modelul chimic elaborat. S-a găsit că la 440°C (temperatura optimă pentru disproporționarea toluenului) ponderea principalelor reacții în proces este următoarea:

disproporționare xileni > izomerizare xileni > disproporționare toluen.

BULETINUL INSTITUTULUI POLITEHNIC DIN IAŞI
Tomul XXXVII (XLI), Fasc. 1—4, 1991
Secţia II
CHIMIE ŞI INGINERIE CHIMICĂ

C.D. 676.2.023 ; 668.473

L'ENCOLLAGE DU PAPIER AVEC DU TALLOÏL

PAR

SAVEL IFRIM et FREDIRICH SCHIEBER

1. Introduction

L'encollage du papier est une opération très importante dans le processus technologique de la fabrication de ce produit, beaucoup sollicité dans l'activité sociale. Une bonne opération d'encollage détermine les qualités du papier, notamment du celui utilisé pour écriture à l'encre ou bien pour impression.

La qualité de l'encollage d'un papier destiné à l'écriture courante est acceptable lorsque la précision des signes typographiques est bien gardée, la pénétration des liquides polaires dans les microcapillaires de la feuille étant empêchée. Un bon encollage détermine aussi une résistance meilleure du papier. Le papier mal encollé permet la pénétration de l'eau et également des autres liquides polaires dans les microcapillaires du celui-ci, ce qui détermine la destruction des liaisons hydrogène interfibres et aussi de celles entre les macromolécules de cellulose et par conséquent résulte une diminution de la résistance du papier.

On peut réaliser l'encollage du papier par deux voies : l'encollage de surface, qui s'applique dans les cas spéciaux et l'encollage en masse, qui est une méthode généralisée dans la technique [1].

Pour l'encollage en masse on utilise plusieures substances, à savoir : colophane, colle animal, paraffine, amidon, résines synthétiques, dispersions de polymères synthétiques, colophane modifié, policolle, etc. Parmi ces produits le colophane est le plus utilisé.

Dans ce travail on montre la possibilité d'utiliser le talloïl brut comme agent d'encollage du papier.

Le fait que le talloïl représente une matière première pour obtenir le colophane constitue un argument en faveur de son utilisation comme agent d'encollage en masse du papier. Sans doute le talloïl présente encore beaucoup d'autres utilisations [2], [3].

2. Partie théorique

Une condition importante qui doit être satisfaite par un produit chimique dans le but de son utilisation comme agent d'encollage en masse du papier, est représentée par sa propriété de former des dispersions très fines dans le milieu aqueux, capables à bloquer l'accès des liquides dans les microcapillaires du papier. Cette condition est satisfaite également par le talloïl.

On peut obtenir le talloïl à partir du savon sulfatique, qui est un sous-produit résultant dans le processus de la fabrication de la cellulose par le procédé „sulfate" en utilisant le bois de conifères. Il est un mélange homogène et complexe de substances organiques, qui appartiennent aux acides résiniques,

aux acides gras saturés et nonsaturés, aux produits insaponifiables [4], comme les alcohols, les stérols et les hydrocarbures [5]. De même le talloïl peut contenir aussi un pourcentage très réduit de substances volatiles, ainsi que des traces d'eau.

Dans un travail précédent [6] on a déterminé quelques caractéristiques du talloïl brut, séparé au Combinat de Fibres, Cellulose et Papier, Dej, mettant en évidence les pourcentages des acides résiniques, des acides gras, des substances insaponifiables, de la cendre, de l'humidité, etc.

Les résultats obtenus dans ce travail montrent que le talloïl provenu du Combinat de Dej contient un pourcentage relativement élevé d'acides résiniques, qui varie entre 61 % et 70%. Compte tenu que l'agent le plus utilisé pour l'encollage du papier, le colophane — produit obtenu à partir des résines de conifères — possède dans sa composition aussi un pourcentage élevé d'acides résiniques (particulièrement d'acide abiétique) conduit à la conclusion qu'on peut utiliser même le talloïl brut comme agent d'encollage du papier.

Les acides organiques de la série des acides résiniques et des acides gras, par traitement en milieu alcalin peuvent être saponifiés. La présence d'un pourcentage de 14...15% des acides gras dans le talloïl, par traitement avec du carbonate ou hydroxyde de sodium, détermine la formation des savons de sodium. Ces savons manifestent des propriétés tensio-actives et d'émulsionnement et ceux-ci déterminent le passage en état de dispersion fine aussi des substances insaponifiables, qui existent dans le talloïl brut. En conséquence, par dilution dans l'eau apparaîtront des dispersions stables.

Les recherches effectuées dans le laboratoire et au stade de pilot ont prouvé que les dispersions de talloïl brut, obtenus par saponification avec du carbonate de sodium, déterminent l'encollage du papier d'emballage, notamment du papier nonblanchi. Puisque le talloïl est un produit de couleur brune, son utilisation comme agent d'encollage pour le papier blanc déterminera une diminution du degré de blanc. Même dans ce cas d'encollage du papier, pour la correction du pH de la pâte de cellulose on utilise aussi le sulfate d'aluminium.

Excepté l'agent de l'encollage, il est connu que le degré d'encollage dépend également d'autres facteurs à savoir: le type de fibres cellulosiques, la manière, d'usinage de celles-ci, la manière de préparation des dispersions d'encollage, le pH, la qualité de l'eau etc.

3. Partie expérimentale

En vue d'obtenir les émulsions nécessaires à l'encollage du papier dans le laboratoire on a procédé de la manière suivante : dans un verre Berzelius de 100 ml on a introduit 6 ml de l'eau distillée et 4 g carbonate de sodium cristallisé et on a chauffé sur bain à l'eau pour dissoudre le carbonate. Puis on a introduit 10 g talloïl brut, sous agitation. Dans quelques minutes on observe un gonflement du contenu du verre, ce qui démontre la présence de l'acidité dans le talloïl. Le gonflement est de très courte durée. On maintient sur le bain de l'eau à l'ébullition et sous agitation pendant 120 min. Pendant la durée de chauffage, due à l'évaporation, il s'avère nécessaire à ajouter une petite quantité d'eau ; selon le cas, on ajoute 2...3 gouttes. Ensuite commence une dilution graduelle avec d'eau chaude jusqu'à un volume total de 400 ml. On

poursuit l'agitation mécanique encore 30 min. Paragitation la dispersion écume un peu, ce qui démontre la présence du savon, résulté par neutralisation des acides gras se trouvant dans le talloïl brut. Cette dispersion a une concentration de 25 g/l, un pH=10,5. elle est stable à long terme et est utilisée à l'encollage du papiers.

La réaction générale de neutralisation de l'acide abiétique avec le carbonate de sodium se déroule selon la schéme:

$$2C_{19}H_{29}-COOH+Na_2CO_3 \rightarrow 2C_{19}H_{29}-COONa+CO_2+H_2O$$

La quantité de carbonate de sodium utilisée à la préparation de la dispersion se trouve en excès pour neutraliser l'acidité minérale, qui accompagne le talloïl brut.

Les épreuves de l'encollage sont réalisées au stade de laboratoire de pilot et plus tard cette méthode a été appliquée dans l'industrie, au Combinat de Cellulose et Papier, Suceava.

1. Au stade de laboratoire on a utilisé la dispersion obtenue tout comme on a indiqué ci-dessus. La quantité de talloïl dispersé, introduite dans la pâte de cellulose blanchie, a été entre 20 et 30 Kg/t. Pour la formation et le séchage de feuilles de papier on a utilisé toujours l'apparail Rapid-Köthen.

De même on a effectué des épreuves d'encollage mixte avec du colophane et du talloïl, en rapport de 10 Kg colophane pour 1 tonne de cellulose et 15 Kg talloïl. Le pH de travail a été toujours 5,5...6. Le contact entre l'agent d'encollage et la pâte de cellulose doit être d'environ 25...30 min. après la correction du pH avec du sulfate d'aluminium. Le degré d'encollage a été verifié par la métode des lignes, étant toujours correspondant, mais le degré de blanc (controlé avec le leucomètre) Zeiss diminue avec 4...5% par rapport à l'épreuve témoin.

Dans les cas des expériences avec de la cellulose naturelle (non-blanchie) la quantité de talloïl nécessaire pour un bon encollage est beaucoup plus petite, environ 5...6 Kg/t.

2. Au stade pilot on a procédé de la manière suivante : 700 Kg cellulose naturelle avec 20% humidité, ce qui correspond à 518 Kg cellulose séchéee, a été moulue et préparée pour lancement sur le tamis.

La dispersion du talloïl a été réalisée dans un réacteur ayant un agitateur mécanique et manteau chauffant. Dans 1 800 ml d'eau on a dissous 1 200 g carbonate de sodium cristallisé et on a introduit en petites quantités 3 Kg de talloïl brut sous agitation lente. Après l'introduction du talloïl il apparait un gonflement de la masse de réaction qui se maintient quelques minutes. On continue le chauffage et l'agitation pendant 120 min. Il apparaît une pâte homogène. Le contenu du réacteur a été avec de l'eau chaude sous agitation jusque'à un volume de 150 l. Le pH de cette dispersion a été aussi de 10,5.

La dispersion du talloïl obtenue de tel façon a été introduite dans la pâte de cellulose sous agitation mécanique. Le pH a été diminué à 5,5 en ajoutant du sulfate d'alluminium.

Pendant le processus d'obtention du papier par cette méthode il n'apparaît aucune écume, le processus découlent d'une façon normale.

Le papier résulté par cette voie présente un degré d'encollage correspondant, quoique la quantité du talloïl utilisé ne dépasse pas 6 Kg/t de cellulose.

Cette expérience au stade pilot démontre, sans ambiguïté, la possibilité d'utiliser le talloïl pour l'encollage du papier nonblanchi.

4. Application industrielle

La méthode de l'encollage du papier avec du talloïl est appliquée, dans l'industrie, au Combinat de Cellulose et Papier, Suceava. La saponification du talloïl a été réalisée à l'aide du hydroxyde de sodium.

Les premières quantités de papier encollé avec du talloïl ont été obtenues en 1987, en utilisant le talloïl séparé dans ce combinat.

Les installations nécessaires pour la transformation du talloïl en dispersion propre au processus d'encollage, en utilisant l'hydroxyde de sodium sont assez simples, en étant constituées par: a) un réservoir antiacide pour le stockage du talloïl, avec la possibilité de mesurer le produit utilisé ; b) un récipient pour la solution d'hydroxyde de sodium ayant de même la possibilité de mesurer la quantité de solution ; c) un réacteur avec agitateur mécanique et source de chauffage, nécessaire à la réaction de saponification ; d) un réservoir (cca 100 m^3) pour dilution et stockage de la dispersion de talloïl qui sera utilisé à l'encollage.

La saponification du talloïl est réalisée à 40°C en certaines conditions bien définies.

On utilise une quantité de 4,5...5 Kg de talloïl par tonne de cellulose naturelle, le pH de travail étant 5,5...6.

Pour vérifier l'efficacité de cette méthode on a encollé deux sortes de papier ; pour chaque sorte on a utilisé à l'encollage du talloïl et du policolle, en même rapport. On a déterminé les caractéristiques du papier obtenu, qui sont présentées dans le Tableau 1.

Tableau 1

Papier naturel résistant, d'emballage, satiné sur une face				Papier naturel, résistant, pour sac	
Caractéristiques	Unités de mesure	Policolle	Talloïl	Policolle	Talloïl
Grammage	g/m^2	59,6	60,2	71,2	71,6
Grosseur	mm	0,1	0,1	0,12	0,125
Densité	g/cm^3	0,594	0,591	0,609	0,572
Porosité	sec.	18	18	20	18
Résistance au crevassement	Kgf/cm^2	2,08	2,0	2,40	2,45
Résistance à la traction	daN/15				
longitudinale	cm	5,53	5,49	7,38	8,30
transversale		3,04	3,66	3,49	2,90
Allongement	%				
longitudinal		2,4	2,3	2,1	2,3
transversal		2,3	2,1	4,0	4,4
Déchirement	gf. cm/cm				
longitudinal		75	75	110	95
transversal		100	88	105	141
Absorption-Cobb	g/m^2	19,1	18,9	10,9	12,7
Encollage	mm	1,5	1,5	1,5	1,5

Les données obtenues montrent que par l'encollage du papier naturel avec du talloïl, au stade industriel, les caractéristiques du produit ne diminuent pas par rapport aux ceux du papier encollé avec du policolle. L'avantage de l'encollage à l'aide du talloïl est une conséquence du caractère plus économique de ce produit par rapport au policolle ou bien au colophane.

Compte tenu que le talloïl est un mélange de grande valeur de produits organiques il s'avère comme opportune sa séparation dans tous les fabriques de cellulose.

5. Conclusions

On étudie la possibilité de l'encollage du papier avec du talloïl séparé au Combinat Dej.

On établi, dans le laboratoire, les conditions d'obtention des dispersions du talloïl à l'aide du carbonate de sodium.

Les épreuves obtenues au stade de laboratoire et au stade pilot montrent qu'on peut encoller le papier naturel avec du talloïl, le degré d'encollage étant correspondant. Pour la cellulose blanchie le degré de blanc diminue.

La méthode de l'encollage avec du talloïl est appliquée au stade industriel au Combinat Suceava, pour le papier naturel (nonblanchi) ; on constate que les caractéristiques du papier encollé avec du policolle ou avec du talloïl ne diffèrent pas. L'utilisation du talloïl pour l'encollage du papier est plus économique que l'encollage à l'aide du policolle ou avec le colophane.

Reçue le 9 juillet 1990

Institut Polytechnique, Jassy,
Chaire de Chimie générale et Technologie
et
Combinat de Cellulose et Papier, Suceava

BIBLIOGRAPHIE

1. Diaconescu V., Obrocea P., *Tehnologia celulozei şi hîrtiei*. Vol. **II**, Ed. Tehnică, Bucureşti, 1976, 172.
2. Трофимов А. Н., Бочарников Е. Б., Узлов Г. А., Тобурдановская Л. А., Коган В. В., Гидрол. и лесохим. пром., *2*, 10 (1974).
3. Узлов Г. А., Жукова И. П., Гидрол. и лесохим. пром., **2**, 12 (1973).
4. Casy J. P., Pulp and Paper, **I B**, 489 (1987).
5. Lorens C., Peintures—Pigments—Vernis, **47**, 7, 388 (1971).
6. Ifrim S., Luchian Cr., Bourceanu M., Bul. Inst. polit., Iaşi, **XXXV (XXXIX)**, *1—2*, s. II, 79 (1989).

ÎNCLEIEREA HÎRTIEI CU ULEI DE TALL

(Rezumat)

Prin cercetări de laborator se arată posibilitatea încleierii hîrtiei cu ulei de tall, separat la Combinatul de Celuloză şi Hîrtie, Dej.

Se stabilesc condiţiile ce trebuie respectate în laborator pentru obţinerea dispersiei de ulei de tall brut, folosind carbonat de sodiu cristalizat.

Probele obţinute în laborator şi în fază pilot arată că hîrtia nealbită pentru ambalaj poate fi încleiate cu ulei de tall brut, obţinîndu-se un grad de încleiere corespunzător ; în cazul celulozei albite este necesară o cantitate mult mai mare de ulei de tall pentru o încleiere corespunzătoare, ceea ce determină scăderea gradului de alb. Încleierea cu ulei de tall se aplică industrial, pentru obţinerea hîrtiei nealbite, la Combinatul de Celuloză şi Hîrtie, Suceava. Caracteristicile hîrtiei încleiată cu ulei de tall sau cu policol nu diferă. Încleierea hîrtiei cu ulei de tall este mai economică decît în cazul folosirii colofoniului sau a policolului.

BULETINUL INSTITUTULUI POLITEHNIC DIN IAŞI
Tomul XXXVII (XLI) Fasc. 1—4, 1991
Secţia II
CHIMIE ŞI INGINERIE CHIMICĂ

RECENZII BROOK REVIEWS

LAFONT O., MAYRARGUE J., VAYSSIÈRE M., *Exercices de chimie organique*. Technique et Documentation, Lavoinier, Paris, 1989, VII+215 pp., ISBN 2-85206-543-6.

Le volume présente 104 exercices de chimie organique, correspondant, en partie, au cours de première année, et en partie, au cours de deuxième année, enseignés aux étudiants en Pharmacie, en Médecine ainsi qu'en Chimie. Les auteurs de cette version revue et corrigée de l'ouvrage sont des spécialistes reconnus dans ce domaine: Olivier Lafont — Professeur à la Faculté de Médecine et de Pharmacie de l'Université de Rouen, Joëlle Mayrargue — Maître de Conférences à la Faculté des Sciences Pharmaceutiques et Biologiques de l'Université de Paris-Sud, Michel Vayssière — Pharmacien des Hôpitaux et Chef de service à l'Assistance Publique de Paris.

Leu auteurs ont conçu les exercices, à la fois, comme une illustration du cours magistral, une introduction aux enseignements dirigés, ainsi qu'une préparation aux épreuves finales.

Les exercices sont presentés en deux parties. La première, „Exercices commentés", comprend les enoncés des 44 exercices suivis par leurs solutions très détaillées. Elles constituent une illustration du cours magistral et une introduction aux enseignements dirigés. La seconde partie, „Exercices non commentés", contient 60 exercices ou questions dont seulement les réponses sont indiquées. Cette partie est ainsi plutôt une préparation aux épreuves finales.

Le volume peut être considéré comme un model de recueil d'exercices pour les étudiants en Médecine, en Pharmacie ainsi qu'en Chimie.

I. Siminiceanu

RICHARDSON L. (Ed.). *Chemistry, Agriculture and the Environment*. The Royal Society of Chemistry / Thomas Graham House, Cambridge, 1991, XIV+546 pp., ISBN 0-85186-228-4.

The book begins with a Foreword and two Prefaces. The Foreword belongs to HRH The Duke of Edinborough, a best known defender of the nature. We must cite several sentences from this beautiful Forward: „There is no doubt that agriculture has been made more efficient and productive by the use of chemicals as fertilizers, pesticides, herbicides, insecticides, fungicides and growth regulators. It is also true that the world's human population has, and is still, increasing and therefore there is a need to produce more food. The question is, at what cost to the rest of the living world? (...) The Challenge for the future is to find an acceptable compromise between the interests of humanity and the integrity of the biosphere on which future generations will have to depend". These words remind us of the Sir William Crookes' adress to the British Association for the Advancement of Science, in September 1898. In that adress, Sir William Crookes warned the „England and all civilised nations

stand in deadly peril of not having enough to eat". However, he then pointed the way to a possible solution to the problem, using the following prophetic words: „It is the *chemist* who must come to the rescue of the threatened communities. It is through the *laboratory* that starvation may ultimately be turned into plenty..."

Now, we must realy optimize, or to find a compromise between the proved optimism of Sir William Crookes and the realism of the Duke of Edinborough. This idea is further developped in the first Preface, signed by the Lord Lewis of Newham, Professor, a past President of the Royal Society of Chemistry. The second Preface belongs to the editor, Mervyn L. Richardson, a Past Chairman of the Royal Society of Chemistry's Chemical Information Group, a former committee member of the Environment Group, etc.

The basic text includes 28 chapters written by 39 eminent scientists from 14 different countries (UK 13 chapters / 16 authors, Netherlands 2/2, France 1/3, Hungary 1/1, Poland 1/1, Italy 2/4, Germany 1/2, Israel 1/1, Norway 1/2, China 1/1, Costa Rica 1/1, USA 1/2, India 1/2, Nigeria 1/1). The editor has attempted to minimize overlap between chapters. However, in dealing with such important topics: pollution of biosphere from gaseous emissions, water, nitrates and pesticides, soil pollution from substances as diverse as silage, animal slurries, some overlap is inevitable.

Finally, the material has been very well arranged, the twenty eight chapters being grouped into five parts: I. *Introduction* (ch. 1...5), II. *Sources of Information* (ch. 6,7), III. *Pollution of the Biosphere — Fertilizers* (ch. 8...13), IV. *Pollution of the Biosphere — Pesticides* (ch. 14...18), and V. *Human Health Aspects* (ch. 19...28).

Chapter 28, *Epilogue*, belongs to M. L. Richardson, the editor. We find here many valuable conclusions and advises, such as „prevention is better than cure".

The book provides an opportunity for a reflection on the risk to the environment from the use of agrochemicals. It is a matter to be considered seriously by all those having responsibilities for producing or handling these chemicals, ranging from those synthesising agrochemicals to those applying such chemicals to soil or crops.

I. Siminiceanu

DUNDERDALE J. (Ed.), *Energy and the Environment*, Royal Society of Chemistry / Thomas Graham House, Cambridge, 1990, XIII + 321 pp., ISBN 0185186-647-6.

The volume includes eighteen papers presented at the „Symposium organized jointly by the Inorganic Chemicals Group and the Environment Group of the Industrial Division of the Royal Society of Chemistry, University of Leeds, April 3rd—5th, 1990". The purpose of the symposium was to consider the relative environmental impact of each step in each of the major energy producing and using processes.

The book covers the types and quantities of polluants produced by these processes, looks at the interaction of these polluants with the atmosphere, and reviews the use of renewable sources as possible alternatives.

The first paper („The Problem", by I. Fells) relates the energy consumption and the consequent two problems — „greenhouse effect" and „acid rain" — to population growth and improved lifestyle. The remaining papers fall into several groups.

The first group (papers 2...5) deals with the chemical interactions of the gaseous emissions, from all energy producing and using processes in and with atmosphere and biosphere.

The second group (papers 6...10) looks in detail at the polluants arising and the control measures adopted at each stage in the production of *nuclear power* from mining to generation, including waste disposal, fuel reprocessing, accidental releases and decommissioning. The last paper of this group („Fusion

Reactors and the Environment", by R. Hancox) the environmental impact of fusion reactors is compared with the impact of fission reactors. The main conclusions of the author is that „fusion reactors appear to offer sufficient environmental advantages to justify the development of this major alternative source of energy for the next century".

The third group (papers 11 ... 13) concerns fossil fuel processes : coal, oil and gas.

The forth group (papers 14 ...16) discusses the environmental legislation, in U.K. and EEC, which applies to energy producers and users and the means taken to meet these requirements.

The last two papers (17 and 18) consider renewables (wind, geothermal, solar, hydropower, biofuels, landfillgas) and conservation, as well as the impact of fuel cells on the environment.

The book is an essential text for chemists, biologists and chemical engineers.

I. Siminiceanu

ORSZÁGOS MŰSZAKI INFORMÁCIÓS KÖZPONT ÉS KÖNYVTÁR 1883

40822